

IN SITU CHARACTERIZATION of  $\alpha 6\beta 1$  INTEGRIN PROTEIN  
ASSOCIATIONS IN EARLY AGGRESSIVE PROSTATE CANCER

by

James Hinton

---

Copyright © James Hinton 2019

A Dissertation Submitted to the Faculty of the  
GRADUATE INTERDISCIPLINARY PROGRAM IN CANCER  
BIOLOGY

In Partial Fulfillment of the Requirements

For the Degree of

DOCTOR OF PHILOSOPHY

WITH A MAJOR IN CANCER BIOLOGY

In the Graduate College

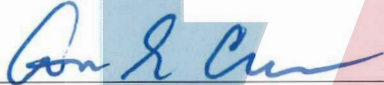
THE UNIVERSITY OF ARIZONA

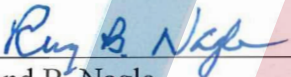
2019


THE UNIVERSITY OF ARIZONA  
GRADUATE COLLEGE


As members of the Dissertation Committee, we certify that we have read the dissertation prepared by: James Hinton, titled: In situ Characterization of  $\alpha\beta 1$  Integrin Protein Associations in Early Aggressive Prostate Cancer


and recommend that it be accepted as fulfilling the dissertation requirement for the Degree of Doctor of Philosophy.

  
\_\_\_\_\_  
Anne Cress Date: 12/19/2019

  
\_\_\_\_\_  
Raymond B. Nagle Date: 12/19/2019


  
\_\_\_\_\_  
Katerina Dvorak Date: 12/19/2019

  
\_\_\_\_\_  
Esteban A. Roberts Date: 12/19/19

  
\_\_\_\_\_  
Ghassan Mounceimne Date: 12/19/19

Final approval and acceptance of this dissertation is contingent upon the candidate's submission of the final copies of the dissertation to the Graduate College.

I hereby certify that I have read this dissertation prepared under my direction and recommend that it be accepted as fulfilling the dissertation requirement.

  
\_\_\_\_\_  
Anne Cress Date: 12/19/19  
Dissertation Committee Chair  
Cancer Biology Graduate Interdisciplinary Program

## ACKNOWLEDGEMENTS

This journey to achieve a doctorate in Cancer Biology from the Graduate Interdisciplinary Program has been a difficult and extremely trying time in my life. As the only son of a single mother raising three children I was always instructed that education would be the key to success and that I should not allow anyone to discourage me from trying to obtain the knowledge and education to reach this goal. I would like to thank the members of my committee primarily my advisor Dr. Anne Cress for her mentorship, invaluable advice and tutelage throughout this process. The moment that I completed my masters defense I knew that I had to have you as my primary mentor and that I would learn so much. I would also like to thank the members of my committee: Dr. Raymond Nagle and Dr. Katerina Dvorak for their immeasurable guidance and direction. I would also like to thank Dr. Esteban Roberts for his continuous encouragement and scientific advice and Dr. Ghassan Mouneimne for advice and suggestions.

Special thanks to my current fellow graduate students Julie McGrath, Kendra Marr, Daniel Hernandez-Cortez and undergraduate student, Nadia Ingabire. I would also like to thank the previous lab mates and collaborators who have completed their degrees, Dr. Cynthia Rubenstein, Dr. Lipsa Das, Dr. Mengdie Wang, and our lab manager Jamie Gard. I would never have made it without your support and comradery.

Last, and certainly not least, I would like to thank my family. Your love, guidance and strength keep me going at my darkest times. Without you, I would never have made it.

## **DEDICATION**

I would like to dedicate this endeavor to my mother. I have felt so lost without you but I made a promise to you that I would finish and I have kept my promise. I only wish I could have finished sooner to share this with you and see your smile when I did. I love you so much!

## TABLE OF CONTENTS

LIST OF FIGURES.....	7
LIST OF TABLES.....	9
LIST OF SUPPLEMENTAL FIGURES.....	10
ABSTRACT.....	11
<b>I. Main introduction.....</b>	<b>13</b>
PROSTATE CANCER.....	13
LAMININ BINDING INTEGRINS (LBIs): $\alpha 6\beta 4$ , $\alpha 3\beta 1$ , $\alpha 6\beta 1$ .....	16
$\alpha 6$ INTEGRIN and uPA/uPAR IN PROSTATE CANCER.....	21
COLLECTIVE TUMOR INVASION AND MIGRATION.....	26
DISSERTATION OBJECTIVES.....	28
<b>II. Loss of <math>\alpha 6\beta 4</math> and <math>\alpha 3\beta 1</math> integrins in PCa track with early PCa progression.....</b>	<b>29</b>
ABSTRACT.....	29
INTRODUCTION.....	30
RESULTS.....	36
DISCUSSION.....	41
<b>III. <math>\alpha 6</math> integrin and uPAR co-distribution in early aggressive PCa.....</b>	<b>43</b>
ABSTRACT.....	43
INTRODUCTION.....	44
RESULTS.....	48
DISCUSSION.....	52
<b>IV. <math>\alpha 6</math> integrin and E-cadherin co-distribution in early aggressive PCa.....</b>	<b>54</b>
ABSTRACT.....	54
INTRODUCTION.....	55
RESULTS.....	59
DISCUSSION.....	71
<b>V. Multiplex IHC detection of <math>\alpha 6</math>, <math>\alpha 3</math> integrins and E-cadherin localization in PCa progression.....</b>	<b>75</b>
ABSTRACT.....	75
INTRODUCTION.....	76
RESULTS.....	79
DISCUSSION.....	87

<b>VI.</b>	<b>Cohesive collective tumor invasion in PCa.....</b>	<b>90</b>
	ABSTRACT.....	90
	INTRODUCTION.....	91
	RESULTS.....	95
	DISCUSSION.....	107
<b>VII.</b>	<b><math>\alpha</math>6 integrin correlative localization with PTEN and ERG expression... </b>	<b>109</b>
	ABSTRACT.....	109
	INTRODUCTION.....	110
	RESULTS.....	116
	DISCUSSION.....	123
<b>VIII.</b>	<b>Method to reuse archived H&amp;E stained slides.....</b>	<b>126</b>
	ABSTRACT.....	126
	INTRODUCTION.....	127
	RESULTS.....	130
	DISCUSSION.....	142
<b>IX.</b>	<b>Concluding statements and future research.....</b>	<b>145</b>
<b>X.</b>	<b>Tables.....</b>	<b>152</b>
<b>XI.</b>	<b>Materials and methods.....</b>	<b>157</b>
<b>XII.</b>	<b>Supplemental figures.....</b>	<b>165</b>
	<b>Appendix A: Manuscripts.....</b>	<b>169</b>
	<b>References.....</b>	<b>170</b>

## LIST OF FIGURES

Figure 1.1 Normal Gland, PIN, PNI.....	15
Figure 1.2. Integrin receptor family.....	17
Figure 1.3. Schematic diagram of $\alpha 6$ integrin.....	18
Figure 1.4. Structure of laminin.....	20
Figure 2.1. High-grade intraepithelial neoplasia (HGPIN).....	32
Figure 2.2. $\alpha 3$ integrin cooperative signaling with E-cadherin.....	35
Figure 2.3. $\beta 4$ integrin expression is lost in human prostate cancer progression...38	
Figure 2.4. $\alpha 3$ integrin expression is lost in prostate cancer progression.....	40
Figure 3.1. uPAR regulates cleavage of integrin $\alpha 6$ to $\alpha 6p$ .....	46
Figure 3.2. Aggressive prostate tumors invade within peripheral nerves.....	48
Figure 3.3 $\alpha 6$ integrin and uPAR expression localization in normal prostate glands in FFPE tissue.....	49
Figure 3.4. Multiplex IHC detection of $\alpha 6$ integrin and UPAR co-distribution in human prostate tissue.....	51
Figure 4.1. E-cadherin IHC expression in prostate with titration.....	60
Figure 4.2. E-cadherin 1:10 dilution immunostain expression comparison to $\alpha 6$ integrin .....	62
Figure 4.3. E-cadherin expression in DU145 CRISPR Cas9 prostate cancer cells.....	65
Figure 4.4. $\alpha 6$ Integrin expression in DU145 CRISPR Cas9 prostate cancer cells.....	66
Figure 4.5. E-cadherin membrane expression increased with inhibition of cleavage.....	68

Figure 4.6. Schematic of Caged Hapten Proximity Assay for $\alpha 6$ integrin and E-cadherin complex.....	70
Figure 4.7. $\alpha 6$ integrin and E-cadherin form complexes in prostate tissue.....	71
Figure 5.1. $\alpha 6$ integrin, E-cadherin and $\alpha 3$ integrin expression in early progressive gland and PNI.....	81
Figure 5.2. $\alpha 6$ integrin, $\alpha 3$ integrin and E-cadherin expression with chromogen multiplex IHC.....	82
Figure 5.3. $\alpha 6$ integrin, $\alpha 3$ integrin and E-cadherin distribution in prostate cancer.....	84
Figure 5.4. Percent ratio of $\alpha 6$ integrin and E-cadherin indicate stage of progression.....	86
Figure 6.1. DU145 diaphragm tumor burden.....	98
Figure 6.2. Hematoxylin and eosin stained xenograft PCa tissue slides.....	100
Figure 6.3. Inhibition of $\alpha 6$ integrin cleavage reduces tumor invasion sites.....	102
Figure 6.4. Maximum depth of tumor invasion in mouse diaphragms .....	104
Figure 6.5. Loss of $\alpha 3$ integrin increases tumor dissemination to the small bowel and $\alpha 6^{AA}$ reduces dissemination.....	105
Figure 6.6. DU145 $\alpha 3^{KO}$ xenograft $\alpha 6$ integrin and E-cadherin expression.....	106
Figure 7.1. PTEN regulates PIP <sub>3</sub> , FAK and Shc.....	111
Figure 7.2. PTEN, ERG, $\alpha 6$ Integrin and HMWCK+p63 protein expression in prostate cancer.....	117
Figure 7.3. $\alpha 6$ integrin localization is quantitative on immunostained human prostate FFPE slides.....	119
Figure 7.4. $\alpha 6$ integrin cytoplasmic and membrane expression in PNI and PIN..	122
Figure 8.1. Malignant primary prostate adenocarcinoma tissue sample.....	130



Figure 8.2. Sequential slides of human prostate tissue exhibiting cancer (Ca) invading into normal glands and high-grade prostatic intraepithelial neoplasia (HGPIN).....	132
Figure 8.3. Prostate cancer CNBs sample H&E slides with PTEN and ERG IHC DAB stained slides.....	135
Figure 8.4. Prostatic adenocarcinoma sample CNB H&E and Chromogen IHC..	136
Figure 8.5. H&E stained slide image and reused H&E slide selected antibody immunostain comparison with sequential slides in PCa CNBs.....	139
Figure 8.6. H&E stained slide archived 4+ years subjected to de-stain and re-stain procedure compared to sequential sample slide.....	141

## LIST OF TABLES

Table 1. List of antibody diluents.....	152
Table 2. 6-week diaphragm invasion sites.....	152
Table 3. 6-week small bowel tumor incidence.....	153
Table 4. List of tissues, results and parameters for samples used for H&E de-stain.....	154
Table 5. Time Tracking and coverslip parameters.....	155
Table 6. Immunohistochemistry antibodies and Adapted Staining Protocols....	156
Table 7. Comparison of H&E reused and sequential comparator immunostaining intensity scores.....	156

**LIST OF SUPPLEMENTAL FIGURES**

Figure S1. H&E stained slide of DU145 WT 8-week mouse diaphragm.....	165
Figure S2. $\alpha 6$ integrin localization with PTEN and ERG expression.....	166
Figure S3. $\alpha 6$ integrin localization with PTEN and ERG expression.....	167
Figure S4. $\alpha 6$ integrin localization with PTEN and ERG expression.....	168

## ABSTRACT

In prostate cancer (PCa) the laminin binding integrin (LBI)  $\alpha 6\beta 1$  is involved in the extra capsular and muscle invasion of cohesive tumor clusters in part through dissemination via peripheral nerves expressing laminin. This invasion results in part due to the posttranslational modification (PTM) of the  $\alpha 6\beta 1$  integrin ( $\alpha 6$ ) by the serine protease urokinase plasminogen activator (uPA, PLAU) and its cognate receptor (uPAR, PLAUR). The cleavage results in a tumor specific variant form of the  $\alpha 6$  integrin called  $\alpha 6p\beta 1$  ( $\alpha 6p$ ). This leads to altered biophysical adhesive properties of the cohesive cancer clusters. This PTM occurs early in progression from indolent and confined tumors to aggressive and invasive phenotypes. Current strategies have the capability to detect aggressive cancers that have invaded, but are unreliable for identification of tumors that have an early signature of invasiveness. Therefore, an identification of a reliable diagnostic method that stratifies confined and indolent (low risk) tumors that lack migratory capability from one that will progress to early invasive phenotypes will aid informed and objective decisions for specific treatment strategies.

Utilizing an emerging technique of multiplex immunohistochemistry (IHC) detection of primary antibodies specific for protein biomarkers within a single formalin fixed paraffin embedded (FFPE), LBI protein interactions and associations were detected within prostate tissue samples. The interaction of LBI biomarkers with uPAR, the essential cell-cell adhesion protein E-cadherin were detected. In addition, associations with the pathway regulating tumor suppressor protein PTEN in concert with the transcription factor ERG in human prostate tissue samples were

also detected. These interactions were detected in tissues exhibiting various stages of PCa disease progression. These protein interactions and associations were also the basis for generating image analysis algorithms to quantify protein expression. Using brightfield multiplex and standard DAB IHC image analysis, two separate quantitation algorithms were created and tested utilizing multiplex chromogen and IHC DAB detections. One quantitative algorithm allowed differentiation of individual chromogenic stain intensities and co-incidence of LBIs and E-cadherin biomarkers within focal regions of interest in PCa tissues. The results also displayed increased ratio of  $\alpha 6$  integrin and E-cadherin cell-cell co-distribution in early pre-malignant events compared to aggressive tumors. The other algorithm designed identified specific localization patterns of  $\alpha 6$  integrin in association of PTEN and ERG status. This indicated that localization of  $\alpha 6\beta 1$  integrin correlating to PTEN and ERG status could be used as an indicator of PCa aggressiveness.

In this study, the role of the  $\alpha 6\beta 1$  integrin cleavage plays in cohesive tumor invasion through muscle was characterized. A CRISPR Cas9 mouse model muscle invasion assay with DU145 prostate tumor cells injected with a transfected uncleavable  $\alpha 6$  mutant ( $\alpha 6^{AA}$ ) exhibited significantly reduced tumor onset and extravasation (6 weeks) while mice injected with cells with a transient knockout of  $\alpha 3\beta 1$  integrin ( $\alpha 3$ ) increased tumor burden and invasion sites in xenograft tissues. Analysis of xenograft sample tissue confirmed a significant decrease in tumor burden and reduced muscle invasion. Overall, these results suggest a loss of  $\alpha 3$  integrin plays a role in aggressive tumor burden and muscle invasion in PCa via

the cleavage of  $\alpha6\beta1$  integrin. Also, the results indicate a blockage of the  $\alpha6\beta1$  integrin cleavage demonstrate a promising mechanism to inhibit the progression of aggressive disease.

## I. Main introduction

### PROSTATE CANCER

Prostate cancer (PCa) is the most common type of cancer in males and second leading cause of cancer deaths (after lung and bronchus) in males (Harryman *et al.*, 2019; Chapter 10; Siegel *et al.*, 2019). It has been estimated that 174,650 new cases of prostate cancer (20% of all cancer cases) will be diagnosed in 2019 (Siegel *et al.*, 2019). Of these cases 31,620 (10% of all cases) will result in death. It is a unique type of cancer that presents with two phenotypes, an indolent confined form and aggressive an invasive form. Cancer that is localized (confined to the gland) is considered curable with a 5-year survival rate of almost 100% (Kascinta *et al.*, 2014; Harryman *et al.*, 2016). This 5-year survival rate dramatically decreases to less than 30% with extracapsular tumor escape (Kasinta *et al.*, 2014; Harryman *et al.*, 2019, Chapter 10).

Treatment for prostate cancer is dependent upon the early detection of aggressive disease. Although the diagnostic capabilities have improved over the past decades, the ability to identify invasive potential remains difficult. Most low-risk stage one confined prostate disease will involve watchful waiting and active surveillance. High-risk PCa is treated by radical prostatectomy, external beam

radiation or implanted radioactive seeds. Advanced stage and metastatic PCa is usually treated with prostatectomy, androgen deprivation therapy (ADT) and/or radiation therapy (RT). Although a study showing the combination of prostatectomy and ADT improved overall survival by about 40% (Rusthoven *et al.*, 2016), the cancers will become unresponsive and lead to the highly aggressive castration resistant form in under 3 years and regression of cancer within 12-18 months (Marques *et al.*, 2010; Karatanos *et al.*, 2016). Currently, the inability to stratify low-risk disease from high-risk metastatic PCa leads to overtreatment or misdiagnosis. Therefore, the need for more specific detection methods to identify the cancers with metastatic potential is critical for patient treatment decisions.

Prostate tumor progression is complex process occurring in steps with transition from normal glands (**Figure 1.1, A**), to metastatic tumors. It begins with transition of normal secretory glands to early premalignant lesions called prostatic intraepithelial neoplasia (PIN) lesions (**Figure 1.1, B**). The process begins with the attenuation of basal cell layer and loss of critical laminin components in the extracellular matrix displaying gaps. Following this event, clusters of tumor cells escape through the gaps into the surrounding stroma and then to the laminin rich peripheral nerves for extracapsular escape in a process known as perineural invasion (PNI) (**Figure 1.1, C**). PNI is defined as the invasion of tumor clusters in and around the nerve and is identified as a known pathological feature of aggressive disease. After extracapsular escape via peripheral nerves, the primary metastatic site for prostate tumors is the bone, although ~20% of the time the brain, liver and lung are also common sites for metastatic prostate disease.

The expression of LBIs and other surface proteins play a significant role in invasive tumor migratory capacity through dynamic matrix and cell-cell adhesion modulations. The mechanotransduction of signal cues via interactions with the matrix environment regulate adhesion responses driving migration and directional polarization. Our group and others have previously demonstrated the blocking of integrin function mitigates PCa metastasis (Ports *et al.*, 2009; Degrosellier and Cheresch., 2010; Landowski *et al.*, 2014). Therefore, specific targeting of these functions in conjunction with compensatory signaling molecules may mitigate metastatic colonization.

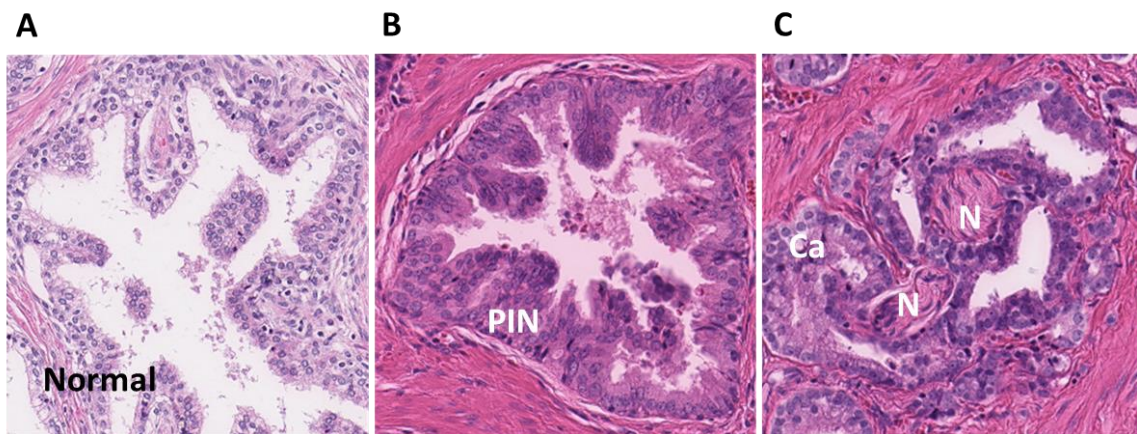


**Figure 1.1. Hematoxylin and Eosin (H\*E) stained prostate tissue slides.** Images representative of stages in prostate cancer progression. **(A)** Image of normal gland. **(B)** Image of early prostatic intraepithelial neoplasia (PIN) lesion. **(C)** Perineural invasion (PNI) with cancer cells (Ca) invading around peripheral nerves (N).

**LAMININ BINDING INTEGRINS (LBIs):  $\alpha6\beta4$ ,  $\alpha3\beta1$ ,  $\alpha6\beta1$ :** Laminin binding integrins are cellular signaling and adhesion molecules that play a critical role in normal human developmental processes such as embryonic development, cellular migration, wound healing and repair, cellular signaling and also a substantial role in cancer progression. Laminin binding integrins are transmembrane cell-surface glycoprotein receptors comprised of non-covalently associated  $\alpha$  and  $\beta$  subunits. There are 18  $\alpha$  and 8  $\beta$  subunits that combine to form at least 24 known integrin heterodimer combinations that demonstrate a ligand binding specificity to substrates in the ECM (Van de Flier *et al.*, 2001; Ports *et al.*, 2009; Barczyk *et al.*, 2010) (**Figure 1.2**). The  $\alpha$  and  $\beta$  integrin extracellular domains function as a receptor for components of the ECM and is required for binding to proteins such as fibronectin, fibrinogen, vitronectin, laminin, and collagen. The cytoplasmic tails connect to proteins of the cytosol (Delwel *et al.*, 1995). They also have the capability to bind vascular and coagulator proteins such as thrombospondin, von Willebrand's factor, factor X and other cellular adhesion molecules (CAMs) (Makrilia *et al.*, 2009). Integrins are involved in bidirectional signal transduction when activated by intracellular and/or extracellular signals. Intracellular signals induce conformational alterations in the ligand binding properties and is known as inside-out signaling, whereas ligation with extracellular proteins constitute outside-in signaling for activation of cellular processes. These integrin-protein associations are essential for integrin regulation of normal functions such as gene expression, cell polarity, cell survival and proliferation, cell cycle progression, cellular adhesion, development, stem cell homing, morphogenesis and wound healing (Makrilia *et*



*al.*, 2009). Integrins are also key mediators of epithelial cell migration and metastasis (Landowski *et al.*, 2014).

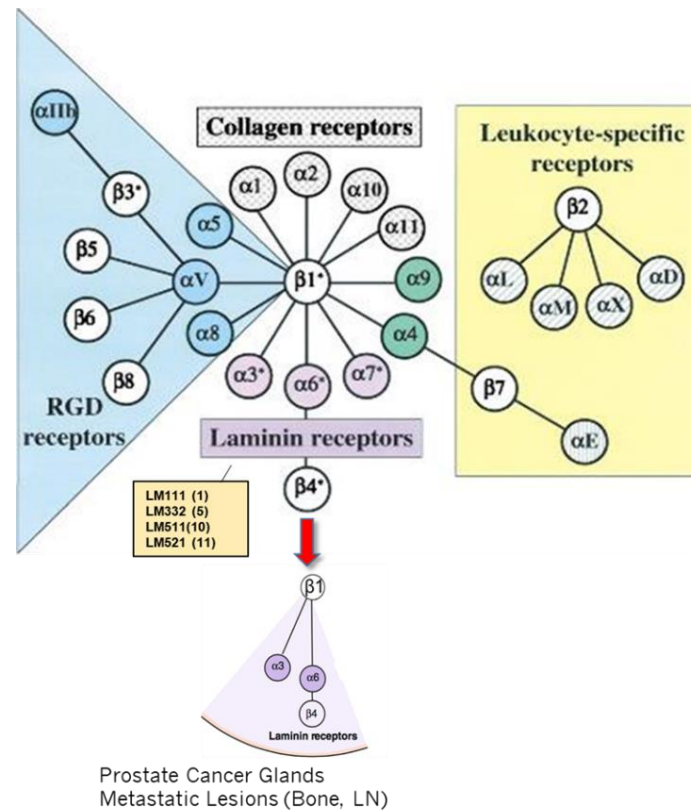


**Figure 1.2. Integrin receptor superfamily and associated extracellular ligands.** The 18  $\alpha$  and 8  $\beta$  integrin subunits and associated extracellular ligand or Ig-super family counter receptor specificities for the 24 different heterodimer conformations. (Modified from Hynes, 2002).

The  $\alpha 6$  integrin subunit primarily forms a heterodimer with the  $\beta 4$  or  $\beta 1$  subunit respectively to form the laminin binding integrin conformations. The  $\alpha 6$  integrin (P23229) is 1073 amino acids in length and contains two polypeptides linked by a disulfide bridge between the 110-kDa N-terminal heavy chain and 30-kDa light chain (Sonnenberg *et al.*, 1987; Tamura *et al.*, 1990., Hogervorst *et al.*, 1991) (**Figure 1.3**). There are two known splice variants of  $\alpha 6$ , each containing similar

heavy chains and two variable light chains  $\alpha 6A$  and  $\alpha 6B$  (Hogervorst *et al.*, 1991). The  $\alpha 6A$  isoform (Alpha6X1) is the most common form (Delwel *et al.*, 1995), is found in prostate cancer and the isoform studied here. The heavy chain has an 875-amino acid extracellular region and a cytoplasmic domain that contains a highly conserved five amino acid residue GFFKR sequence motif that is necessary for heterodimerization to  $\beta$  integrin subunits for cell surface expression (De Melker and Sonnenberg., 1996; De Melker *et al.*, 1997).

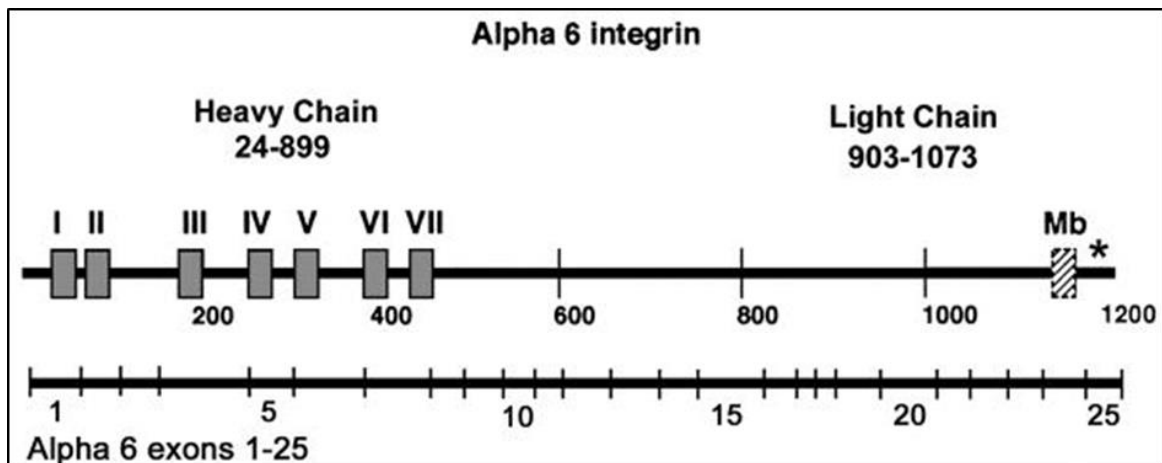


**Figure 1.3. Schematic diagram of the full-length  $\alpha 6$  integrin and the tumor specific variant  $\alpha 6p$ .** A schematic representation of the  $\alpha 6$  integrin sequence with amino acid heavy chain region at 24-899 and light chain amino acid region at 903-1073 (Modified from Davis *et al* 2001).

The LBIs  $\alpha 6\beta 4$  (CD104),  $\alpha 6\beta 1$  (CD49f) and  $\alpha 3\beta 1$  (CD49c) are required for normal cellular adhesion to laminin, a major component of the basal lamina (basement membrane), as their extracellular ligand. Laminins are members of a family of 800 kDa heterotrimeric basement membrane glycoproteins that contain three chains; one  $\alpha$ ,  $\beta$  and  $\gamma$  subunit that are crosslinked by disulfide bonds that form the shape of a cross-like structure with two shorts arms and one long arm (Chang *et al.*, 1995;

Durbeej., 2010) (**Figure 1.4**). The primary laminins recognized by these integrins are laminins 111, 332, 551, and 521 (laminins 1, 5, 10 and 11 respectively). The  $\alpha 6\beta 4$  integrin is associated with the nucleation of hemidesmosomes and intermediate filaments (Kurpakus *et al*, 1991., Jones *et al.*, 1991., Cress *et al.*, 1995). The  $\alpha 6\beta 1$  integrin is found to be a constituent of focal adhesions and is associated with cytosolic molecule vinculin (Hogervorst *et al.*, 1993., Cress *et al.*, 1995). Of the LBIs,  $\alpha 6\beta 1$  has the broadest specificity binding to all laminin isoforms with preference for laminin 111, laminin 332 and laminin 511 (Nishiuchi *et al.*, 2006) and can support the undifferentiated growth of human stem cells (Miyazaki *et al.*, 2008). In normal tissue, the primary laminin for  $\alpha 6\beta 4$  is laminin 332 (LMN 5) which is expressed in basal lamina of normal prostate glands. In normal tissue the primary laminin ligand for  $\alpha 6\beta 1$  is laminin 551 (LMN 10), which is a key constituent of the normal basal lamina of the prostate gland and the muscle stroma. However, of all the LBIs, the  $\alpha 6\beta 1$  integrin has the ability to bind all laminin isoforms it may encounter, with laminin 511 as the most preferred ligand (Nishiuchi *et al.*, 2006). These are crucial factors involved in aggressive tumor dissemination into surrounding tissues for successful metastasis through laminin lined microenvironments.

Early PCa progression from normal glandular epithelium is considered by many to be initiated by early pre-malignant prostatic intraepithelial neoplasia (PIN) precursor lesions. This involves the attenuation of basal cells, the intermittent preservation of ECM laminin-5 expression in which remaining basal cells are bound, the loss of hemidesmosomes which coincide with the downregulation of

the  $\alpha6\beta4$  and  $\alpha3\beta1$ . This has been suggested to potentially be of high predictive value for adenocarcinoma (Wang *et al.*, 1999; Soares *et al.*, 2002). Laminin-10 expressed within the stroma becomes available for tumor cell interaction due to the intermittent expression of the laminin-5. The gaps of laminin 5, provide access to laminin-10 ligation of  $\alpha6\beta1$ . This event is then exploited by proliferating invasive tumor cells. Our understanding of these associations may ultimately lead to defining a signature for first step invasiveness and with that foundation, the ability to target and inhibit the invasion.

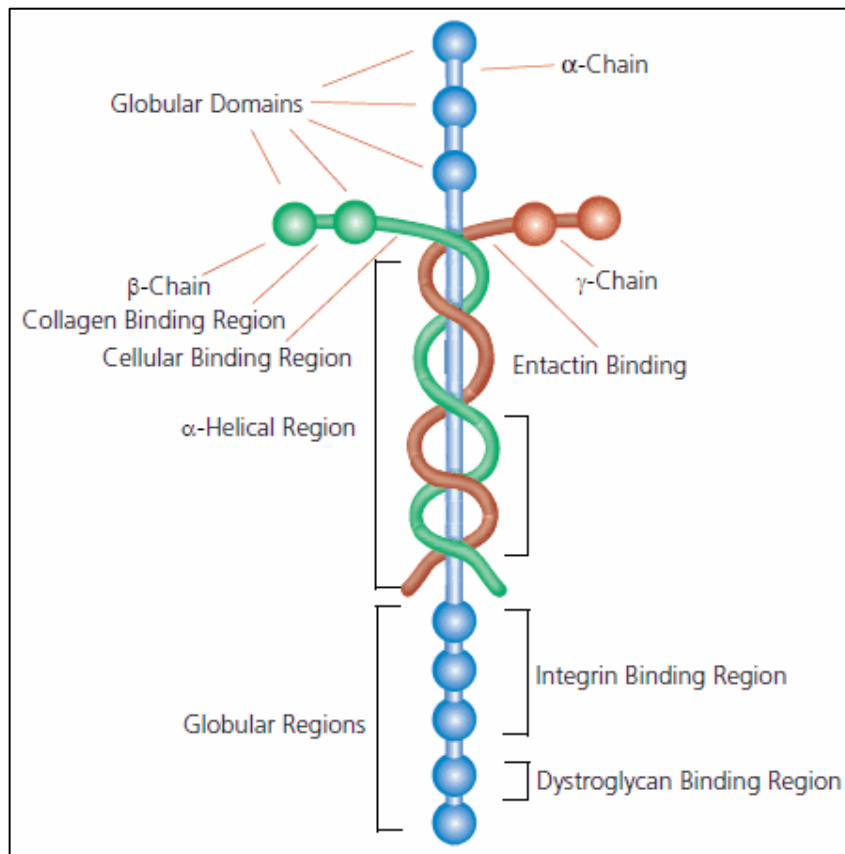


**Figure 1.4. Structure of laminin.** Schematic representation of laminin-1. The heterotrimeric laminin structure with  $\alpha$ ,  $\beta$  and  $\gamma$ -chains comprising of globular domains. The laminin structure encompasses the long  $\alpha$ -chain contain three globular domains in the top region that associate with components of the ECM and a lower region containing 5 globular regions, three for integrin binding and two for dystroglycan binding. The  $\alpha$ -chain is associated by the  $\beta$  and  $\gamma$ -chains both with two globular domains coiled in a helical formation. Note: The  $\alpha 5$  and the  $\alpha 3$  chains for laminin 10 and laminin 5 are different from the illustration depicted here. (*Image courtesy of MilliporeSigma, the Life Science Business of Merck KGaA, Darmstadt, Germany. Sitterley, George. BioFiles 2008, 3.8, 11*).

## **$\alpha 6$ INTEGRIN AND UPA/UPAR IN PROSTATE CANCER**

Although  $\alpha 6\beta 4$  ( $\beta 4$ ) and  $\alpha 3\beta 1$  integrins play an integral role in progression from non-neoplastic to neoplastic lesions in PCa, events leading to progression of cancer is due to the absence of protein epitope expression. The  $\alpha 6\beta 1$  integrin role in tumor invasiveness is critical specifically due to the posttranslational modification event. Previous work by our group has demonstrated that an invasive PCa specific variant form of  $\alpha 6\beta 1$  integrin called  $\alpha 6p\beta 1$  ( $\alpha 6p$ ) is mediated by the protease uPA when it is associated with its receptor called uPAR. This modification precedes the progression of indolent or confined tumors to a more cohesive aggressive phenotype with the propensity of capsular penetration and muscle invasiveness into surrounding tissues.

*$\alpha 6$  Integrin.* Along with  $\alpha 3\beta 1$  integrin, the  $\alpha 6\beta 1$  integrin is the common laminin binding integrin heterodimer receptor pair that remains expressed in prostate cancer (Cress *et al.*, 1995., Nagle *et al.*, 1995., Ports *et al.*, 2009). In invasive prostate carcinomas, most of the integrin heterodimers are downregulated and not

expressed on the cellular surface (Cress *et al.*, 1995). However, between 10% and 69% of those invasive cancers express  $\alpha3\beta1$  and  $\alpha6\beta1$ , respectively (Demetriou and Cress., 2004). A previous study by our lab incorporating 135 prostate cancer biopsies from 61 patients observed that approximately 80% of those cases expressed either  $\alpha3$  or  $\alpha6$  integrin (Schmelz *et al.*, 2002; Demetriou and Cress., 2004). Various other studies have implicated these integrins in other aggressive cancers such bladder cancers, colorectal cancers, glioblastoma and pancreatic adenocarcinomas (Weinel *et al.*, 1995; Rabinovitz and Mecurio., 1996).

The increased cell surface expression of  $\alpha6\beta1$  integrin is linked with progressive downregulation of  $\beta4$  integrin in the natural history of prostate cancer involving prostatic intraepithelial neoplasia (PIN), carcinoma in situ, and adenocarcinoma invasion of adjacent structures and lymphoid involvement and metastasis to bone (Cress *et al.*, 1995). The decreased expression of  $\beta4$  integrin subunit coincides with the decreased expression of the associative laminin-5. There remains laminin-10 in which the  $\alpha6\beta1$  has a preferred specificity (Nishiuchi *et al.*, 2006). Although the  $\alpha3$  integrin subunit has been demonstrated to be functional receptor for laminin-10 in vivo, other studies have shown that laminin-5 was the preferred ligand (Kikkawa *et al.*, 2000). The increased exposure of laminin-10 and the preference for laminin-5 binding is accompanied by downregulation of  $\alpha3$  subunit. Thus, an increased qualitative association of the  $\alpha6$  with the  $\beta1$  and corresponding increased surface expression of  $\alpha6\beta1$  which activates downstream signaling pathways (Fornaro *et al.*, 2001; Goel *et al.*, 2008).

The increased surface expression of  $\alpha 6\beta 1$  (here by referred to as  $\alpha 6$  integrin), results in integrin clustering. The pathways activated are involved in cancer cell survival, proliferation, adhesion, cytoskeletal reorganization and regulation of cancer cell motility such as the focal adhesion kinase (FAK) which is a non-receptor tyrosine kinase (Ilic *et al.*, 1995; Goel *et al.*, 2009). Once phosphorylated, FAK interacts with various other signaling factors that are found altered in PCa such as Cas, Src kinases, paxillin and phosphatidylinositide 3-kinase (PI3K) that has been shown to promote prostate cancer cell invasion (Goel *et al.*, 2009).

*uPA/uPAR*. The serine protease uPA and its glycosylphosphatidylinositol (GPI) - anchored receptor uPAR are key molecules in several normal developmental, wound healing and maintenance functions. These molecules also been discovered to have pleiotropic functions in pathogenesis of inflammation, fibrinolysis, innate and adaptive immunity and pathology (Modino and Blasi., 2004). They also function as key facilitators of ECM degradation and remodeling, intracellular signaling, migration, tumor invasion, and are attributed to the production of  $\alpha 6\beta 1$  variant in prostate adenocarcinoma. The inactive precursor form of uPA (pro-uPA), secreted by cells, remains in an inactive soluble form until activation. The anchored uPAR is composed of three domains (D1, D2 and D3) that together have a high affinity for pro-uPA (zymogen), uPA and ECM protein vitronectin (Mondino and Blasi., 2004). The activation of uPA occurs once bound to the GPI anchored uPAR, which not only localizes uPA but regulates signaling activity and cellular differentiation and migration through the ECM (Busso *et al.*, 1994; Shariat *et al.*, 2007). The activated uPA catalyzes the conversion of the inactive zymogen

plasminogen to the active plasmin form. The active plasmin form activates matrix metalloproteases (MMPs) that actively cleave protein components of the ECM to allow dissolution of the membrane (LeBeau *et al.*, 2015). In turn, this process releases various growth factors, cytokines and other molecules from within the matrix. The activated plasmin also feeds into the proteolytic positive feedback loop by the cleavage and activation of the pro-uPA resulting in increased expression of the uPA/uPAR complex. This is a key event during tumor growth, invasion and metastasis (Mahmood *et al.*, 2018).

Once the uPA is bound to the uPAR, this stimulates membrane receptor clustering, potentially within detergent-resistant cholesterol rich regions known as lipid rafts (Cunningham *et al.*, 2003; Smith and Marshall., 2010). This clustering enhances vitronectin binding resulting in increased associations with integrins, particularly with  $\alpha 6\beta 1$  integrin. The uPA/uPAR complex can also activate downstream signaling pathways involved in proliferation, migration and invasion such as Ras-mitogen-activated protein kinase (MAPK), Signal transducer and activator of transcription (STAT), FAK, Janus kinase (JAK) and phosphatidylinositide 3-kinase (PI3K)-Akt (Ma *et al.*, 2001; Li and Cozzi., 2007, Smith and Marshall., 2010). However, the signaling through the uPA/uPAR complex is independent of the uPA proteolytic activity but dependent upon transmembrane co-receptors such as integrins (Nusrat *et al.*, 1991; Smith and Marshall., 2010).

The proteolytic activity of uPA is regulated by members of the serine protease inhibitor (serpine) superfamily, plasminogen activator inhibitors type I and 2 (PAI1 and PAI2) and by uPAR (Li and Cozzi., 2007). In return, uPA has the ability to



cleave the uPAR in the linker between the D1 and D2 domain regions resulting in soluble D1 fragment and leaving a membrane bound D2-D3 fragment (Smith and Marshall., 2010). This in turn inactivates the proteolytic activity of the complex by mitigating the uPA binding to the uPAR. The proteolytic cleavage of the GPI linker could also result in soluble full length and D2-D3 fragments (Smith and Marshall., 2010). The activated uPA bound to uPAR is recruited to cells of the leading edge of migrating cells bordering the ECM for localized pericellular remodeling of the matrix molecules promoting the invasive potential (Friedl., 2004; Friedl *et al.*, 2004; Friedl *et al.*, 2009). The presence of the uPA/uPAR complex is highly increased in many malignant human cancers and expression is frequently prognostic of poor survival, predictive of invasion and metastasis (Smith and Marshall., 2010). The expression of uPAR has also been shown in populations of inflammatory cells such as tumor associated macrophages (TAMs) and also within stromal cells of interstitial tissues of PCa (Li and Cozzi., 2007). This demonstrates an intricate process by which normal cellular migration and movement proceeds within the complex environment. This exploitation of deregulated processes by invasive tumors is a major reason why specific targets indicative of early aggressiveness are extremely difficult to elucidate.

Overall, the involvement of the uPA/uPAR complex as a mediator of tumor progression and dissemination through the ECM has been determined to involve the association of laminin binding integrins  $\alpha6\beta1$  and  $\alpha3\beta1$ . It is noted that uPA and uPAR as well as  $\alpha6\beta1$  expression is increased in aggressive prostate cancer (Sroka *et al.*, 2011). However, the specific role of  $\alpha3\beta1$  in this progression has not

been fully discerned. The increased expression of uPA/uPAR has been shown to be responsible for the significantly increased pericellular proteolysis in patients with advanced PCa (Lippert *et al.*, 2016). Pericellular proteolysis includes the production of a tumor-specific receptor that is a laminin binding integrin variant, a novel form of the  $\alpha 6$  integrin with altered biophysical adhesion properties. Our lab has previously characterized the production of the tumor specific variant  $\alpha 6\beta 1$  resulting from PTM of the laminin binding domain of  $\alpha 6\beta 1$  due to the proteolytic activity of the uPA/uPAR complex. It is evident that although the mechanistic pathways that initiate this modification has yet to be uncovered, the association of these proteins “bear fruit” to phenotypic switches that precedes the metastatic potential and thus may be targeted as proteins of interest for early invasiveness.

### **COLLECTIVE TUMOR INVASION AND MIGRATION**

Tumor invasion and migration of cohesive tumor cells through muscle to distant sites involves the laminin binding integrin association with various critical adhesion molecules such as Kindlin-2, Talin and integrin-linked kinase (ILK) and protein receptors E-cadherin, beta-catenin. Initial testing using formalin fixed paraffin embedded (FFPE) tissues involved developing a diagnostic assay to evaluate the uPA and  $\alpha 6\beta 1$  ( $\alpha 6$ ) association. This initially was to become a dual detection immunostain using antibodies against uPAR and  $\alpha 6$  integrin. The purpose was to profile the potential posttranslational modification of  $\alpha 6$  integrin in early invasive tumors by utilizing chromogen multiplex detection. However, the antibody utilized against the uPAR lost viability and was discontinued by the vendor leaving this particular pathway unavailable for further pursuit. Therefore, the integrin

association with cell-cell adhesion proteins, such as E-cadherin, became the prevailing focus. There are three hallmarks that characterize collective cell migration (Friedl *et al.*, 2009). Collective tumor invasion through tissues involves cell-cell and cell-matrix proteins that allow physical and functional connectivity of the cohesive groups of cancer cells to retain integrity of the adhesive junctions for preservation of cellular motility and migration. These proteins transduce signals that initiate groups of cells to organize their actin cytoskeleton in a polarized fashion to generate traction and protrusion forces for migration. They migrate through the extracellular matrix (ECM) as collective sheets, chords or clusters that also involves structural tissue remodeling and modification of the ECM that may result in basement membrane deposition.

## **DISSERTATION OBJECTIVES**

The discovery and detection of a biomarker signature in prostate cancer tissues that is a definitive indication of aggressive disease that will disseminate to distant tissue remains an elusive undertaking. When prostate cancer invades, it breaches through the smooth muscle walls of the prostatic capsule and migrates in a single cell fashion or a cellular cohesive collective. Our initial focus was to utilize various antibody detection strategies such as standard immunohistochemistry, chromogen multiplexing and proximity assays on human prostate tissues to target the distribution of cell surface protein expressions. This would allow our lab to develop an IHC assay to recognize an early cohesive migratory cancer phenotype. This cohesive group utilizes several substrate and cell-cell adhesion proteins to remain pliable and intact during dissemination. The secondary objective of this research was to develop a model assay system that would interrogate the associations between these proteins and allow detection and quantification of protein expression levels to identify an early signature related to invasiveness.

## II. Loss of $\alpha6\beta4$ and $\alpha3\beta1$ integrins in PCa track with early PCa progression

### ABSTRACT

This chapter characterizes the roles of  $\alpha6\beta1$  and  $\alpha3\beta1$  integrins in early prostate cancer progression through IHC detection methods to visualize protein expression in human FFPE tissues. Immunohistochemistry assays utilizing antibodies specific for these receptors were developed to determine expression patterns associated with early PCa progression. The transformation of normal prostate glandular epithelium to neoplastic lesions initiates with changes to the microenvironment that include altered expression and function of the  $\alpha6\beta4$  and  $\alpha3\beta1$  integrin at the surface membrane of basal cells for most epithelia. The epithelium of normal glands consists of a contiguous layer of stable hemidesmosome structures accentuated by the expression of  $\alpha6\beta4$  ( $\beta4$  integrin) at the cell-ECM contact and  $\alpha3\beta1$  ( $\alpha3$  integrin) localized to the cell-ECM focal adhesion sites. In early transition of these normal glands an attenuation of the basal cell layer is observed along with the loss in polarization of  $\beta4$  integrin localized surface expression and subsequent loss of  $\alpha3$  integrin. These precursory lesions are called prostatic intraepithelial neoplasia (PIN) lesions and result in loss of homeostasis and are considered in situ carcinoma. In the progression from PIN lesions to high grade PIN (HGPIN) then onto aggressive PCa, the increasing loss of the  $\beta4$  and  $\alpha3$  integrin is demonstrated in most PCa tissues. The protocols utilizing IHC with 3, 3'-diaminobenzidine (DAB) were optimized for *in situ* detection of protein expression of the  $\beta4$  and  $\alpha3$  integrin epitopes in human prostate cancer tissues. Utilizing these

detection strategies, it is evident that the loss of  $\beta 4$  and  $\alpha 3$  integrin play a critical role leading to progression of invasive prostate cancer and with further understanding of mechanisms initiating this event that may lead to defining the factor specific for initiating the early transition to the aggressive phenotype.

## INTRODUCTION

The laminin binding integrins  $\alpha 6\beta 4$  and  $\alpha 3\beta 1$  are transmembrane surface proteins that are expressed in abundance on epithelial cells to facilitate adherence to the basement membrane. The laminin specificity for either of these integrins is laminin-332 (laminin-5) and laminin 511 (laminin 10) (Nishiuchi *et al.*, 2006). Although they display a common functionality as laminin-5 receptors, these integrins are recruited to distinctly separate structures for cellular adhesion (DiPersio *et al.*, 1997). The  $\beta 4$  integrin functions as a key factor in nucleation of hemidesmosomes to stabilize and anchor basal keratinocytes to the basement membrane in normal epithelia tissue. The  $\alpha 3$  integrin, although is also found within the basement membrane in human epithelia in various tissues, is primarily recruited to focal contacts of the keratinocytes and other cells and plays a role in facilitation of linking the ECM to components of the cytoskeleton (Carter *et al.*, 1990b; DiPersio *et al* 1995).

Historically, in the lifetime of the average male, what typically occurs within the normal prostate during the 3<sup>rd</sup> and 4<sup>th</sup> decade of life is an observed histological contextual change to the microenvironment that continues to increase with advancing age (A. Sakr *et al.*, 1996; Harryman *et al.*, 2019). The evidence of that transformation has begun within these glands is visualized with loss of basal cells

lining the glands leading to PIN lesions. PIN lesions are associated with focal loss of the normal morphological associations of the epithelium to the environment of the stroma (Bonkhoff and Remberger., 1995; Montironi *et al.*, 2002; Nagle and Cress., 2011). PIN lesions demonstrate sporadic basal cell presence and disordered layers of luminal cells with incomplete differentiation. Also, the nuclei become enlarged with prominent nucleoli and begin to demonstrate traits of loss of homeostasis with visual evidence of heterochromatic appearance and pleomorphic attributes (**Figure 2.1**). The loss of the normal basal cell component is a key factor initiating PIN that results in gaps in laminin-5 resulting in cellular exposure to a new environment of laminin-10 and growth factor enriched surrounding muscle stroma (Rosario and DiSimone., 2010; Harryman *et al.*, 2019). There has been a growing evidence that confirm PIN lesions are the pre-malignant stage (Bostwick., 1996; Bostwick *et al* 2004., Wang *et al.*, 2017). The continued genomic instability and loss of homeostatic environment of PIN lesions result in HGPIN lesions that are indicative of early invasive PCa development. HGPIN lesions are defined by increased loss or attenuation of the basal cell layer and ECM (Bostwick *et al* 2004., Wang *et al.*, 2017). HGPIN also displays proliferation of the glandular epithelial cells with increasing cytological atypia (Zhou., 2018). This chapter investigates the ability to detect the loss of surface expression of  $\beta 4$  integrin and  $\alpha 3$  integrin in progression from normal prostate glandular epithelium in human prostate tissue that are associated with progression to invasive PCa.



**Figure 2.1. High-grade intraepithelial neoplasia (HGPIN).** Hematoxylin and eosin stained image of HGPIN showing large heterochromatic nuclei (black arrow), and prominent nucleoli (white arrow). (Reprinted with permission of MedReviews®, LLC. Bostwick DG, *et al*. High-grade prostatic intraepithelial neoplasia. *Rev Urol.* 2004; 6:171–179. All rights reserved).

*$\alpha 6 \beta 4$  Integrin.* Normal human prostate glands exhibit an ordered layer of basal cells with continuous surface expression of  $\beta 4$  integrin that is necessary to anchor basal cells via laminin-5 present in the ECM to hemidesmosomes to stabilize the adhesion (Nagle *et al* 1995., Wang *et al* 2017). HGPIN lesions have a discontinuous layer of  $\beta 4$  integrin because of the attenuation of basal cell attachment to the basal lamina. The discontinuous layer of  $\beta 4$  integrin is also indicative of laminin-5 loss of expression. The loss in laminin-5 results in gaps in



the defective basal layer which promotes cellular budding and migration of dedifferentiated cell clusters. These gaps also give rise to exposure to laminin-10 expressed in the muscle stroma, contributing to tumor escape and dissemination via  $\alpha 6$  integrin. These results demonstrate the loss of  $\beta 4$  integrin is involved in the initial steps of tumor progression.

*$\alpha 3\beta 1$  Integrin.* Similar to  $\beta 4$  integrin,  $\alpha 3$  integrin also demonstrates an abundant cell surface expression on normal cells in the basement membrane of normal prostate glandular epithelium. The  $\alpha 3$  integrin has also been described as a weak receptor for other ECM proteins such as fibronectin, collagen, laminin-1, thrombospondin and nodogen (DiPersio *et al.*, 1995, DiPersio *et al.*, 1997). Although  $\alpha 3$  integrin exhibits overlapping functions with laminin-5 similar to  $\beta 4$  integrin,  $\alpha 3$  integrin is suggested to demonstrate a post-adhesion role in basement membrane integrity (DiPersio *et al.*, 1997). It is also suggested that  $\alpha 3$  integrin may be required to maintain strength and integrity of the basement membrane independently of initial assembly of the receptor (DiPersio *et al.*, 1997). This strengthens the narrative that  $\alpha 3$  integrin can act as a negative regulator of motility, which studies utilizing  $\alpha 3$  null keratinocytes showed enhanced migration in vitro and faster wound healing (Margadant *et al.*, 2009; Stipp ., 2010).

One particular mechanism in which  $\alpha 3$  integrin maintains strength and membrane integrity is by transduction of signals through Abl kinase family to restrain Rho GTPase activity (**Figure 2.2**). This restraint supports the activation of the Hippo pathway suppressor function of inhibiting proto-oncogenic transcriptional

activators YAP/TAZ, in turn restraining a transition to prostate cancers with anchor-independent growth, migratory and invasive capabilities (Varzavand *et al.*, 2016). The Hippo pathway has been shown to regulate extracellular inputs such as cellular adhesion, cellular detachment, cell-cell contact and growth factor signaling from cell receptor-ECM association (Johnson and Hadler., 2014; Piccolo *et al.*, 2014; Yu *et al.*, 2015; Varzavand *et al.*, 2016). It is also noted that the Hippo pathway is influenced by cell adhesion. In addition, the adherens junction homodimer E-cadherin, was identified as one of the few adhesion receptors with upstream inputs to influence the pathway. Varzavand *et al.* 2016 presented evidence that  $\alpha 3$  integrin can also be included as one of those influential receptors.

Interestingly, separate studies using HT-29 and CaCo-2 colon adenocarcinoma cells showed that  $\alpha 3$  integrin adhesion to laminin-5 promoted E-cadherin localization to cell-cell adherens junctions (Schreider *et al.*, 2002; Chartier *et al.*, 2006). This particular function is believed to be the result of collaborative signaling of  $\alpha 3$  integrin and laminin-5 with E-cadherin to induce stabilized cell-cell adhesion complexes. This signaling reduces the downstream activity of Rho-GTPase and the induction of effectors such as Rho-associated kinase (ROCK) and Diaphanous related formin (mDia). These effectors initiate cellular migration. It should be noted that Rho activity is required for cell-cell adhesion but is tightly regulated since increased levels of Rho cause a disruption in cell-cell adhesions (Zhong *et al.*, 1997).

Other groups providing evidence that signaling from  $\alpha 3$  integrin ligated to laminin-5 inactivates RhoA. However, they demonstrated that this activity in squamous cells promoted migration and invasion through upregulated Cdc42/Pak1 activity whereas collagen bound  $\alpha 2\beta 1$  integrin strongly activated RhoA enhancing focal contact formation and impeding migration (Zhou *et al.*, 2005). These results contrasted with the work by Nguyen *et al.*, 2001 that showed  $\alpha 3$  integrin ligation to laminin-5 would activate RhoA-dependent adhesion of human foreskin keratinocytes. These results, compared to results of our studies and various others, indicate that there is a clear difference in responses depending on the specific cell type utilized in testing models and type of integrin receptor ligation elicited.

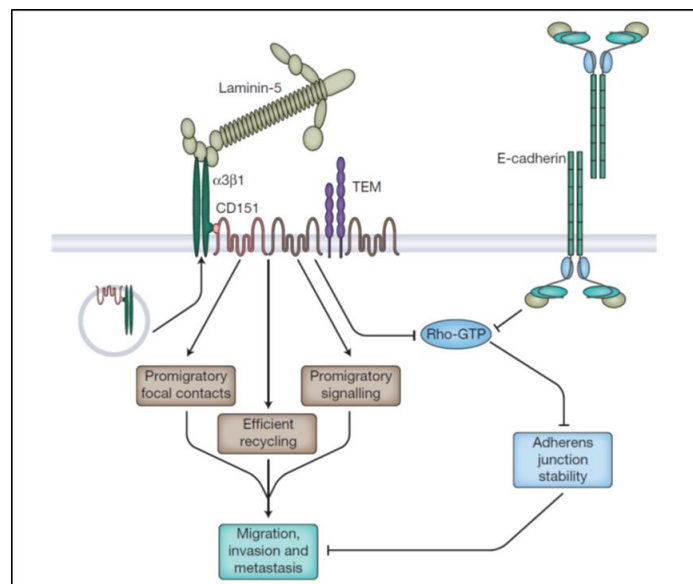


**Figure 2.2. The  $\alpha 3$  Integrin cooperative signaling with E-cadherin.** The  $\alpha 3$  integrin associated with tetraspanin CD151 allows collaboration with E-cadherin to inhibit activity of Rho-GTPases that may elicit anti-migratory activity counteracting the  $\alpha 3$  integrin promigratory function (Adapted from Stipp, 2010).

## RESULTS

*Loss of  $\alpha6\beta4$  in PCa Progression.* A rat anti-human antibody (BD Pharmingen) specific for the  $\beta4$  integrin subunit was initially formulated for immunostaining on FFPE human prostate tissue at a 1:100 dilution in several antibody diluents to test for specificity and non-specific immunostaining of endogenous proteins and structures. An immunostaining protocol was prepared for the Ventana Benchmark ULTRA platform (Benchmark ULTRA) utilizing high temperature (72°C) deparaffinization (de-waxing) step, a heat induced epitope retrieval (HIER) step at 95°C and antibody incubation time of 60 minutes at 36°C. The detection kit used was a modified Ventana *ultraView* Universal DAB Detection kit (uV Detection) with a substitution of the (mouse) Universal Multimer linker dispenser with a DISCOVERY rat anti-human Ultramap HRP multimer. De-identified prostate tissue samples were sequentially sectioned and an H&E stained slide prepared from the initial sectioning for evaluation by a board-certified pathologist for normal and tumor histological content. The execution of the protocol resulted in selection of the optimal results in  $\beta4$  integrin immunostaining with the 1:100 dilution in Tris HCL buffer with Brij-35. Membrane localization of the  $\beta4$  integrin was observed in normal prostate basal cells. Furthermore, as expected, positive immunostaining was observed in endothelial cells of vessels and on the peripheral nerves (**Figure 2.3, A and D**). Also, the loss of a continuous layer of  $\beta4$  integrin expression in the basal lamina is indicative of early transformation to an invasive PCa in human prostate tissue. The loss of basal cells was evident in tissues containing pre-malignant PIN lesions that demonstrated increased proliferation of staggered

patterns of luminal cells, enlarged nuclei and nucleoli in clusters of cells budding through gaps in the discontinuous layer (**Figure 2.3, B and E**). The results also demonstrate the loss of  $\beta 4$  integrin in cohesive tumor collectives invading perineural spaces (via PNI) surrounding laminin coated myelinated nerves that exhibited positive  $\beta 4$  integrin expression (**Figure 2.3, C and F**). This optimized procedure allowed for the demonstration of membrane specific localization of the  $\beta 4$  integrin within each tissue sample and for reproducibility across multiple sampling sizes.

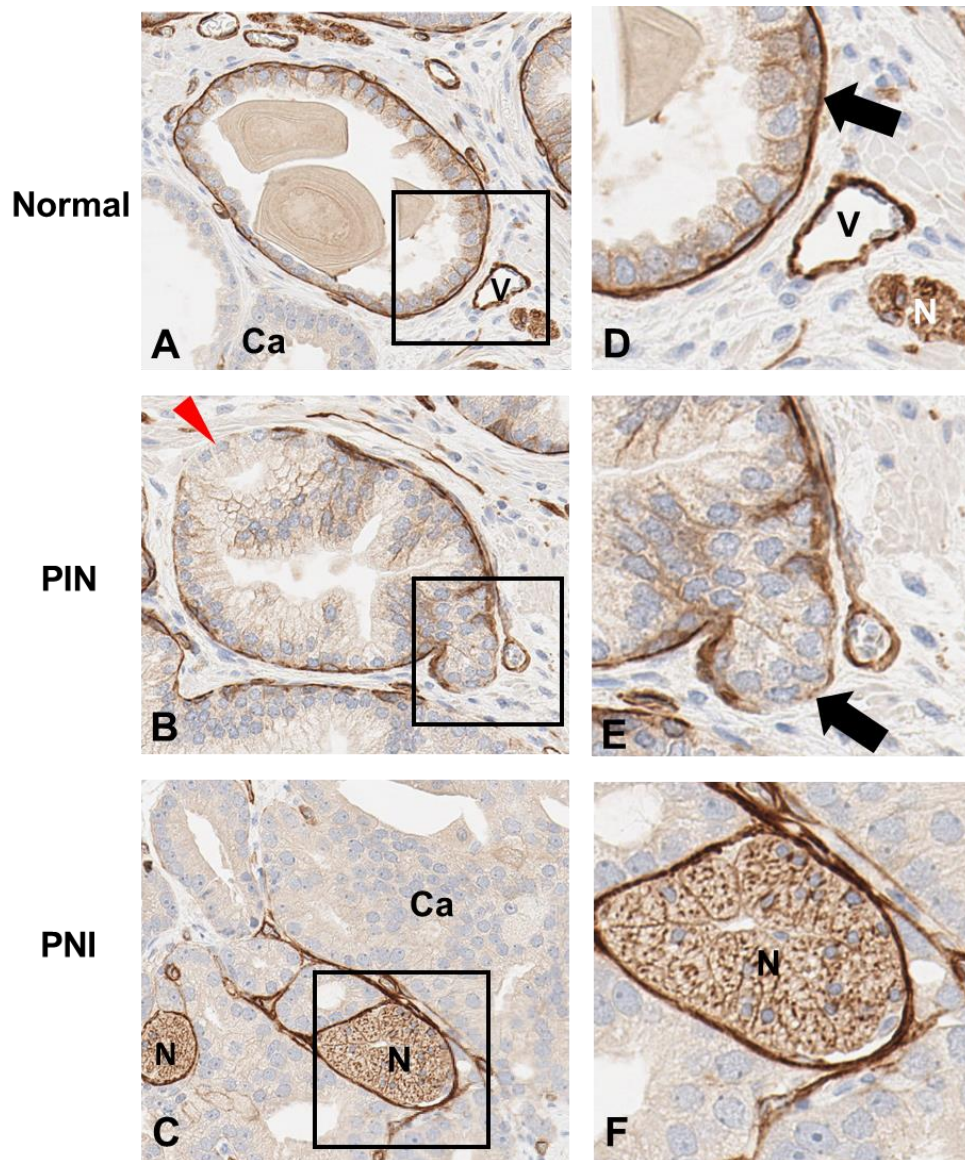


**Figure 2.3.  $\beta 4$  Integrin expression is deregulated in human prostate cancer progression.**

Images **A-C** are 20x magnification. **(A)** De-identified FFPE prostate tissue resection IHC stained with anti- $\beta 4$  antibody exhibits continuous basal expression in normal gland bordered by cancer (Ca) lacking expression. **(B)** HGPIN lesion depicted demonstrating discontinuous expression of  $\alpha 6\beta 4$  integrin in attenuated basal cell layer (red arrowhead). **(C)** Lack of anti- $\beta 4$  intensity in cancer (Ca) region of PNI. **(D-F)** Enlarged views of the indicated fields at 40x. **(D)** Positive controls Vessels (V) and nerves (white N) in normal glands, **(E)** cellular cluster budding through layer absent of  $\beta 4$  integrin, **(F)** Tumor demonstrates negative immunostaining for anti- $\beta 4$  surrounding nerve (N) that is positive for  $\beta 4$  integrin expression.

*Loss of  $\alpha 3\beta 1$  integrin in PCa progression.* To demonstrate the expression of  $\alpha 3$  integrin in human FFPE prostate tissue samples, the rabbit polyclonal antibody (clone HPA008572) specific for the transmembrane domain was used. After optimizing the antibody formulation similar to  $\beta 4$  integrin testing, a 1:200 dilution of the anti- $\alpha 3$  integrin antibody utilized in IHC testing on human prostate FFPE. The results revealed immunostaining localized to areas similar to  $\beta 4$  integrin in the basal cells of normal prostate glands (**Figure 2.4, A and D**). As expected, the loss of  $\alpha 3$  integrin expression was evident in pre-malignant PIN lesions in a similar fashion to  $\beta 4$  integrin (**Figure 2.4, B and E**). Although, previous work distinguished three prostate tumor phenotypes based on integrin expression. Type I co-expressing  $\alpha 6$  and  $\alpha 3$  integrins, type II expressing only  $\alpha 6$  integrin and type III expressing  $\alpha 3$  integrin only (Schmelz *et al.*, 2002). Since the  $\alpha 3$  integrin was not observed in the tissue samples containing primary tumors, this may indicate that these tumors were of the type II phenotype observed in Schmelz *et al.*, 2002. Also, it was noted that the  $\alpha 3$  integrin expression was absent in endothelial cells of vessels and was not expressed in peripheral nerves or prostate tumor cells invading the peripheral nerve space via PNI (**Figure 2.4, C and F**).

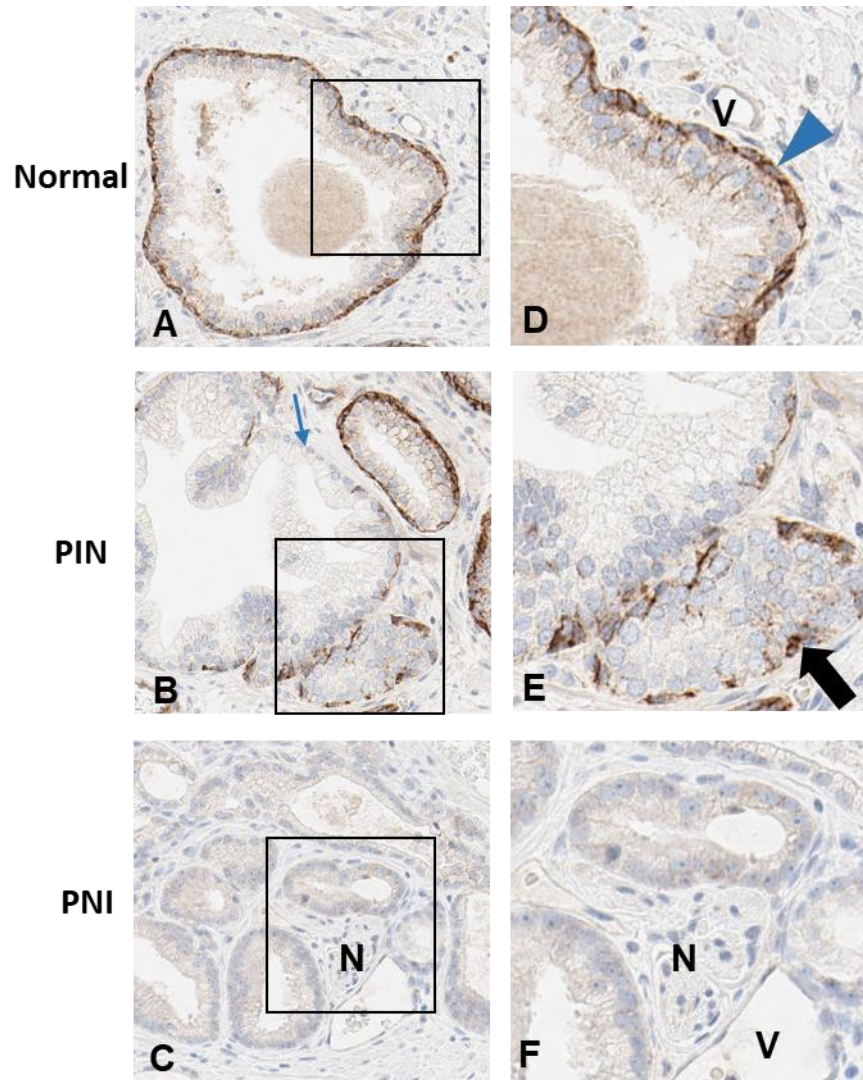


**Figure 2.4.  $\alpha 3$  integrin expression is lost in prostate cancer progression.** Images **A-C** are 20x Magnification. **(A)** De-identified prostate FFPE tissue sample slides immunostained with anti- $\alpha 3$  antibody demonstrating continuous basal cell expression in normal prostate gland. **(B)** An observed pre-malignant PIN lesion with discontinuous  $\alpha 3$  integrin expression (blue arrow). **(C)** Lack of  $\alpha 3$  integrin expression exhibited in peripheral nerves of prostate, endothelial cells of vessels and tumor cells within PNI. **(D-F)**. Enlarged views of indicated fields are 40x. **(D)** Normal glands with intact basal cell layer positive for  $\alpha 3$  integrin (blue arrowhead). **(E)** Evidence of tumor cluster budding through discontinuous layer of  $\alpha 3$  integrin (black arrow). **(F)** Nerves (N) and vessels (V) lack  $\alpha 3$  integrin expression.



## DISCUSSION

The loss of  $\beta 4$  and  $\alpha 3$  integrin expression in the normal cells of the basal cell layer in human prostate tissues indicate a clinically relevant event in which loss in homeostasis, impaired cell-ECM adhesion and attenuation of critical ECM proteins result in destabilization of epithelial morphology. This hallmarks the transition from normal to pre-malignant architecture. We investigated the expression patterns of these protein biomarkers utilizing antibodies in de-identified patient prostate tissue samples to determine if the downregulation of these biomarkers could be detected. Our results demonstrate that the specificity and sensitivity of these antibodies for *in situ* detection, in patient samples, could translate into a potent tool necessary for accurate diagnostic and predictive indicators of early invasive phenotypes. Because our lab (and others) have previously assessed how the loss of each of these integrin receptors impact the cellular adhesion to critical ECM components in mice (Raymond *et al.*, 2004) and facilitates invasion via cord networks in model systems of 3D Matrigel, it was prudent that the expression levels were determined in human clinical samples.

Studies showed that highly invasive subpopulations of PCa were selected by the decrease in  $\beta 4$  and  $\alpha 3$  integrin expression leading to the propensity of metastatic invasion (Dedhar *et al.*, 1993). Although, it has been stated that the relationship of  $\alpha 3$  integrin expression in PCa is complex because heterogeneous nature of the tumors result in several phenotypes that display either positive or negative expression of  $\alpha 3$  integrin (Schemlitz *et al.*, 2002). The scientific community often

disagrees on the specific role that  $\alpha 3$  integrin expression plays in the progression or inhibition of PCa. Some groups have suggested  $\alpha 3$  integrin induces migration (Nguyen *et al.*, 2001; Stipp., 2010, Zhou *et al.*, 2014). Other groups have demonstrated shown that  $\alpha 3$  integrin inhibits migration (Kim *et al.*, 1992; Varzavand *et al.*, 2013., Varzavand *et al.*, 2016; Ramovs *et al.*, 2019).

Our lab has was postulated that the loss of  $\alpha 3$  integrin would promote a migratory phenotype in prostate cancer by increasing  $\alpha 6$  integrin internalization. In order to test this hypothesis, an *in vitro* model interrogating gene edited DU145 cell lines in SCID xenografts was used as the working model. For the testing, the cells used were DU145 WT, DU145 cells transfected with a small interference RNA (siRNA) to knockdown (KD)  $\alpha 3$  integrin (si $\alpha 3$ ) expression and DU145 cells transfected with siRNA to knockdown  $\alpha 6$  integrin (si $\alpha 6$ ). This working model showed the loss of  $\alpha 3$  integrin increased  $\alpha 6$  integrin internalization rates and accumulation to Rab4 early endosome antigen 1 (EEA1) containing vesicles. This ultimately promoted recycling the  $\alpha 6$  integrin to cell-cell lateral membranes increasing tumor cell migration by 1.8-fold (Das *et al.*, 2017 unpublished). The increase in fold migration was dependent upon the  $\alpha 6$  integrin function and cleavage regulated by uPAR.

### III. $\alpha 6$ integrin and uPAR co-distribution in early aggressive PCa

#### ABSTRACT

This chapter describes the co-distribution of  $\alpha 6$  integrin and uPAR in progression from normal prostate cells to invasive and metastatic prostate cancer. Metastatic cancer is a progressive cascade in which the invasion beyond primary tumor to colonize distant tissue occurs. The progression to metastatic disease is regulated by mechanisms that involve the change in the adhesive properties of  $\alpha 6$  integrin due to modification regulated by uPAR. The co-distribution of these proteins initiates a phenotypic switch from non-malignant to aggressive and invasive tumors by co-opting a mechanism that is traditionally reserved for events in early embryogenesis. These include embryonic tissue and organ development, response to foreign agents, and tissue repair. This has been found to be an aberrant event that leads to aggressive tumors. An IHC detection assay was developed utilizing antibodies targeting the laminin binding N-terminal domain of the  $\alpha 6$  integrin and the uPAR. The purpose was to characterize the expression of each of these target epitopes in human FFPE prostate tissue to further develop a chromogen multiplex assay with the potential of identifying a quantifiable signature for early invasion. The results indicated that the co-distribution of these two biomarkers can be detected and is linked with tumor grade and invasiveness.

## INTRODUCTION

Previous studies have demonstrated that during progression from normal prostate glands to perineural intraepithelial neoplasia (PIN), an attenuation of basal cells combined with the loss of  $\alpha 6\beta 4$  occurs along with gaps in LMN 5 deposition leading to the exposure of LMN 10 in the muscle stroma (Nagle *et al* 1995., Davis *et al.*, 2001., Nagle and Cress., 2011., Wang *et al.*, 2017). This exposure of LMN 10 (laminin 511) is significant since laminin 511 is the most preferred ligand for laminin binding integrins and has the highest affinity, as determined by dissociation constants, for  $\alpha 6\beta 1$  integrin (Nishiuchi *et al.*, 2006). The increased exposure of LMN 10 enhances the association of  $\alpha 6\beta 1$  integrin with both the urokinase plasminogen activator (uPA) and its receptor (uPAR, CD87). The attenuation of the basal lamina and loss of laminin expression are both hallmarks of progressive prostate disease and coincide with the attenuation of  $\alpha 6\beta 4$ . The  $\alpha 6$  and  $\alpha 3$  integrins are stated to be expressed in 80% of prostate cancers (PCa) with ~26% exhibiting loss of  $\alpha 3$  and increased expression of  $\alpha 6$  (Schmelz *et al.*, 2002). Both of these LBIs are considered to be crucial factors in cohesive prostate cancer migration and invasion. However, due the heterogenous nature of PCa the expression of  $\alpha 6$  and/or  $\alpha 3$  is phenotypically dependent. Incidentally, recent studies suggest that  $\alpha 3$  integrin inhibits progression to aggressive PCa via transduced signals to the Abl kinase-Hippo tumor suppressor pathway to restrain Rho GTPase activity and inhibit activity of YAP/TAZ cell proliferation transcription factors (Varzavand *et al.*, 2016). The reduction in  $\alpha 3$  integrin in promotion of aggressive disease, as also

shown by Ramovs *et al.*, 2019 in the Her2 driven breast cancer, shows the importance of  $\alpha 3$  integrin loss in the initiation and progression of various types of aggressive cancers.

A switch to a more dynamic “quick-release” adhesion event occurs through the interaction of the  $\alpha 6$  integrin and uPA which generates a tumor specific post translational modification (PTM) producing a variant of  $\alpha 6\beta 1$  called  $\alpha 6p\beta 1$ , lacking the laminin binding domain. The variant is produced on the tumor cell surface by PTM (cleavage) action of the uPA. The interaction is postulated to be a result of redistribution of  $\alpha 6$  integrin to uPAR due to the loss of  $\alpha 3$  integrin. The uPAR was shown to preferentially complex with  $\alpha 3$  integrin in previous studies (Wei *et al.*, 2001). The uPAR was also shown to be increased in aggressive tumors, including prostate cancer (Miyake *et al.*, 1999; Usher *et al.*, 2005). Thus, the loss of  $\alpha 3$  integrin not only increases  $\alpha 6$  integrin surface expression (Das *et al.*, 2017) but is postulated to result in increased interaction of  $\alpha 6$  integrin with uPAR and increased production of the tumor variant in aggressive tumors. uPA is initially secreted in zymogen form (pro-uPA) that binds to uPAR and is then cleaved by plasminogen to its active single chain form. This interaction results in increased production of the  $\alpha 6p$  integrin variant due to uPA cleavage culminating into aggressive prostate cancer (**Figure 3.1**). This mechanism is responsible for the permissive migration within the ECM and within and around the laminin rich peripheral nerves. This has also been reported in the promotion of HER-2 driven breast cancer in vivo (Ramovs *et al.*, 2019).

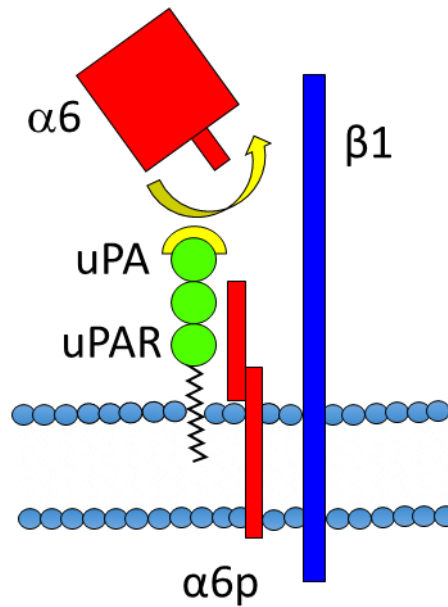


**Figure 3.1. uPAR regulates cleavage of  $\alpha 6$  integrin to  $\alpha 6p$ .** Schematic representation of posttranslational modification of integrin  $\alpha 6$  by proteolytic activity of uPA bound to uPAR.

In addition to association of  $\alpha 6$  integrin with uPAR (Wei *et al.*, 2001; Kacsinta *et al.*, 2014), it has been reported that  $\alpha 6$  integrin complexes with E-cadherin in metastatic liver disease (Marchio *et al.*, 2012). E-cadherin and integrin crosstalk is a crucial factor in invasion and metastasis in various types of cancers (Marchio *et al.*, 2012; Canel *et al.*, 2013; Weber *et al.*, 2011; Mui *et al.*, 2016). This cross talk between integrins and E-cadherin mediates the dynamic interplay that contributes to the plasticity of tumor cells in response to environmental cues and allows effective migration (Canel *et al.*, 2013). This plasticity is necessary for intact and functional cell-cell adhesion of these tumors to migrate through the muscle. Some of the reported modes of tumor migration are single cell, chords, sheets and as a cohesive collective. Collective migration of cohesive cells is a mechanism that is utilized in developmental events and embryogenesis (Llense and Martin-Blanco.,

2008; Friedl and Gilmour., 2009). E-cadherin and  $\alpha 6$  are co-distributed intermittently within these cohesive tumor collectives. The expression of this complex is found on the lateral cell-cell associations within the migrating tumor clusters and is believed that integrin signaling may have a significant role in the destabilization of E-cadherin-mediated adhesion complexes (Giehl and Menke., 2008). This loosening of the adhesive cell-cell association is sufficient to permit collective migration and invasion (Canel *et al.*, 2013). In prostate cancer, a major sign of disease progression is capsular escape of these groups via PNI or Endoneural invasion (ENI) (**Figure 3.2**). These cohesive groups surround the nerve (PNI) or invade into nerves (Harryman *et al.*, 2016). Once these cohesive tumors have escaped via the nerves, this is called extracapsular extension (ECE). ECE, is associated with an increased risk of biochemical recurrence, distant metastases and lower prostate cancer-specific survival (Fleshner *et al.*, 2016; Grignon *et al.*, 2018). Since migration, invasion and colonization of distant tissues is likely to depend upon integrins as stated by Goel *et al.*, 2008 (reviewed in Fornaro *et al.*, 2001 and Felding-Habermann., 2003), mitigating aberrant integrin functionality may be critical for inhibiting extracapsular escape.

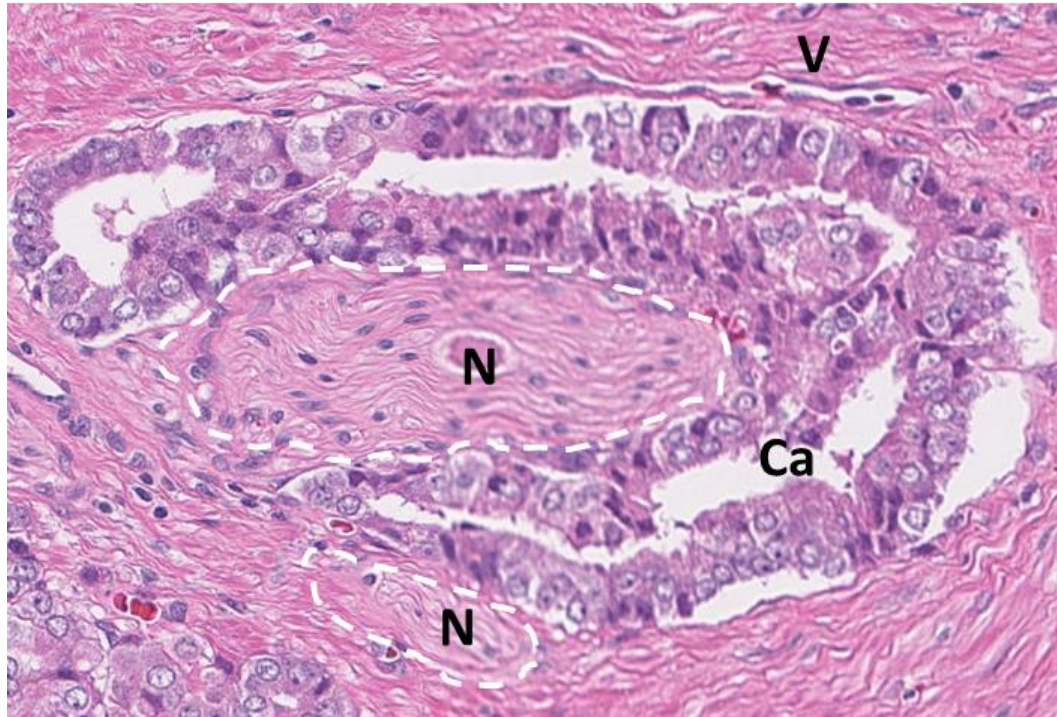


**Figure 3.2. Aggressive prostate tumors invade within peripheral nerves.** H&E image of FFPE human prostate tissue perineural invasion (PNI) of cohesive cancer cell cluster (**Ca**) invading in and nerves (**N**, annotated dashed lines) and nerve tissue containing vessels (**V**). [Magnification image 40x]

## RESULTS

*IHC detection of  $\alpha 6$  integrin and uPAR in Human PCa tissue.* The rabbit polyclonal antibody, anti- $\alpha 6$  (AA6NT), recognizes the full-length  $\alpha 6$  integrin and targets the laminin binding extracellular domain. This antibody also recognizes the cleaved N-terminal fragment of the  $\alpha 6$  remaining attached to laminin the ECM. The mouse monoclonal antibody (ADG3937) recognizes the receptor for urokinase plasminogen activator. The AA6NT was optimized at a 1:800 titration in Tris HCL diluent with Brij-35. The protocol for  $\alpha 6$  integrin detection was executed with a 64-minute heat induced epitope retrieval (HIER) at 100°C and antibody incubation time of 24-minutes at 36°C. This protocol resulted in the detection of the  $\alpha 6$  integrin



expression in the membrane of basal cells in glands of normal prostate tissues (**Figure 3.3, A**). In contrast, the uPAR exhibited an apical cytoplasmic expression localized in the luminal cells of normal prostate glands (**Figure 3.3, B**). The AA6NT also displayed membranous basal lateral expression in HGPIN lesions and primary tumors and membranous and/or cytoplasmic expression in higher-grade tumors in FFPE PCa tissues.

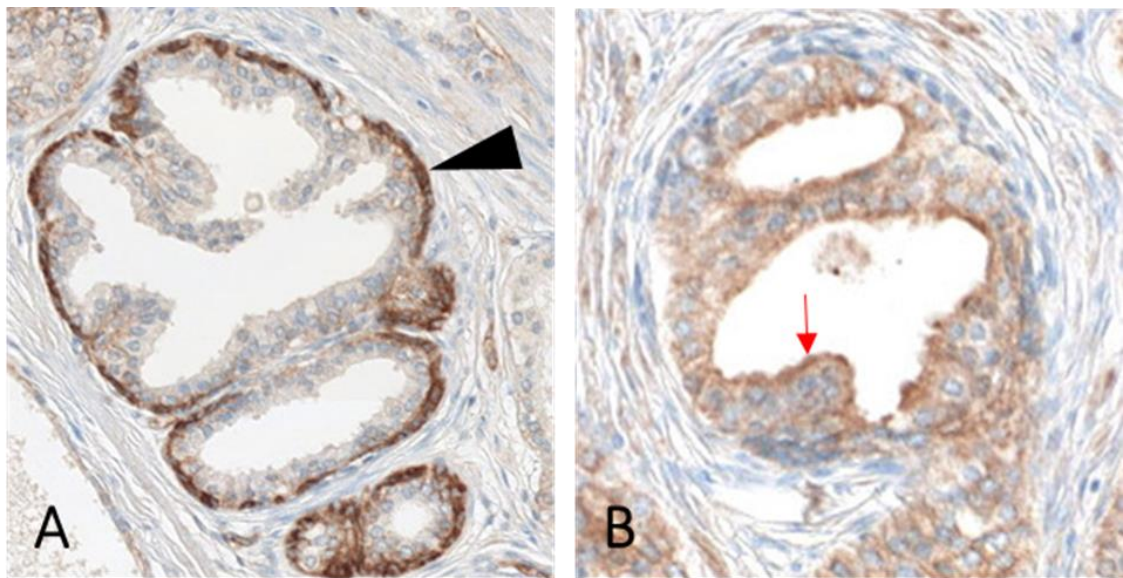


**Figure 3.3.  $\alpha 6$  integrin and uPAR expression localization in normal prostate glands in FFPE tissue.** (A) IHC DAB immunostaining using anti- $\alpha 6$  antibody demonstrates the expression of  $\alpha 6$  integrin in basal cells of normal epithelial glands (black arrowhead). (B) Immunostaining with anti-uPAR antibody demonstrates the expression of uPAR in apical regions of luminal cells in normal gland (red arrow). [Magnification images, 40x]

*Dual Chromogen IHC of  $\alpha 6$  integrin and uPAR reveal co-distribution:* Serial sections were prepared from de-identified human prostate tissue samples blocks. H&E stained slides were prepared from the first sample slide in the series. A board certified pathologist evaluated the H&E stained slides for normal glandular structures, tumor composition and specific Gleason grades. Samples selected for

testing contained normal prostate glands, Gleason grade 3+3 primary tumor and Gleason 4+4 tumor (**Figure 3.4, A**). We performed a dual chromogen IHC immunostaining using the anti- $\alpha 6$  and anti-uPAR specific antibodies. The normal prostate glands demonstrated polarized  $\alpha 6$  integrin expression with chromogen detection (teal) in the basal cell layers in comparison to the apical localization of uPAR detected chromogen (yellow) in luminal cells, as expected (**Figure 3.4, B**). In the Gleason 3+3 sample, the loss of the basal layer (evident by the loss of  $\alpha 6$  integrin expression) was observed and expression of the  $\alpha 6$  integrin associated with uPAR exhibited a co-associative chromogen mix (teal + yellow = green). The absence of the  $\alpha 6$  integrin was observed in the Gleason 4+4 sample suggesting the laminin binding domain was not available for antibody detection. However, the uPAR expression remained evident. This may suggest the cleavage product ( $\alpha 6p$ ) could be the prevalent form in aggressive high-grade tumors which may account for the invasive potential.

An image-merge was performed to compare the amount of  $\alpha 6$  integrin and uPAR co-distribution within the regions of interest (**Figure 3.4, C**). The merge revealed little to no co-distribution of  $\alpha 6$  integrin and uPAR in normal glands but an increase in co-distribution was demonstrated with the image merge of the Gleason 3+3 primary tumor region (**Figure 3.4, D**). This result suggests the initiation of PTM of the laminin binding region of the full-length  $\alpha 6$  integrin and a phenotypic switch to a more mobile tumor.

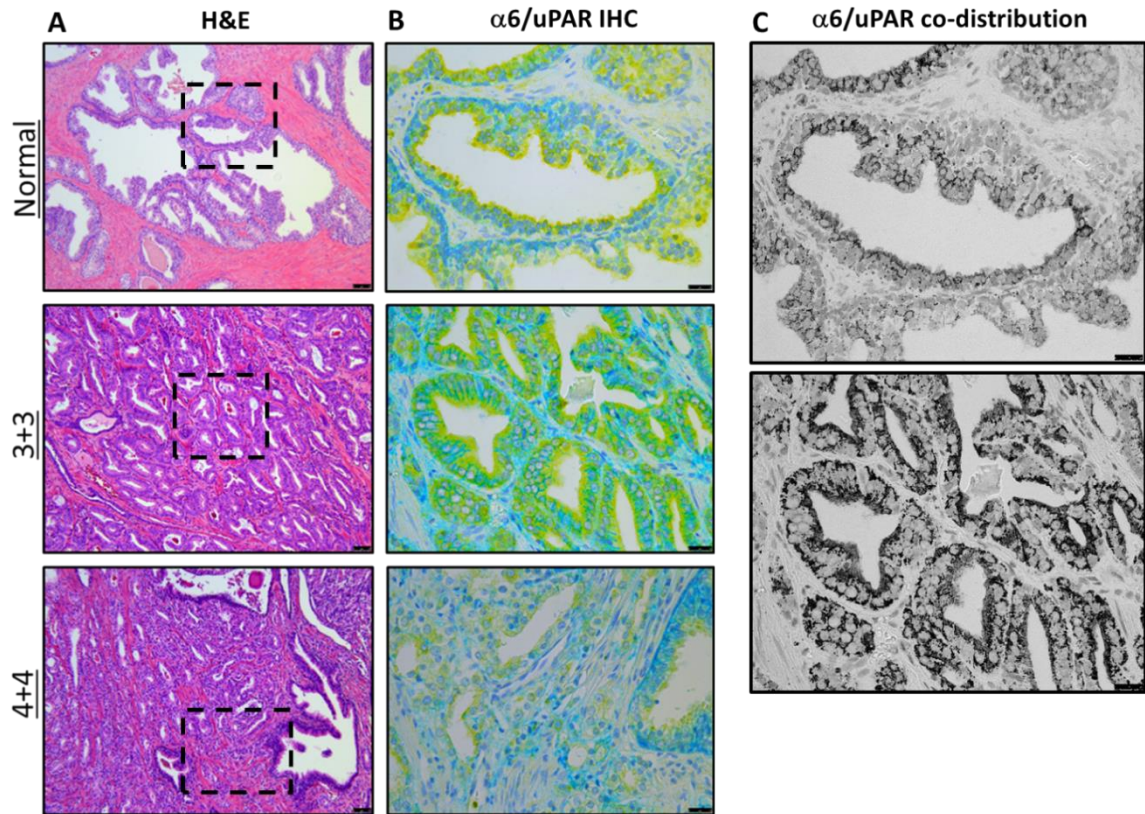


**Figure 3.4. Multiplex IHC detection of  $\alpha 6$  integrin N-terminal domain and uPAR co-distribution in human prostate tissue.** Columns (A-B) Depicting architecture of human prostate in FFPE. (A) H&E stained slides of prostate tissue stages of Normal, Gleason 3+3 (low-grade tumor) and Gleason 4+4 (high-grade tumor). (B) Dual chromogen IHC using anti- $\alpha 6$  and anti-uPAR antibodies. Normal demonstrates  $\alpha 6$  integrin N-terminal polarized localization in basal layer (blue) as expected and uPAR expression in luminal region (yellow). Low-grade tumor (3+3) displays loss of basal polarity of  $\alpha 6$  integrin and intracellular localization demonstrating chromogen co-distribution color (green) in with association uPAR. High-grade tumor (4+4) exhibits loss of  $\alpha 6$  integrin N-terminal domain expression in tumor region and retention of uPAR luminal expression with comparative adjacent normal gland retaining  $\alpha 6$  integrin expression in basal region. (C) Single channel merged images of normal and low-grade tumor image (Panel B) depicting co-distribution of  $\alpha 6$  integrin N-terminal domain and uPAR. [Scale bars, 25 $\mu$ m]

## DISCUSSION

Integrins are considered key uPAR signaling co-receptors that have an intricate association that is critical for normal early processes such as tissue remodeling, organ development and wound repair (Smith and Marshall., 2010). Integrins mediate cell-ECM adhesion and regulate the signaling pathways that control cell proliferation, differentiation and ECM remodeling (Smith and Marshall., 2010). The uPAR is a key regulator of coordinated ECM proteolysis, cell-ECM interactions and cell signaling (Smith and Marshall., 2010). In addition, uPAR regulates the activity of the plasminogen activation system and proteolysis of a range of components of the ECM (Smith and Marshall., 2010). The uPAR association with uPA activates the plasmin proteolytic function of the plasminogen which reciprocally activates the uPA-uPAR axis. This activation of plasminogen activity by bound uPA-uPAR facilitates pericellular proteolysis directing cellular migration through the ECM (Smith and Marshall., 2010). Together,  $\alpha 6$  integrin regulation of signaling pathways for cell-ECM adhesion and cellular migration and uPAR regulation of ECM remodeling are postulated to create the condition for invasive tumor dissemination.

During the progression from normal prostate to aggressive and invasive prostate tumors, the increased surface expression of  $\alpha 6$  integrin and uPAR results in subsequent co-distribution (as seen in Gleason 3+3 sample in **Figure 3.4, B**). The co-distribution may result in a PTM event that produces a tumor specific variant ( $\alpha 6p$ ), as detected by loss of the N-terminal epitope of  $\alpha 6$  integrin in higher grade tumor. Previous work has shown that loss of the N-terminal epitope is the same

as loss of the laminin binding domain of the receptor (Davis *et al.*, 2001; Demetriou *et al.*, 2004). Since the ligand binding domains of both the  $\alpha$  and  $\beta$  subunits of integrins are required for activation (Hynes., 2002), it is expected that the PTM would result in aberrant cell signaling that drives progression signifying a specific switch from confined primary tumor to aggressive and invasive phenotype. Utilizing an antibody specific for  $\alpha 6$  integrin detection in human prostate tissues demonstrates  $\alpha 6$  integrin is expressed in a uniform polarized basolateral expression in basal cells in normal prostate epithelia. The immunodetection of uPAR using a specific antibody demonstrates an apical expression within luminal cells in normal prostate glands. It remains to be determined if the conversion of low grade (indolent) to high grade (aggressive) lesions is accompanied by a conversion of  $\alpha 6$  integrin (N-terminal domain):uPAR complexes to loss of the N-terminal  $\alpha 6$  integrin membrane signal. Loss of the N-terminal ligand binding domain from the tumor cell surface is expected to mark aggressive disease since recent experimental systems using gene editing have shown preventing the PTM will prevent aggressive disease (Rubenstein *et al.*, 2019).

#### IV. $\alpha 6$ integrin and E-cadherin co-distribution in early aggressive PCa

##### ABSTRACT

As the focal point of tumor cell dissemination shifts towards cohesive invasion, the discussion involving the role of cellular adhesions and crosstalk between integrin and cadherin-mediated adhesions has intensified. The current chapter characterizes how the co-distribution of  $\alpha 6$  integrin and E-cadherin is involved with early PCa progression and how their association shows potential for indication of tumor stage. Individual IHC DAB assays were developed to investigate protein distribution and modulation in prostate progression. In FFPE prostate tissues containing various stages of prostate cancers, IHC assay showed localization of  $\alpha 6$  integrin lateral (cell-cell) and intracellular (cytoplasmic) expression within tumor regions and demonstrated co-distributive expression with E-cadherin. Deletion of  $\alpha 3$  integrin in aggressive tumor model resulted in downregulation of the E-cadherin protein, which correlated with low membrane expression of tumor cells. In addition, the deletion of  $\alpha 3$  integrin resulted in production of the tumor specific variant  $\alpha 6p$ , as expected, indicating a role of PTM in  $\alpha 6$  integrin expression with the loss of  $\alpha 3$  integrin. The inhibition of  $\alpha 6$  integrin PTM resulted in a 1.8-fold increase in E-cadherin protein density in tumor cells, in conjunction with inhibiting production of  $\alpha 6p$ .

These results indicate that coordination between  $\alpha 3$  and  $\alpha 6$  integrin expression exists and that deletion of  $\alpha 3$  integrin, in aggressive tumor model, correlates with  $\alpha 6p$  production. Reduction in  $\alpha 3$  integrin protein expression in a migratory tumor

phenotype model also identified a role the reduction of E-cadherin plays in tumor progression. A co-distribution of  $\alpha 6$  integrin and E-cadherin was also observed in aggressive FFPE tumors in tissue with IHC detection. A coordination between  $\alpha 6$  integrin and E-cadherin was demonstrated by upregulation of E-cadherin protein during  $\alpha 6$  integrin PTM inhibition in an aggressive tumor model. This upregulation of E-cadherin increased tumor cell-cell adhesive clustering and may decrease migratory potential. A loss in E-cadherin can promote invasive and metastatic behavior in epithelial tumors (Birchmeier and Behrens., 1994). These data suggest phenotype switch to non-migratory phenotype via E-cadherin positive pathway activation.

## **INTRODUCTION**

Early prostate tumor progression from confined to an invasive tumor phenotype employs dynamic cell-cell and cell-ECM interactions for migration through the surrounding environment and for dissemination to distant tissue environments. This is associated with a coordinated modulation of E-cadherin mediated cell-cell adherens junctions and integrin-mediated focal adhesions that are in contact with the ECM (Canel *et al.*, 2013).

E-cadherin is a calcium dependent transmembrane glycoprotein that is a crucial component of the adherens junctions, which is a structure that is necessary for the adhesive interactions of adjacent cells and the stability of the epithelium (Cousin *et al.*, 2017). The extracellular domain of E-cadherin (and all cadherins) is

important for cell-cell adhesion due to a conserved tryptophan residue (Trp2) in the extracellular domain that forms a side chain that docks to a hydrophobic pocket in the extracellular domain of the partner cadherin (Huang *et al.*, 2016). The extracellular domain contains five 100 amino acid sequence tandem repeats (E1-E5) with  $\text{Ca}^{2+}$  binding domains between the repeats. The adhesive activity is retained in the biggest part of the N-terminal of the repeats (Pecina-Slaus., 2003). The extracellular domains form homodimers with parallel domains that interdigitate with the dimers of a neighboring cell to form points of adhesion and stabilize the cell-cell adherens junction (Pecina-Slaus., 2003).

E-cadherin is linked to the actin cytoskeleton through a series of cytoplasmic adaptor proteins (Itoh *et al.*, 1997., Ghadimi *et al.*, 1999; Turner *et al.*, 2009; Hwang *et al.*, 2012). The most notable of these cytosolic adaptor proteins are  $\beta$ -catenin and p120-catenin, which link the E-cadherin to the actin cytoskeleton through  $\alpha$ -catenin (Canel *et al.*, 2013). It is reported that the  $\beta$ -catenin acts to chauffeur a newly synthesized E-cadherin to the plasma membrane and remains in complex while the p120-catenin stabilizes the complex at the membrane (Chen *et al.*, 1999; Ireton *et al.*, 2002; Canel *et al.*, 2013). The E-cadherin cell surface levels are controlled by the regulation of cadherin trafficking (Davis *et al.*, 2003; D'Souza-Schorey., 2005; Canel *et al.*, 2013).

Several studies have stated that the decrease of E-cadherin cell surface expression (or altered localization) in advanced high-grade tumors may be linked to higher incidence of metastasis and tumor recurrence (Birchmeier and Berhens., 1994; Berx and van Roy., 2009; Canel *et al.*, 2013). It is also noted that E-cadherin



and  $\beta$ -catenin remain expressed in lower grade PCa adenocarcinomas that result in survival advantage of the tumor cells (Nagle and Cress., 2011). But E-cadherin may also exhibit suppression of tumor invasion because it may decrease the cellular motility rate by polarizing the direction of cell migration (Nagle and Cress., 2011). Overall, these studies indicate that the most common cause of the reduction of E-cadherin surface expression is the transcriptional silencing by the hypermethylation of its promotor or upregulation of the zinc finger family transcriptional repressors SNAIL, SLUG, SIP1 and ZEB1, which target the E-cadherin promoter region (Berx and van Roy., 2009; Canel *et al.*, 2013) and alter  $\beta$ 4 integrin expression (Drake *et al.*, 2010). Histone deacetylation has also been suggested as a negative regulator of E-cadherin expression (Mareel and Leroy., 2003; Giehl and Menke., 2008). This reduction of E-cadherin surface expression and the “weakening” of the cell-cell adhesion is a crucial step in epithelial-mesenchymal transition (EMT) process (Kalluri and Weinberg.2009; Canal *et al* 2013). However; this reduction in membrane expression may simply be associated with the increased rate of cycling of the protein from the surface to the cytoplasm and back to the surface as a result of the plasticity in collective tumor migration. In fact, previous studies observed that reduction in E-cadherin did not cause dissociation of cellular clusters in *Xenopus* cranial neural crest cells (Huang *et al.*, 2016).

*E-cadherin and  $\alpha$ 6 integrin crosstalk in prostate cancer.* Multiple studies showed the evidence of integrin and E-cadherin crosstalk in cellular adhesion, migration and contraction (Yano *et al.*, 2004; de Rooij *et al.*, 2005; Martinez-Rico *et al.*,

2010). The crosstalk between the  $\alpha 6$  integrin and E-cadherin occurs during the lateral cell-cell associations in which lateral expression of  $\alpha 6$  integrin primarily occurs during tissue remodeling events, such as wound healing or early embryonic events of organ formation involving tubulogenesis, or during the progression of tumors. This  $\alpha 6$  integrin lateral association occurs with the attenuation of basal cells. The objective was to determine if the loss of  $\alpha 3$  integrin would modulate  $\alpha 6$  integrin and E-cadherin co-distribution. To test this, anti- $\alpha 6$  (AA6NT), anti- $\alpha 3$  antibody formulations in addition to a ready to use E-cadherin commercial product (RTD) with subsequent dilution titers were immunostained on FFPE tissues. CRISPR Cas9 DU145 cell lines (WT,  $\alpha 3^{KO}$ ,  $\alpha 6^{KO}$ ,  $\alpha 6^{AA}$ ) were tested with anti- $\alpha 6$  and E-cadherin in western blot analysis and cell line pellets were immunostained with anti-E-cadherin for membrane surface expression.

The initial titrations of E-cadherin antibody were prepared by opening a ready to use product dispenser (0.314 $\mu$ g/mL) and transferring calculated amounts from the standard dispenser into user fillable dispensers containing calculated volume of RTD proprietary Avidin antibody diluent containing a B5 blocker at 1:2 and 1:4 dilutions. The 0.314 $\mu$ g/mL solution was considered the baseline for E-cadherin immunostaining intensity and the anti- $\alpha 6$  antibody (or AA6NT) and anti- $\alpha 3$  antibody (CD49c) were tested on sequential sample slides as comparators for protein expression. The expression of both the  $\alpha 6$  and  $\alpha 3$  integrin is polarized in the basal layer in non-neoplastic tissue while the  $\alpha 6$  expression will transition to

less polarized expression in HGPIN and upregulated primary adenocarcinomas while  $\alpha 3$  integrin will exhibit downregulation of expression (Goel *et al.*, 2008).

## RESULTS

The immunostaining procedures executed on VENTANA Benchmark ULTRA instrument using protocols optimized for VENTANA OptiView and *ultraView* IHC DAB Detection Kits resulted in high intensity for E-cadherin. The results for the initial dilutions proved to be inconclusive as the 1:2 and 1:4 dilutions proved to demonstrate comparable immunostaining intensity to the 0.314 $\mu$ g/mL concentration with little to no visible drop in intensity (**Figure 4.1, A**). This result prompted an increase in titer range to identify a specific extreme in which to determine a threshold. The next range of titers therefore were 1:100 and 1:500 titers. The previous experimental procedures were repeated utilizing the same de-identified sample tissues (n=4). The results of the 1:100 titer concentration demonstrated only a diffuse blush within the tissue while the 1:500 titer demonstrated a completely negative result (**Figure 4.2, B**). Immunostaining intensities were plotted in **Figure 4.1, C**. These results suggested that the optimal titer that would demonstrate any substantial information concerning the E-cadherin membrane of cytoplasmic distribution would not be beyond the 1:100 titer from the 0.314 $\mu$ g/mL concentration.

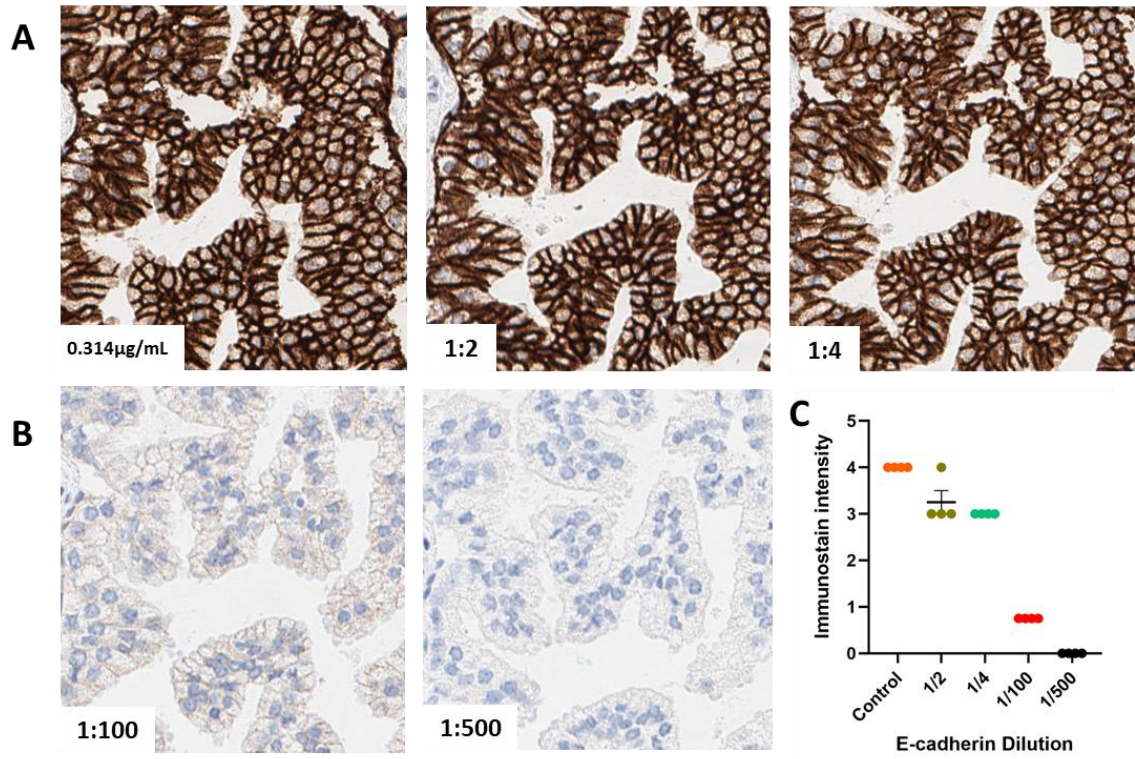


**Figure 4.1. E-cadherin IHC expression in prostate with titration.** Images are 20x magnification. E-cadherin expression was observed for decrease in saturated immunostaining intensity. (A) 0.314µg/mL concentration expression was compared to a 1:2 and 1:4 dilution titer. (B) Dilution titers of 1:100 and 1:500 demonstrated decrease in immunostaining intensity. (C) Immunostain intensities scores analyzed using one-way ANOVA GraphPad analysis (n=4).

This prompted the investigation of dilutions of 1:10 and 1:50 to determine if the range was sufficient for visible immunostaining intensity. The process was repeated utilizing the same tissue samples and the results indicated the 1:10 dilution formulation titrated from the ready to use dispenser to be the appropriate dilution to visualize differential expression localization of E-cadherin in PCa tissues containing aggressive tumors compared to HGPIN and normal glands. The 1:10 dilution of anti-E-cadherin demonstrated an observable membrane localization in normal glands (Figure 4.2, A) and exhibited primarily peripheral membranous

intensity and membranous and cytoplasmic localization in a tissue sections containing cribriform lesion (**Figure 4.2, B**). This data would support the findings of previous studies reporting a reduction in E-cadherin staining within aggressive migrating collective tumors (Bronsert *et al.*, 2014). This would indicate plasticity of lateral E-cadherin localization and redistribution within aggressive migrating collective tumors and may be an indication of poor outcome and disease advancement. This will also suggest that studies reporting the dependence on  $\beta 1$  integrin function for invasive migratory collective tumors were correct in their assumption (Hergerfedlt *et al.*, 2002).

The comparative sample immunostained with the anti- $\alpha 6$  antibody exhibited the expected basal expression within normal glands (**Figure 4.2, C**) and a pattern of localization in the cribriform lesion similar to E-cadherin with peripheral intracellular membrane expression and centrally cytoplasmic expression in the within the same sample on sequentially cut slides. This similar expression pattern may indicate a complex association of the  $\alpha 6$  integrin with the E-cadherin and potentially the presence of the  $\alpha 6p$  tumor specific variant within focal areas of low membrane expression of  $\alpha 6$  integrin (**Figure 4.2, D**). The study by Bronsert *et al.*, 2014 using 3D melanoma explant demonstrated that budding cell clusters exhibited decreased membranous staining and a shift to cytoplasmic staining of E-cadherin. Several studies targeting *Xenopus* Cranial Neural Crest (CNC) migration have suggested that while the downregulation of E-cadherin is necessary for the formation and migration action of the CNC, that some E-cadherin presence is also necessary of migration (Schafer *et al.*, 2014; Cousin *et al.*, 2017). The CNC is a

population of early embryonic cells that require cadherin mediate cell-cell contact to migrate collectively to form the head of the *Xenopus* embryo.

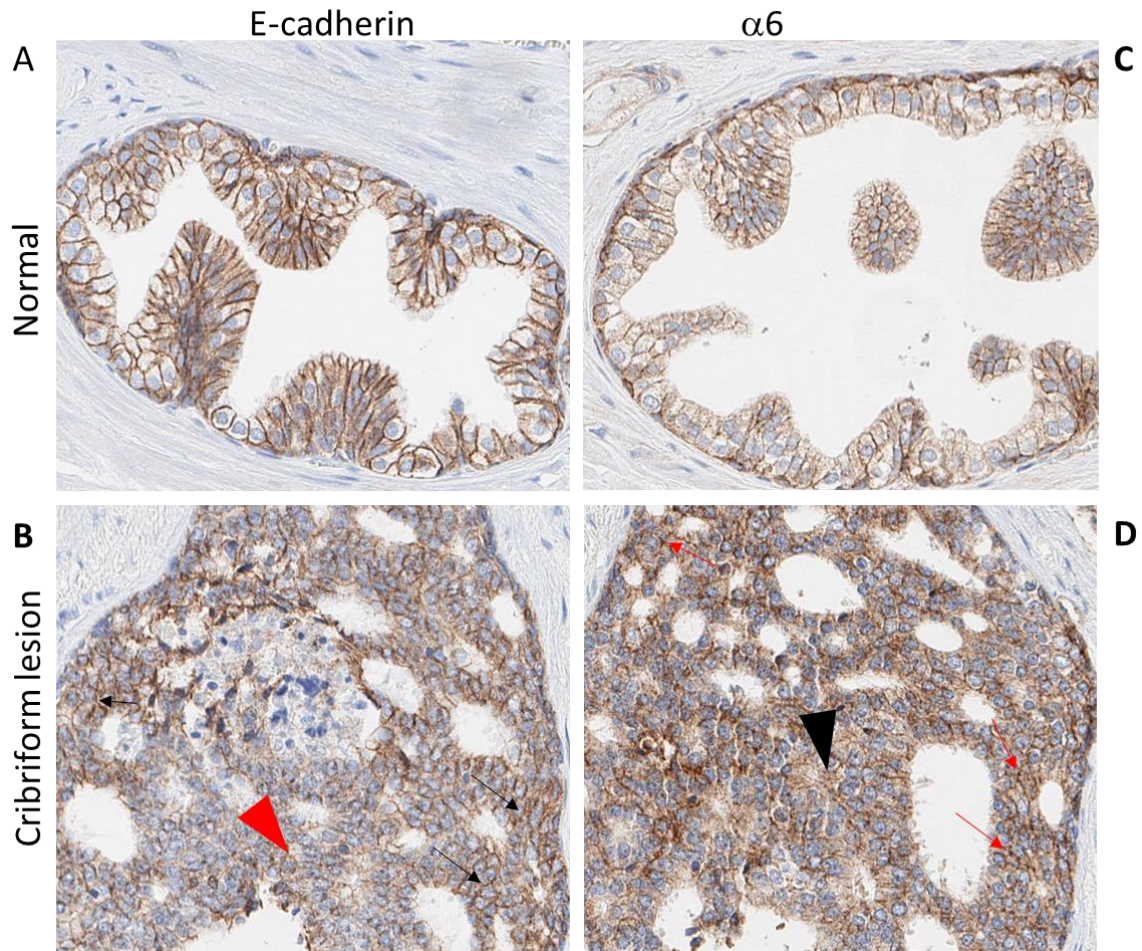


**Figure 4.2. Optimized detection of cell-cell distribution of E cadherin and  $\alpha 6$  integrin in prostate normal and cancerous tissue.** Images captured are 20x magnification. Two different prostate tissue sections are captured, one with normal glands and one with prostate tumor. **(A)** Human prostate FFPE sample with prominent E-cadherin membrane expression with 1:10 antibody dilution in normal prostate gland. **(B)** E-cadherin cell-cell distribution and membrane staining pattern (black arrows) in PCa aggressive cribriform lesion (Gleason Score 4+4) and cytoplasmic localization in central regions (red arrowhead). **(C)**  $\alpha 6$  Integrin expressed in expected basal and suprabasal pattern in normal prostate gland. **(D)**  $\alpha 6$  Integrin demonstrates peripheral membrane associated pattern, Black arrows and central cytoplasmic localization similar to E-cadherin in cribriform lesion.

*Inhibition of  $\alpha 6$  integrin cleavage by  $\alpha 6^{AA}$  increases E-cadherin protein expression:*

Here, the important task was to further interrogate the findings of the anti-E-cadherin antibody titration testing. The goal was to determine if loss of  $\alpha 3$  integrin surface expression would alter the  $\alpha 6$  integrin and E-cadherin distribution. Previous work in experimental models had shown that depletion of  $\alpha 3$  integrin expression resulted in redistribution of  $\alpha 6$  integrin to an observed cell-cell staining pattern that is consistent with a suprabasal distribution observed in epidermis and early PIN lesions in PCa and a two-fold rate increase in internalization (Das *et al.*, 2017). Since others had observed a cross-talk of  $\alpha 6$  integrin and E-cadherin function (reviewed in Canel *et al.*, 2013), we performed a protein expression analysis with the anti-E-cadherin antibody at a 1:10 dilution with DU145 CRISPR Cas9 cell lines. The cell lines tested were DU145 wild type, DU145  $\alpha 3^{KO}$ , DU145  $\alpha 6^{KO}$ , and DU145  $\alpha 6^{AA}$ . Western blot analysis revealed samples with the deletion of the  $\alpha 3$  gene resulted in > 2-fold reduction from the DU145 WT in the protein expression of E-cadherin (**Figure 4.3**). These data are consistent with the view that loss of the  $\alpha 3$  integrin surface expression correlates with a progression toward the loss of E-cadherin expression. In contrast, blocking the PTM function of the  $\alpha 6$  integrin (DU145<sup>AA</sup> cells) significantly increased E-cadherin expression. These data are consistent with previous observations that blocking the PTM function of the  $\alpha 6$  integrin will block bone metastasis progression (Ports *et al.*, 2009; Landowski *et al.*, 2014) and more recently, the muscle invasion of prostate cancer cells (Rubenstein *et al.*, 2019). An  $\alpha 6$  integrin protein assessment was also accomplished using the AA6NT antibody with these cell lines demonstrating the

deletion of  $\alpha 3$  integrin promotes  $\alpha 6$  integrin cleavage to  $\alpha 6p$ . As expected, the  $\alpha 6^{AA}$  mutant was unable to be cleaved and only expressed the full length  $\alpha 6$  integrin (**Figure 4.4**). The increased expression of E-cadherin support our findings (Rubenstein *et al.*,2019) in which gene editing of the  $\alpha 6$  extracellular region to eliminate the PTM function will generate a new biophysical phenotype of increased cell-cell adhesive clusters and reduced invasiveness. This may be the result of activation of an unknown pathway initiated by the dominant activity of the uncleavable full length  $\alpha 6$  integrin. The dramatic phenotype switch and E-cadherin expression suggest a major point of regulation dictated by the  $\alpha 6$  integrin ectodomain. It remains to be determined which specific integrin signal transduction pathways are responsible.



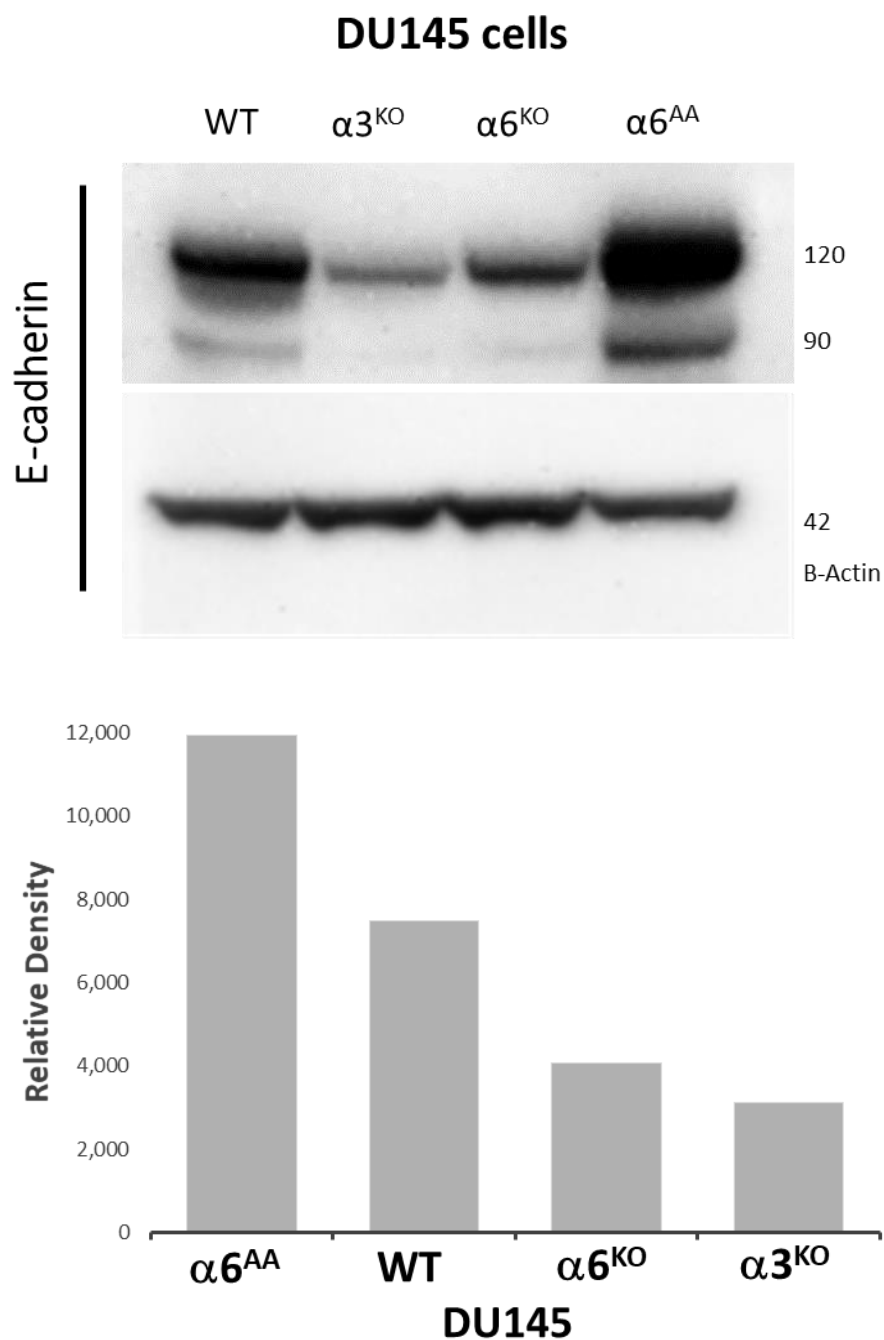


**Figure 4.3. E-cadherin expression in DU145 CRISPR Cas9 prostate cancer cells.** Western blot total protein analysis of cell lysates with anti-E-cadherin antibody at 1:10 dilution and relative expression of E-cadherin was quantified exhibiting downregulation with  $\alpha 3^{KO}$  and significant increase with  $\alpha 6^{AA}$  cleavage inhibition. Slight recovery of E-cadherin expression observed with  $\alpha 6^{KO}$ .

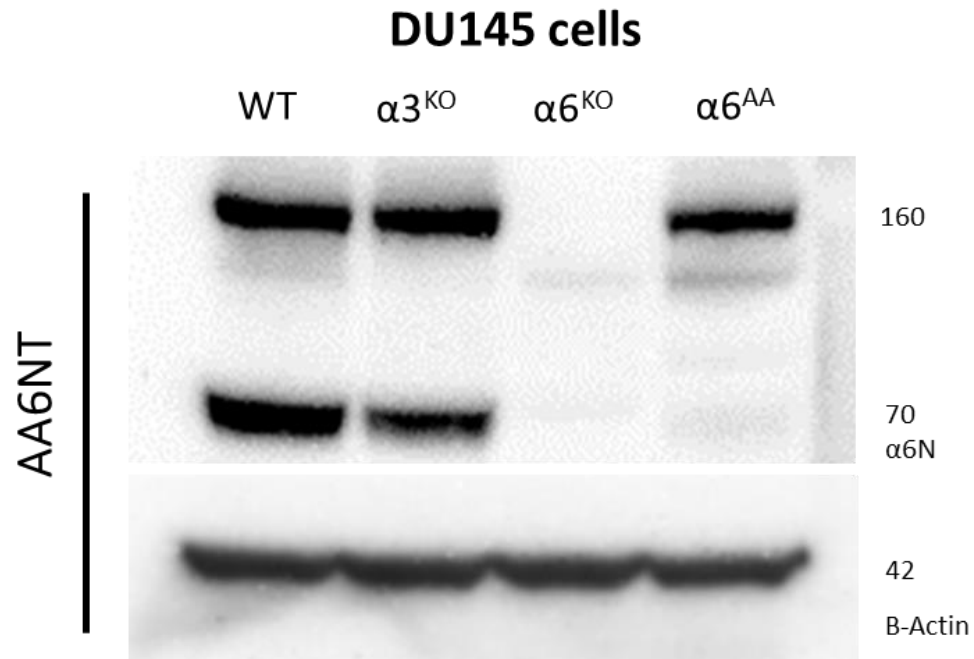


**Figure 4.4.  $\alpha 6$  integrin expression in DU145 CRISPR Cas9 prostate cancer cells.** Western Blot total protein analysis of DU145 cell lysates with anti- $\alpha 6$  (AA6NT) antibody revealed production of  $\alpha 6$  integrin cleavage product in  $\alpha 3^{KO}$  cells and inhibition of the cleavage product with  $\alpha 6^{AA}$ .

*$\alpha 6^{AA}$  increases E-cadherin membrane expression and cohesive tumor cell clustering:* The objective was to determine if the increased total protein expression that was demonstrated in the western blot analysis because of the  $\alpha 6^{AA}$  gene editing would correlate to increased tumor cell membrane expression and upregulated cell-cell adhesiveness in tumor cells. The observations showing increased E-cadherin protein expression could have potentially been the result of the inhibition of protein degradation pathways which could have also accounted for upregulated presence of E-cadherin protein. Therefore, we investigated E-cadherin membrane expression in the matching DU145 cells. We theorized the  $\alpha 6^{AA}$  induced a phenotypic switch that activated unknown signaling factors that

promoted E-cadherin recycling to the membrane surface for stronger adherens junctions and tighter cell-cell associations.

To perform this testing, single slides containing DU145 cell pellets for WT,  $\alpha 3^{\text{KO}}$ ,  $\alpha 6^{\text{KO}}$ , and  $\alpha 6^{\text{AA}}$  that had been paraffin embedded and serially sectioned were immunostained with anti-E-cadherin. As expected, the DU145 WT exhibited variable E-cadherin cell surface expression but did not appear to demonstrate increased cell-cell adhesion as a result of the protein expression (**Figure 4.5, A**). The DU145  $\alpha 3^{\text{KO}}$  cells exhibited a complete lack of E-cadherin membrane expression, using an ultra-sensitive detection system, as mentioned earlier. This is significant since the western blot only detected a decrease in total protein expression. (**Figure 4.5, B**). The DU145  $\alpha 6^{\text{KO}}$  exhibited variable E-cadherin membrane expression that induced some cell-cell adhesion but did not display a significant amount of cells forming adhesive clusters (**Figure 4.5, C**). This may indicate a potential E-cadherin association with  $\alpha 3$  integrin, or other cell surface receptors such as tetraspanin CD151 at lateral cell surface (Chattopdahyay *et al.*, 2003). Although the role of  $\alpha 3$  integrin has been defined in cell-ECM focal adhesions, results from work characterizing the PTP $\mu$  (transmembrane protein tyrosine phosphatase) gene expression in cadherin-mediated adhesion, suggests a distinct pool of  $\alpha 3$  integrin locates to the lateral membrane in complex with CD151. This complex can associate with proteins of cell-cell adhesion complex including E-cadherin (Fitter *et al.*, 1999; Yanez-Mo *et al.*, 2001; Chattopdahyay *et al.*, 2003). Still, it did not appear the DU145  $\alpha 6^{\text{KO}}$  were able to facilitate a significant increase in cell-cell adhesive aggregates (clusters). However, as expected, the

DU145 cells with  $\alpha 6^{AA}$  inhibition of the cleavage event resulted in significant increase in E-cadherin membrane expression (**Figure 4.5, D**). The tumor cells also demonstrated a dramatic increase in cell clusters, creating pockets of cells that appeared to exhibit a tight adherence to neighboring cells. Also observed, were spaces in between the cell clusters that further suggested increased adhesion.

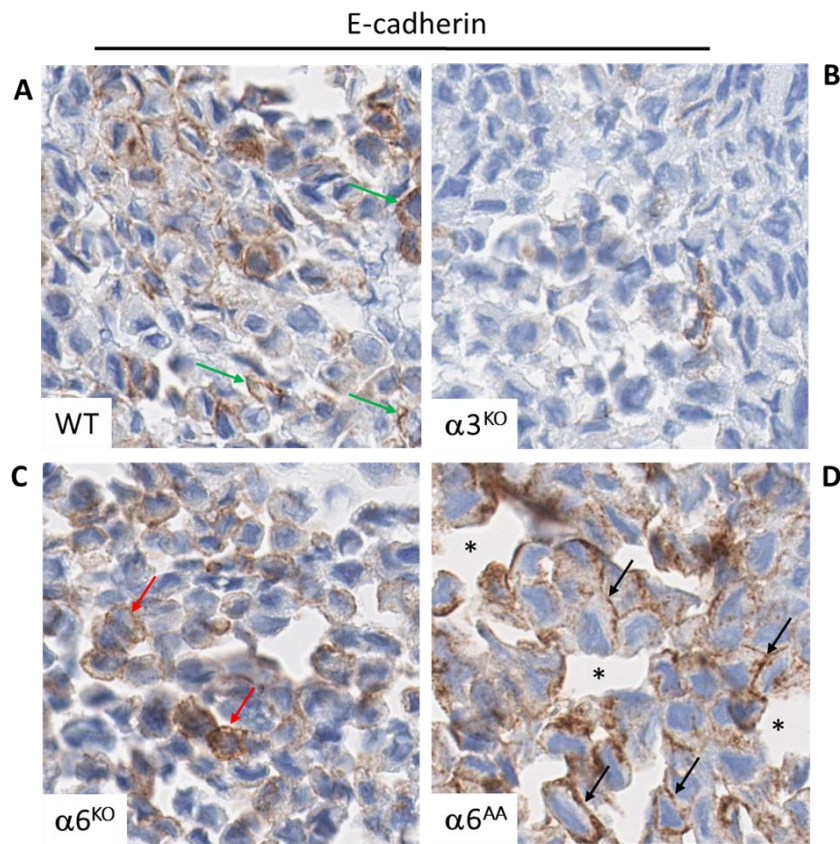


**Figure 4.5. E-cadherin membrane expression increased with inhibition of  $\alpha 6$  cleavage.** DU145 cell pellets for WT,  $\alpha 3^{KO}$ ,  $\alpha 6^{KO}$ , and  $\alpha 6^{AA}$  cells were paraffin embedded IHC immunostained with anti-E-cadherin. **(A)** DU145 WT exhibited variable membrane expression (green arrow). **(B)** E-cadherin surface expression was relatively absent in DU145  $\alpha 3^{KO}$  cell pellets. **(C)** DU145  $\alpha 6^{KO}$  cell pellets demonstrated focal membrane expression (red arrows). **(D)** DU145  $\alpha 6^{AA}$  cell pellets show significant membrane localization of E-cadherin (black arrows) and increased tumor cell clusters with increased spacing between the cell clusters (\*) indicating tight adhesions. Images are 40x magnification.

*Proximal detection of  $\alpha 6$  integrin and E-cadherin in PCa prostate tissue:* To test the theory that  $\alpha 6$  integrin and E-cadherin were truly complexed in tissues as Marchio *et al.*, 2012 suggested, an innovative proximity detection assay (PDA) was employed. The PDA (from RTD) utilizes a “caged hapten” proximity readout that is followed by IHC detection. The PLA is described in the materials and methods section of this dissertation. The execution of the proximity assay was accomplished using three human prostate FFPE tissue samples consisting of normal and tumor elements. The assay was designed to detect proximal protein events with enzymatic biochemical conformational interactions if indeed proximal association occurs (**Figure 4.6**). In the sample with normal glands, the presence of proximal event was demonstrated with intense immunostaining because of the proximal association of  $\alpha 6$  integrin and E-cadherin. (**Figure 4.7, left panel**). In contrast, the tissue containing aggressive PNI element, the punctate immunostaining was evident in focal areas (**Figure 4.7, right panel**). These results indicate that  $\alpha 6$  integrin and E-cadherin form complexes in prostate tissues that is associated with disease progression, confirming the findings in Marchio *et al.*, 2012. In aggressive PCa, cleavage of  $\alpha 6$  integrin occurs and the invading tumor cells utilize the tumor variant  $\alpha 6p$  lacking the laminin binding domain to migrate along the nerve.

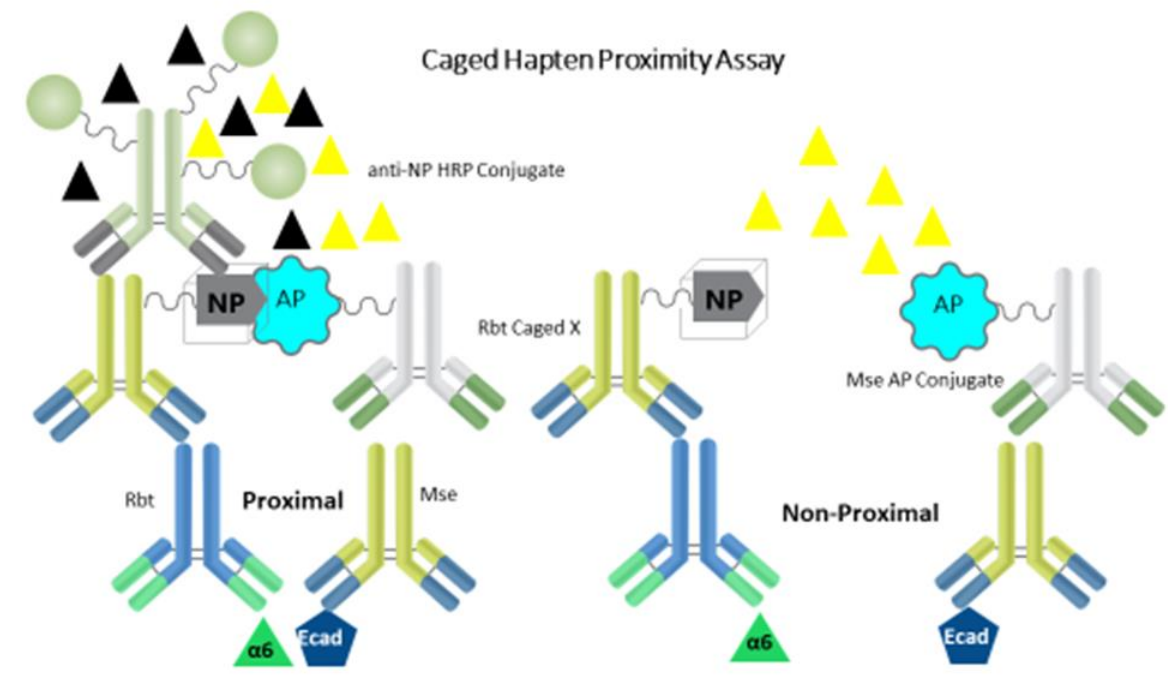


**Figure 4.6. Schematic of Caged Hapten Proximity Assay for  $\alpha 6$  integrin and E-cadherin complex.** Proximal events, allow conformational change of secondary conjugated quinone methide precursor (NP) due to interaction with enzymatic alkaline phosphatase (AP) secondary to allow deposition of tertiary with anti-NP horseradish peroxidase (HRP) for detection (left region) (yellow and black arrows). Lack of proximity negates activation and results in lack of detection (right region).

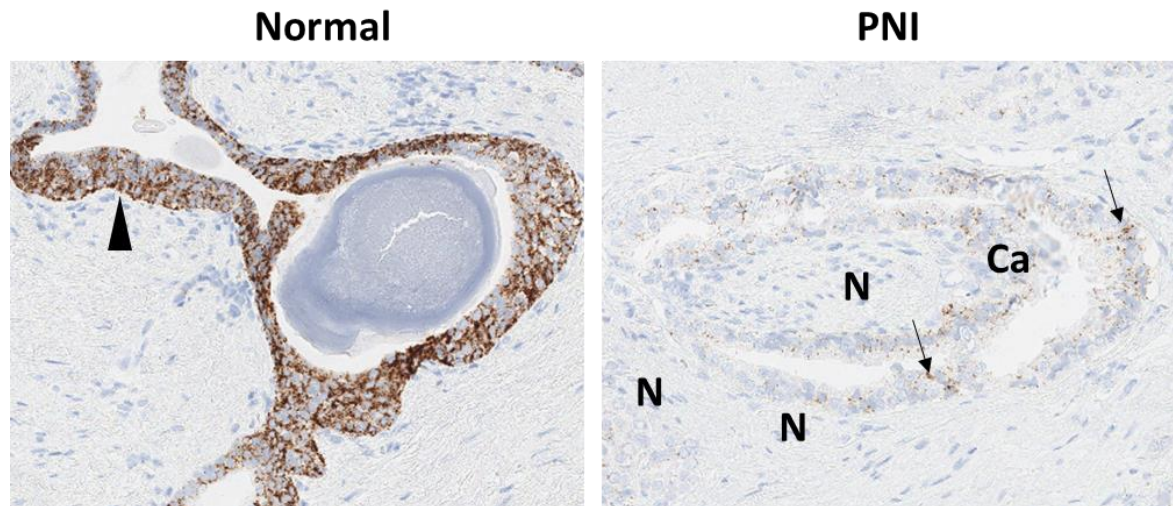


**Figure 4.7.  $\alpha 6$  integrin and E-cadherin form complexes in prostate tissue.** Proximity ligation assay using antibody for laminin binding region of  $\alpha 6$  integrin and E-cadherin. Tumor clusters (Ca) invading around nerves (N) via perineural invasion (PNI), demonstrate low proximity expression with punctate immunostaining (black arrows) indicating laminin binding region of  $\alpha 6$  integrin are unavailable (left panel). Normal prostate gland demonstrates intense immunostaining (black arrowhead), indicating proximal complexes of  $\alpha 6$  integrin and E-cadherin (right panel). [Images 10x magnification].

## DISCUSSION

Tumor cells invading as a cohesive collective utilize activation of signaling pathways that control cytoskeletal dynamics and turnover of cell-matrix and cell-cell junctions (Friedl and Alexander., 2011). In doing so, the collective adopts various morphological strategies to invade in to surrounding areas, although it depends on the cell type and environment being invaded (Friedl and Alexander., 2011). These multicellular collective tumors move as sheets, strands, clusters or ducts (Friedl and Gilmore., 2009). The collective tumors can recapitulate the types and mechanisms utilized by normal, non-neoplastic cell processes to migrate but lack the physiological “stop signals” that immobilize and anchor cells that inhibit

mobility (Cox *et al.*, 2001; Friedl and Alexander., 2011). During collective migration, the cell-matrix integrin-mediate regulation of cell-cell adherens junction molecules, specifically E-cadherin, contributes to the plasticity of the collective to perpetuate translocation through the tissue structures. It is suggested that the alterations of the cell-cell and cell-matrix adhesion, through signal transduction, cytoskeletal signaling, cellular mechanics and protease activity determine the migration mode (Friedl and Wolf., 2010).

The upregulation of  $\alpha 6$  integrin in aggressive PCa has been well established. Our lab has previously defined the role that cleavage of  $\alpha 6$  integrin to the variant  $\alpha 6p$  plays in progression to the invasive tumor phenotype (Demetriou and Cress., 2004; Demetriou *et al.*, 2004; Pawar *et al.*, 2007). Our group has also demonstrated that blocking the  $\alpha 6$  integrin cleavage event could potentially offer a significant non-toxic approach for to arrest progressive tumors *in vivo* (Ports *et al.*, 2009; Landowski *et al.*, 2014; Rubenstein *et al.*, 2019). However, it was unknown what other mechanisms and molecular pathways affect the migratory capabilities of these tumors.

Various groups have documented the deregulation of migratory suppressive E-cadherin mediated cell-cell adhesion in many invasive tumor types. It is known that migratory cell clusters demonstrate plasticity through modulating E-cadherin membrane dynamics. In keratinocytes,  $\beta 4$  and  $\alpha 3$  integrins stimulate E-cadherin hemophilic interactions that abrogated cellular motility (Hintermann and Quaranta., 2004; Hintermann *et al.*, 2005; Chartier *et al.*, 2006; Martinez-Rico *et al.*, 2010).



However, it has been determined that upstream signals through exposure to growth factors in ECM, such as TGF $\beta$ , EGF, FGF and Wnt, lead to activation of transcriptional repressors such as ZEB1, Snail, Slug and Twist that inhibit E-cadherin transcription and thus protein translation (Yang *et al.*, 2004; Friedl and Alexander., 2011). The aberrant signaling displayed in these tumor collectives underlie the mechanisms controlling the dynamic membrane and intercellular expressions of E-cadherin and drive these collective cohorts. Uncovering the mechanisms that mitigate the suppression of cell-cell adhesion regulated by E-cadherin would be an attractive target for resolving tumor cohesive migration.

In our results, the increased E-cadherin cell surface protein expression on the DU145  $\alpha 6^{AA}$  cells was an intriguing surprise since the expected outcome was to phenocopy the DU145  $\alpha 6^{KO}$  phenotype. The result indicated a potential activation of undetermined signaling pathways or a gain of function that initiated a cellular phenotypic switch phenotype as a result of expression of the  $\alpha 6^{AA}$  uncleavable full length integrin. This gain of function activity may be due to induction of several endogenous kinases or molecular transcription factors responding to an unspecified transduction of integrin signaling initiated by the activation of the full-length  $\alpha 6$  integrin. It was previously determined by our lab that the  $\alpha 6^{AA}$  functional cleavage inhibition of the  $\alpha 6$  integrin to the tumor specific variant  $\alpha 6p$  form mitigating invasive chords to cohesive clusters was a reproducible outcome (Rubenstein *et al.*, 2019). However, it had not been determined to an extent what other specific protein pathways had been surreptitiously involved. These data indicate that not only inhibiting the  $\alpha 6$  integrin cleavage by uPAR can be a target

for impeding migratory tumors that have invaded but also that it may result in a phenotypic tumor switch to indolent disease.

The results of the proximity detection assay supports the complexing of  $\alpha 6$  integrin and E-cadherin role in normal prostate tissues similar to results of Marchio *et al.*, 2012. The result in aggressive PNI indicating only low intensity and punctate immunostaining would suggest increased PTM of the full-length  $\alpha 6$  integrin to the  $\alpha 6p$  tumor variant. This could mean the tumor variant may be constitutively activated to regulate E-cadherin cell-cell expression to create the plasticity necessary for tumor navigation through the ECM environment and along the nerves for dissemination.

The next task would be to investigate what other critical factors and mechanisms are being activated to upregulate this cellular adhesive potential. The pathways and factors such as Twist activated in tumors are known antagonists of E-cadherin expression (Giehl and Menke., 2008; Schafer et al., 2014). These factors allow dissemination in most cancers and targeted therapies have been developed to mitigate their activity. Understanding the factors upregulating E-cadherin membrane expression in concert with  $\alpha 6$  integrin cleavage inhibition leaves an attractive target for companion therapy that may increase the effectiveness.

## **V. Multiplex IHC detection of $\alpha 6$ , $\alpha 3$ integrins and E-cadherin localization in PCa progression**

### **ABSTRACT**

The detection of protein molecules that are involved in directing specialized adhesions in cancer progression leading to dissemination is vital to being able to elucidate and target the mechanisms regulated by their co-distribution in aggressive transition. The development and optimization of a multiplex chromogen IHC detection assay interrogating the protein expression levels identified localization patterns of  $\alpha 3$  integrin,  $\alpha 6$  integrin and E-cadherin. Here, the primary antibodies targeting  $\alpha 6$  integrin, E-cadherin and  $\alpha 3$  integrin are used in a three-color multiplex IHC panel (3-Plex) that was integral in determination of patterns on one sample slide associated with early disease transition in tissues. Interestingly, tissue regions of early progression demonstrating loss of  $\alpha 3$  integrin, displayed co-distribution of  $\alpha 6$  integrin and E-cadherin. This observation, in theory, may show cellular response to physical stress in the attempt to maintain homeostasis and cell-cell and cell-ECM adherence. This multiplex panel allowed for a deployment of an innovative imaging analysis tool to design an algorithm to quantify regions of  $\alpha 6$ /E-cadherin complexes to identify non-malignant regions from malignant regions. In addition, this innovative assay shows capability to assess the required uniform protein expression levels of E-cadherin necessary for the formation of cell-cell adhesive contacts and migratory inhibition. In addition, this assay also allows the identification of E-cadherin membrane levels associated with downregulation

in proliferative and invasive tumors. Overall, these results show that the multiplex detection of these protein associations in tissue allows identification of non-malignant and malignant tumors. This may also identify a potential path to develop strategies mitigating the capability of aggressive prostate tumors to invade by activating factors that promote E-cadherin expression.

## **INTRODUCTION**

The mechanisms that mediate progression from the early confined prostate cancer to invasive prostate tumors have remained elusive. The transition involves dynamic interplay between cell surface adhesion molecules that control cellular response to the sensing of cues from the surrounding tissue milieu that drive the biophysical functional activity. The association of laminin binding integrins and cadherins involves a complex crosstalk driven by mechanosensing of signals from the microenvironment. Mechanotransduction of these signals into intracellular action potentials likely regulate spatial localization of these receptors and may have an impact on focal adhesion traction forces, intracellular tension and cellular motility. The ability of tumor cells to interact with the microenvironment has a significant impact on behavior through cell-cell and cell-ECM adhesion (Giehl and Menke., 2008).

The mechanisms associated with these tumor cell interactions involve complex activation or downregulation of molecular pathways and proteins that regulate phenotypic switch to aggressive types. Previous chapter (2) mentions the association of E-cadherin with inactivation the Rho family of GTPases (Rho, Rac

and Cdc42) to inhibit cellular migration. In addition,  $\alpha 6$  integrin clustering requires Rho activation (Wei *et al.* 1997). Therefore, the co-distribution of  $\alpha 6$  integrin and E-cadherin may regulate the Rho family activation. Other groups have reported that the stimulation of these factors result in adaptive remodeling of the actin cytoskeleton architecture in response to specific adhesions (Etienne-Manneville and Hall., 2002; Giehl and Menke., 2008; Watanabe *et al.*, 2009; Parsons *et al.*, 2010; Mui *et al.*, 2016). Whether the remodeling on the actin cytoskeleton results in increased lateral clustering of E-cadherin to reinforce cell-cell adhesion or activate de-polymerization depends on mechanical stresses applied. Liu *et al.*, 2010 demonstrated that cell-generated forces regulate the strength of cell-cell adhesions by inducing growth of the adherens junctions, similar to the findings of what occurs at focal adhesions (Maruthamuthu *et al.*, 2011). Together, they provide quantitative data demonstrating an interdependence of cell-cell and cell-ECM forces that regulate the mechanosensing, mechanotransduction that result in dynamic reorganization of these adhesions utilized in invasive cohesive tumors. Therefore, methods to detect and quantify regions of expression of  $\alpha 3$  integrin in association with E-cadherin and  $\alpha 6$  integrin are postulated to be important to distinguish between diagnosing confined or aggressive PCa.

Educated decisions for stratifying patients for treatments traditionally have relied upon detecting biomarkers for targeting aggressive diseases. Primarily, those decisions have relied upon the detection of single biomarkers. Advances in multiplex immunostaining and multispectral imaging have allowed the simultaneous detection and analysis of multiple targets in FFPE that allow accurate

cell detection and spatial information (Gorris *et al.*, 2017). This has given a potential advantage of assessment of potential aggressiveness of cancers in a single tissue slides as opposed to single biomarker labeling on sequential samples which may or may not retain the specific region of interest.

Creating, optimizing and applying immunostaining detection protocols targeting multiple proteins in one sample is a complex task that some studies use primary antibodies (Abs) raised in separate species to prevent cross-reactivity (Gorris *et al.*, 2017). However, procedures developed in this study utilized heated denaturation steps that may allow the use primary Abs of the same species. The use of tyramide signal amplification (TSA) is deployed to minimize limitations to detection with multiple markers in most cases but other biochemically designed amplifications such as Benzofuran haptenated secondaries can be employed. Still, careful optimization processes are still necessary to mitigate damage to epitope, tissue architecture or even primary antibody degradation due to exposure to multiple parameters during sequential immunostaining protocols.

In prostate cancer progression, differential expression of the LBIs has been demonstrated (Chapter 1). The positive correlation between higher Gleason grades and pathological stage with the loss of cell surface expression of  $\alpha 3$  integrin is an important finding (Schmelz *et al.*, 2002). However, the debate concerning the role of  $\alpha 3$  integrin in cancer progression continues as some groups reporting data showing  $\alpha 3$  integrin is involved in disease progression and promotion of migration (Zhou and Kramer., 2005; Zhou *et al.*, 2014). In contrast, others have

demonstrated  $\alpha 3$  integrin to be a negative suppressor of invasion, migration and malignant transformation (Owens and Watt., 2001; Varzavand *et al.*, 2013; Varavand 2016). Results from our lab demonstrate the loss of  $\alpha 3$  integrin coincides with increased expression of  $\alpha 6$  integrin in these progressive PCa tumors that has been linked to reduced patient survival, and increased metastasis (Ports *et al.*, 2009). Increased expression of  $\alpha 6$  integrin in PNI and PCa bone metastasis confirm that it is a significant factor for aggressive designation (Sroka *et al.*, 2010; Landowski *et al.*, 2014). The  $\alpha 6$  integrin cleavage results in the tumor specific variant that is has been demonstrated to be a key contributor to cancer metastasis (Demetriou and Cress., 2004; Demetriou *et al.*, 2008; Ports *et al.*, 2009; Kacsinta *et al.*, 2014). Recently, it was indicated that  $\alpha 6$  integrin and E-cadherin form a complex that interacts with hepatic angiopoietin-like 6 to promote aggressive liver metastasis (Marchio *et al.*, 2012). This supports the work of several other groups indicating a specific cross talk involving the dynamic expression of integrin association with E-cadherin as an important factor in tumor progression, invasion and dissemination (Yano *et al.*, 2004; Giehl and Menke., 2008; Martinez-Rico *et al.*, 2010; Weber *et al.*, 2011; Marchio *et al.*, 2012; Canel *et al.*, 2013; Mui *et al.*, 2016).

## **RESULTS**

Four de-identified human prostate cancer FFPE tissue samples were selected and sectioned with initial slides stained with hematoxylin and eosin (H&E) for content assessment. A board-certified pathologist evaluated the H&E stained slides to

determine tissue architecture, morphology, histological elements and tumor content. The primary focus of this study was to evaluate the location of any elements of normal architecture, pre-malignant PIN lesions (carcinoma in-situ) and aggressive tumors with any notable elements of PNI (perineural invasion). Immunostaining protocols were initially developed utilizing each antibody individually with immunohistochemistry (IHC) detection with 3, 3'-diaminobenzidine (DAB) to maximize immunostaining intensity, sensitivity, specificity and to provide reproducibility. The serial sections were immunostained with the anti- $\alpha 6$  antibody specific for the laminin binding region of  $\alpha 6$  integrin, the HPA008572 antibody clone specific for the extracellular region of  $\alpha 3$  integrin, and the anti-E-cadherin clone (36) for the transmembrane domain of E-cadherin to determine localization.

*Individual chromogen IHC detection:* IHC of  $\alpha 6$  integrin revealed cellular membrane localization in normal prostate glands exhibiting early progression and positive expression in endothelial cells of vessels (**Figure 5.1, A, top left panel**). Although,  $\alpha 6$  integrin primarily displayed intracellular localizations with some membrane expression in tumors invading via PNI (**Figure 5.1, A, bottom left panel**). As expected, peripheral nerve and endothelial cells of vessels also exhibited membranous and cytoplasmic positive expression for  $\alpha 6$  integrin (**Figure 5.1, A, bottom left panel**). The anti-E-cadherin IHC immunostaining exhibited high level of intensity initially demonstrating membrane expression in samples with early progression (**Figure 5.1, A, top middle panel**) and in PNI (**Figure 5.1, B, bottom middle panel**). The  $\alpha 3$  integrin was detected focally in the membrane and showed loss in prostate gland exhibiting early progression (**Figure 5.1, A, top**



right panel), and no expression was detected in the aggressive PNI (**Figure 5.1, B, bottom right panel**).

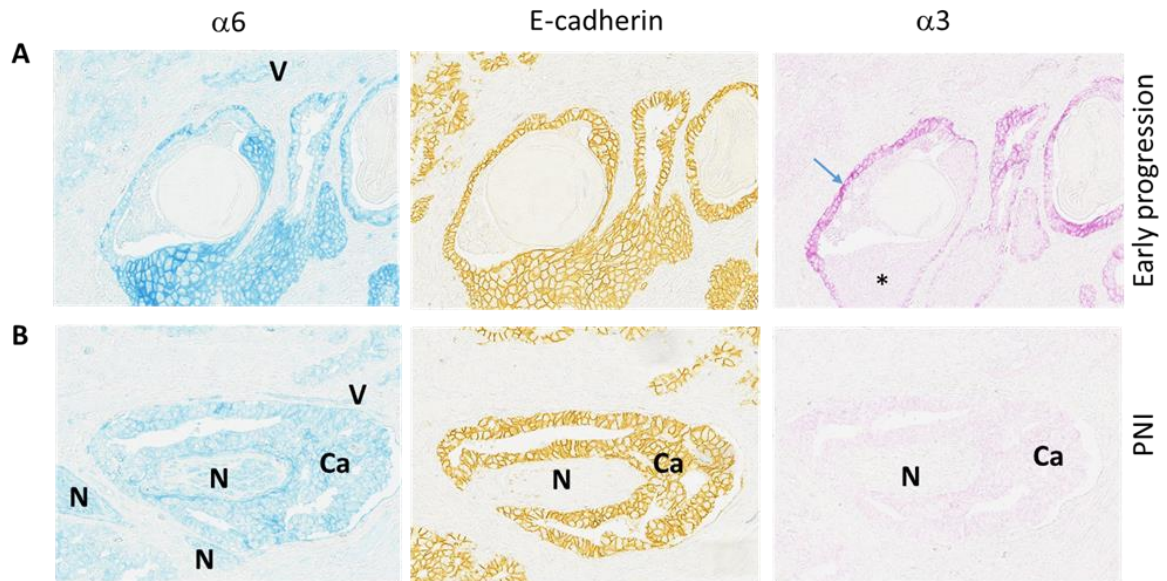


**Figure 5.1.  $\alpha 6$  integrin, E-cadherin and  $\alpha 3$  integrin expression in PCa and PNI.** Individual chromogens were detected in human prostate tissue serial sections with anti- $\alpha 6$  antibody (teal), anti-E-cadherin antibody (yellow) and anti- $\alpha 3$  antibody (magenta). **(A)** Prostate gland demonstrating early progression.  $\alpha 6$  integrin exhibiting membrane expression and positive intensity with vessel endothelial cells (top left panel). Anti-E-cadherin demonstrating strong membrane intensity (top middle panel). Anti- $\alpha 3$  demonstrating focal membrane expression (blue arrow) (top right panel). **(B)** Perineural invasion (PNI) with anti- $\alpha 6$  exhibiting intracellular and some membrane expression in cancer (Ca) invading in and around nerves (N). Alteration in  $\alpha 6$  integrin expression likely due to loss of epitope within in cancer cluster since normal structures exhibit immunostaining (bottom left panel). Anti-E-cadherin demonstrating expression in cancer (Ca) and lack of immunostaining in nerves (N) (bottom middle panel). Anti- $\alpha 3$  showing lack of intensity in Cancer (Ca) or nerves (bottom right panel). [Images at 10x magnification]

*Chromogen multiplex IHC:* The execution of the chromogen multiplex IHC detection yielded similar results as the individual chromogen IHC. The  $\alpha 3$  integrin displayed focal immunostaining within the prostate gland with early progression features (**Figure 5.2, A,**

**red arrowhead**), while  $\alpha 6$  integrin and E-cadherin demonstrate co-distribution within the transitioning area (**Figure 5.2, A, black arrow**). The co-distribution of  $\alpha 6$  integrin and E-cadherin likely indicates a response to increased stress. Similarly, the  $\alpha 3$  integrin did not display signal in sample containing PNI. Although  $\alpha 6$  integrin did show positive expression in nerves and vessels and minimal areas of co-distribution with E-cadherin, it was determined that the  $1.5\mu\text{g}/\text{mL}$  anti-E-cadherin antibody was too high and saturated the intensity level reducing the ability to observe potential detail (**Figure 5.2, B**). Therefore,  $1.5\mu\text{g}/\text{mL}$  anti-E-cadherin antibody was optimized further to an optimal dilution of 1:10 from  $1.5\mu\text{g}/\text{mL}$  anti-E-cadherin antibody concentration (referenced from chapter IV).

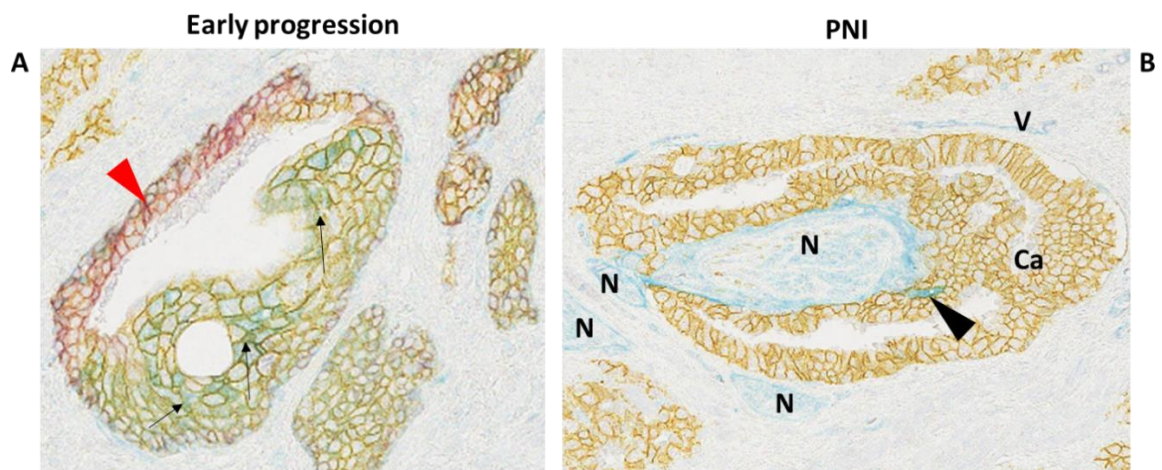


**Figure 5.2.  $\alpha 6$  integrin,  $\alpha 3$  integrin and E-cadherin expression using chromogen multiplex IHC.** Human prostate FFPE tissue immunostained with anti- $\alpha 3$  antibody (magenta), anti- $\alpha 6$  antibody (teal) and anti-E-cadherin antibody (yellow). **(A)** Prostate gland with early cancer progression. Anti- $\alpha 3$  demonstrates focal expression (red arrowhead). Anti- $\alpha 6$  and anti-E-cadherin demonstrate co-distribution intensity (green) within the areas with early progression features (black arrows). **(B)** Perineural invasion (PNI). Anti- $\alpha 3$  downregulated and showing lack of signal. Anti- $\alpha 6$  showing positive expression in nerves (N) and endothelial cells of vessels (V) and demonstrates minimal area of co-distribution intensity (green) with E-cadherin in cancer cluster (black arrowhead). [Images at 10x magnification].

*Loss of  $\alpha 3$  integrin correlates with aggressive prostate cancer.* Serial sections of human prostate cancer tissue were immunostained with chromogen multiplex IHC using antibodies targeting  $\alpha 6$ , and  $\alpha 3$  integrins and the optimized dilution of anti-E-cadherin antibody. A difference in immunostaining pattern was observed in aggressive tumor samples compared to normal glands. In regions of normal architecture, membrane expression of  $\alpha 3$  integrin,  $\alpha 6$  integrin and E-cadherin were co-distributed. Areas of pre-malignant transition and areas of aggressive cancer demonstrated a loss of  $\alpha 3$  integrin and E-cadherin while expressing  $\alpha 6$  integrin (**Figure 5.3, A**).

*Single biomarker localization of  $\alpha 3$  integrin,  $\alpha 6$  integrins and E-cadherin expression with chromogen multiplex IHC:* Image analysis was performed utilizing a hyperspectral research imager (HRI) capable of individual red green blue (RGB) wavelength channel selection. The research imager demonstrated the ability to detect individual colors within a chromogen multiplex array using darkfield unmixed absorbance images. The result demonstrated individual expression levels of  $\alpha 3$  integrin,  $\alpha 6$  integrin and E-cadherin within co-distributed regions and within the tissue where only  $\alpha 6$  integrin and E-cadherin were co-distributed (**Figure 5.3, B**). The co-distribution of  $\alpha 6$  integrin and E-cadherin were distributed to pre-malignant lesions (area of transition) and tumor clusters within normal glands.

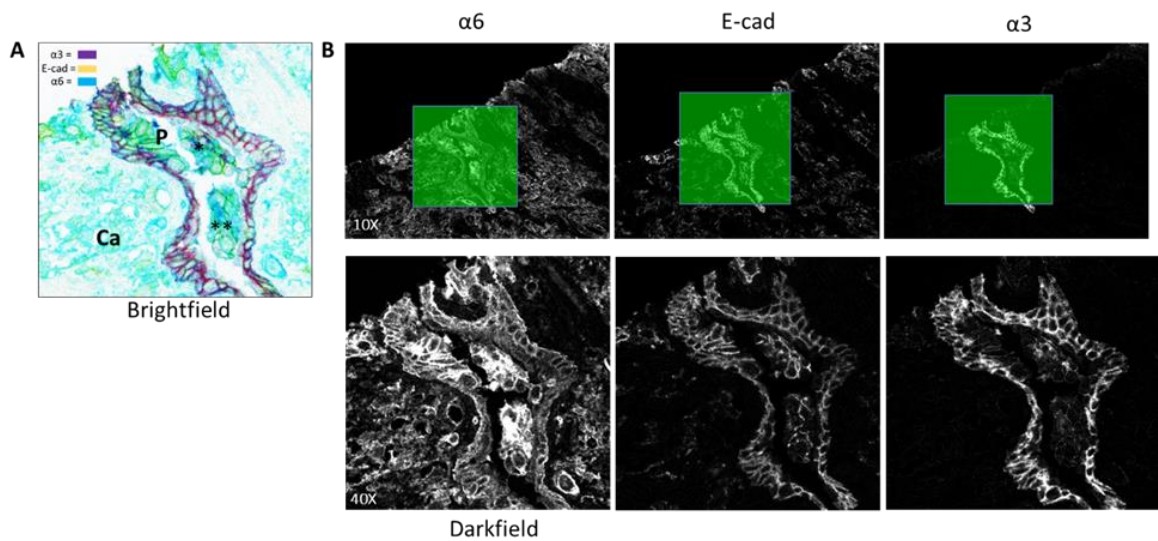


**Figure 5.3.  $\alpha 6$  integrin,  $\alpha 3$  integrin and E-cadherin distribution in prostate cancer.** Serial sections of human prostate cancer tissue were immunostained using chromogen multiplex assay (n=4). Normal gland within cancer area (Ca) with area of cellular transition representative of PIN (P) and cancer clusters within the lumen (\*\*). (A) Brightfield image of antibody chromogen detection with anti- $\alpha 3$  antibody (magenta), anti- $\alpha 6$  antibody (teal) and anti-E-cadherin (yellow). (B) Darkfield unmixed absorbance images of region of interest (ROI) at 10x magnification (green box) of  $\alpha 6$  integrin (top left panel), E-cadherin (top middle panel) and  $\alpha 3$  integrin (top right panel). Bottom panel is magnified image of boxed section of ROI. [Magnification, 40x].

*$\alpha$ 6 integrin and E-cadherin co-distribution ratio correlate to aggressive status:*

Next, a quantitative analysis algorithm was developed to determine the ratio amounts of anti- $\alpha$ 6 and anti-E-cadherin antibody co-distribution within a specific ROI to determine stage of aggression. The ratio of antibody co-distribution would demonstrate the level in which  $\alpha$ 6 integrin and E-cadherin receptors co-distribute, indicating cellular cohesiveness. Each ROI was given an arbitrary designation of "PIN", "high-grade" or "invasion" to categorize each. Absorbance wavelength channel selections, for  $\alpha$ 6 integrin and E-cadherin expression only, demonstrated co-distribution ratios of quantifiable pixel intensities in darkfield images (**Figure 5.4, A**). Heat map conversions of pixel intensities indicated a greater than 40 percent ratio of  $\alpha$ 6 integrin and E-cadherin in pre-malignant "PIN" region, less than 40 percent ratio "high-grade" tumor cluster and low less than 20 percent ratio in the "invasive" cluster (**Figure 5.4, B**). In contrast, only intermittent ratios of low intensity were observed in the aggressive cancer areas outside the gland and were not analyzed. The analysis indicated a decreasing percent ratio of  $\alpha$ 6 integrin and E-cadherin co-distribution occurs as a result of cancer progression (**Figure 5.4, C**). Individual analysis showed that  $\alpha$ 6 integrin increases with tumor progression, whereas a decrease in overall E-cadherin surface expression occurs (**Figure 5.4, D**).

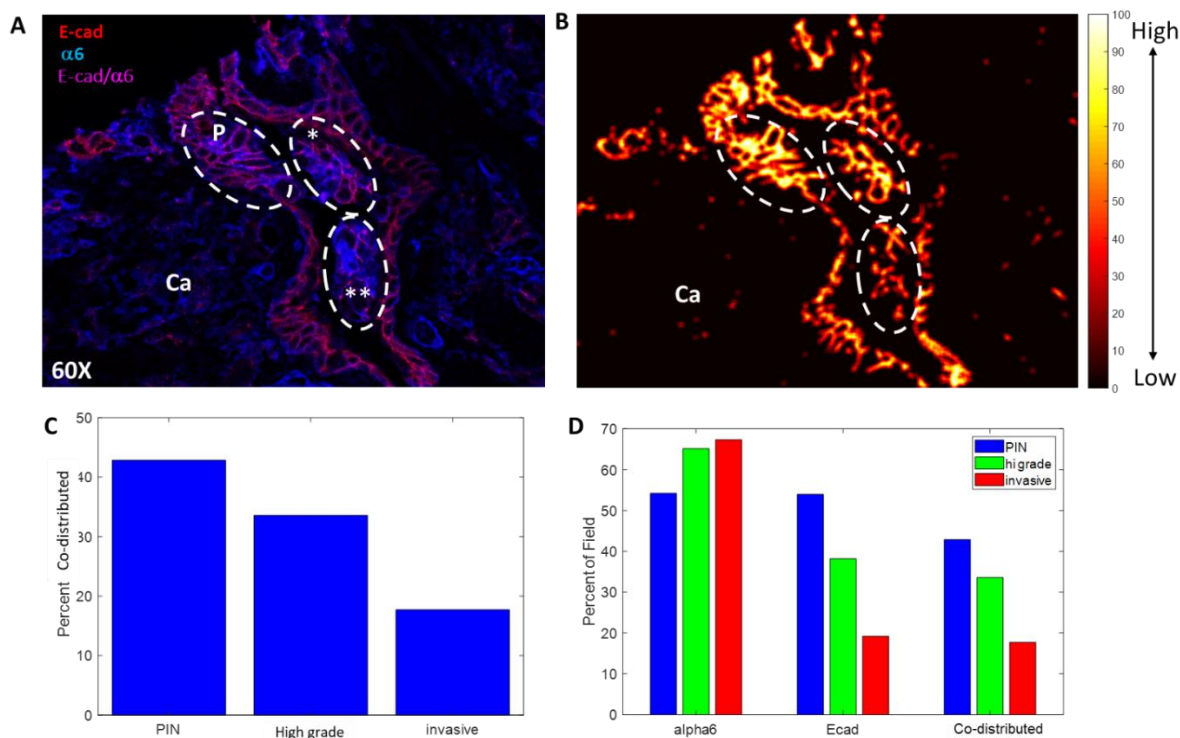


**Figure 5.4. Percent ratio of  $\alpha 6$  integrin and E-cadherin indicate stage of progression.** Unmixed darkfield absorbance image of chromogen multiplex with channel selection for anti- $\alpha 6$  antibody (teal) and anti-E-cadherin antibody (red) only. **(A)** Image of  $\alpha 6$  integrin and E-cadherin dual expression (co-distribution) in ROI with normal gland within cancer area (**Ca**) and annotated area representative of pre-malignant PIN transition (**P**) within normal gland, and annotated tumor clusters representative of high-grade (\*) and invasive (\*\*) within the gland. **(B)** Heat map of panel A depicting of pixel intensity of  $\alpha 6$  integrin and E-cadherin co-distribution in annotated regions (see panel A) and cancer area (**Ca**). **(C)** Box chart analysis representative of  $\alpha 6$  integrin and E-cadherin percent co-distribution ratios within ROIs. **(D)** Box chart analysis representative of individual and co-distributed  $\alpha 6$  integrin and E-cadherin percentage of intensity level detected within each field of interest.

## DISCUSSION

Prostate cancer progression from a confined non-invasive cluster to aggressive and invasive cohesive phenotype requires dynamic regulatory modulation of cell-matrix and cell-cell adhesion. The regulation necessary for generation of intracellular forces, signal transduction and transcriptional events for migration requires a coordinated crosstalk between integrins and E-cadherin (Canel *et al.*, 2013; Mui *et al.*, 2016). This chapter identifies localization expression patterns of  $\alpha 3$  and  $\alpha 6$  integrins in association with E-cadherin in tissues associated with PCa progression. A multiplexed chromogenic assay was used to visualize these localization patterns and to develop a method to quantify protein co-distribution.

The mechanotransduction of signals from the ECM to intracellular components drives the integrin-cadherin crosstalk, which organizes intracellular components for coordination of movement, transcriptional events, polarization and directional migration (Mui *et al.*, 2016). Integrins are the cells signaling molecules and are a critical link between the ECM and the cytoskeleton of the cell (Barczyk *et al.*, 2009). The “outside-in” and “inside-out” signaling transduced by these receptors, in reaction to engagement of external and internal cues (respectively), affect the cellular physiology and activity. The regulation of integrin function is crucial for the formation of dynamic cell-matrix focal adhesive structures for cellular motility. The coordinated assembly and disassembly of these adhesive structures are required for cellular migration (Parsons *et al.*, 2010). The crosstalk between integrins and E-cadherin is thought to be mediated by the physical disruption of cell-cell

adhesions that is driven by integrin-induced alterations in myosin contractility (de Rooij *et al.*, 2005; Martinez-Rico *et al.*, 2010).

The cross talk that occurs between the dynamic interplay between cell-cell adhesion and cell-matrix adhesion signaling contributes to the plasticity of tumor cells allowing them to respond to external cues, driving optimal migration and invasion (Canel *et al.*, 2013). Historically, this action is the process utilized in early embryogenesis and morphogenesis but is co-opted by invasive tumor collectives. Cell migration is complex due to the array of mechanochemical signaling events involving spatiotemporal coordination of cell-cell, cell-matrix and intracellular tension. Fine balance between substrate traction and intercellular adhesion controls tumor collective migration. One group described the crosstalk that occurs between cells, stating that an adherens junction proportional size increase due to increased endogenous stress (Liu *et al.*, 2010; reviewed by Mui *et al.*, 2016). It was also mentioned that increased traction forces from the ECM could affect cell-cell adhesion and result in proportional increase in endogenous tension at cell-cell junctions (Maruthamuthu *et al.*, 2011).

Our results in PCa tissues utilizing multiplex chromogen IHC with antibodies for  $\alpha 3$  and  $\alpha 6$  integrins along with an E-cadherin antibody corroborated these findings, which was demonstrated in the co-distribution of  $\alpha 6$  integrin and E-cadherin in early progressive events. The loss of  $\alpha 3$  integrin would appear to be a key event associated with early tumor progression. Since previous chapters have established that the loss of  $\alpha 3$  integrin plays a role in production of  $\alpha 6$  integrin



tumor variant and regulation of E-cadherin expression, it's likely a factor in mediating crosstalk. Loss of  $\alpha3$  integrin expression in pre-malignant lesions in PCa tissues may suggest increased endogenous stresses leading to signals upregulating  $\alpha6$  integrin and E-cadherin co-distribution and formation of tumor-associated complexes, such as those found in Marchio *et al.*, 2012.

The development of a multiplex detection assay that is quantifiable for localization patterns of protein biomarkers relevant to tumor progression could be important for patients. This allows for detection utilizing one slide, which reduces the need for invasive patient tissue sampling. In addition, it allows interrogation of several targets at one time potentially to assess biophysical associations relevant to disease progression. Additionally, the development of an algorithm applied to the detection of multiplex images is beneficial in assigning numerical value to biological marker co-distribution and creating data sets to categorize tumor aggressiveness. Future research utilizing chromogen IHC (and quantitative algorithms) on proximity detection assays with antibodies for  $\alpha6$  integrin and the tumor specific variant  $\alpha6p$  may provide more information to differentiating tumor aggressiveness.

## VI. Cohesive collective tumor invasion in PCa

### ABSTRACT

Prostate cancer is a unique disease that has two different phenotypes, a slow growing confined form (indolent), and an aggressive form involving invasive cohesive collectives of tumor cells. However, little is known as to which early mechanisms are responsible for initiating an indolent tumor to switch and become aggressive and disseminate. Using gene edited DU145 prostate cancer cell lines in mouse models, we investigated how these tumor collectives invade through the muscle of the diaphragm to model the environment of the ECM. We demonstrated the deletion of  $\alpha 3$  integrin results in increased invasion, suggesting the removal of  $\alpha 3$  integrin plays a role in initiating a more efficient invasive subclass of aggressive tumor collective. We also showed that the deletion of  $\alpha 3$  integrin promotes production of  $\alpha 6$  integrin cleavage product  $\alpha 6p$  with altered biophysical adhesive properties. The perturbation of the  $\alpha 6$  cleavage integrin, by creating an uncleavable product ( $\alpha 6^{AA}$ ) with the substitution of arginine for alanine (R594A-595A) using CRISPR Cas 9 gene editing, reduced tumor collective invasion through the muscle. Interestingly, the inability to cleave the integrin also promoted an increase of E-cadherin protein expression, suggesting a gain of phenotype switch that activates pathways to increase cell-cell adhesion. Together, these data suggest that loss of  $\alpha 3$  integrin in human tumors will promote a metastatic phenotype of cohesive tumor collectives. These collectives utilize the  $\alpha 6$  integrin

cleavage product that enhances migration, but can be inhibited by a function block of the  $\alpha 6$  cleavage that in turn, increases cell-cell adhesion to block invasion.

## INTRODUCTION

Prostate cancer is a neurotrophic disease that arises from the peripheral zone of the prostate gland (reviewed by Harryman *et al.*, 2016). These cohesive tumor-cell clusters develop as intraepithelial neoplasia that migrate through muscle and escape the gland via perineural invasion for hematogenous spread to distant tissues (Harryman *et al.*, 2016). The intratumoral heterogeneity of prostate cancers makes it extremely difficult to identify which tumors may switch and develop the propensity to invade as a cohesive collective. Previous chapters have shown that  $\alpha 6$  and  $\alpha 3$  integrins play a critical role in progression of these invasive tumor clusters. Invasive prostate cancer clusters uniformly express  $\alpha 6$  integrin, and laminin-10, which is the predominant laminin form in muscle and nerve microenvironments (Harryman *et al.*, 2016). The  $\alpha 6$  integrin primarily associates with laminin-10, which is utilized for focal adhesions during cellular migration. Depletion of the  $\alpha 3$  integrin significantly increased dissemination of cohesive tumor clusters to distant tissue.

The current strategies for early stage detection and diagnosis of disease have improved the 5-year survival rate to ~100% and has resulted in a 40% decrease in mortality rates for those with localized prostate cancer. However, the 5-year survival rate of patients presenting with extracapsular escape remains at less than 30% (Siegel *et al.*, 2019). In addition, statistics show that the incidence of

metastatic PCa disease increased 72% between 2004 and 2013 in a sample of more than 700,000 men diagnosed with prostate cancer (Weiner *et al.*, 2016; Harryman *et al.*, 2016). Therefore, in spite of improvements in detection, the incidence of metastatic disease remains a significant issue. The principle modes of tumor dissemination that have long been the focus study of researchers for decades are single cell and collective tumor migration. Single cell migration is the best studied mechanism for cell movement *in vitro* and contributes to *in vivo* physiological motility processes such as tissue development, immune surveillance and cancer invasion and metastasis (Ridley *et al.*, 2003; Friedl and Gilmore., 2009). However, collective cell migration is prevalent in many cancer types and is emerging as a major driver of embryonic development, organogenesis, tissue homeostasis and tumor dissemination (Friedl and Gilmore., 2009; Mishra *et al.*, 2019).

Most research models suggest that metastases are seeded by single cells that have originated from the primary tumor, but increasing evidence is demonstrating that collective tumors traveling together is required for successful seeding (Chueng and Ewald., 2016). Collective cell migration is considered the second mode of cellular movement (Vaughn *et al.*, 1966; Friedl, Hegerfeldt and Tusch., 2004; Friedl and Gilmore., 2009). The migration of cohesive cell collectives is an event that occurs in early embryonic development that is necessary for development of complex tissues and organic systems. This early morphogenetic event is the hallmark of tissue remodeling and development. It is this mechanism of the normal

developmental process that is co-opted by aggressive tumors and is a focus of this study.

One of the most popular hypotheses of tumor cellular invasion and migration postulates the involvement of cellular epithelial-mesenchymal transition or EMT. The concept maintains single cells that are undergoing EMT detach from the primary tumor and disseminate to metastatic sites (Friedl and Wolf., 2010; Bronsert *et al.*, 2014). According to some researchers, metastasis by EMT may primarily occur in epithelial carcinomas, however; this has not been observed among clinical pathologists studying human material (Talmadge and Filder., 2010) and metastasis has been proposed in prostate cancers to occur by tubulogenesis (Nagle and Cress., 2011). EMT is associated with the loss of E-cadherin from the adherens junction and involves the switch from keratin to vimentin, a mesenchymal filament (Hurst and Welch., 2011; Nagle and Cress., 2011). However, it is recognized that the reduction of E-cadherin is not uniform in carcinomas. This was due to findings in a study in which complete deficiency of E-cadherin was found in some cancers whereas only the membranous localization is lost in the dedifferentiated region of the invasive front of tumors (Giehl and Menke., 2008). In addition, some models state that when EMT inducing signals are lost, tumor cells may reverse the process and elicit a mesenchymal to epithelial transition (MET) (Chaffer *et al.*, 2006; Hugo *et al.*, 2007; Nagle and Cress., 2011). Invasive prostate cancer collectives remain epithelial and do not require the transition to an epithelial phenotype making it an EMT-independent event (Nagle and Cress., 2011).

Collective tumor migration requires integrin signaling for migration of cells while simultaneously cell-cell adhesion is necessary for motile cells (Yano *et al.*, 2004). This cell-cell based collective adhesion is necessary for cohesive tumor invasion through the prostate muscle. Friedl and Gilmore have described three key hallmark properties of collective cell migration that are considered basics of the mechanism: (1) cell clusters remain physically connected and cell-cell junctions are preserved; (2) multicellular polarity along with cytoskeleton organization producing adhesive friction and protrusion of the crawling edge of the cluster while preserving cell-cell junctions; (3) cohesive collectives of cells modify the tissue structures of vessels by which they travel, clearing a pathway or by the deposition of elements of the basement membrane (reviewed in Friedl and Gilmore., 2009; Harryman *et al.*, 2016).

These cohesive cellular units are bound together laterally by maintaining what Friedl and Gilmore describe as 'supracellular properties' fostered by the cell-cell protein adhesions at the adherens junctions. These properties offer the tumor cohesive unit the pliability to transverse the extracellular milieu with the use of cellular polarization, directionality and modification. Cellular cues and biochemical signals from the surrounding stromal environment are transduced into action potential that induce cell state plasticity. The cell-ECM presence of  $\beta 4$  and  $\alpha 3$  integrins supports stronger cell-cell affinity in normal cells. However, these receptors are downregulated in cohesive tumor collectives. This leads to increased expression of  $\alpha 6$  integrin and co-distribution with E-cadherin, which involves

“receptor crosstalk” that modulates the cell-cell adherens junctions that allows migration of these cohesive collectives.

Here the loss of  $\alpha 3$  integrin is identified as a key event that leads to the development and exacerbates dissemination of PCa cohesive tumor collectives through muscle. This relies on increased production of the  $\alpha 6$  integrin tumor variant  $\alpha 6p$  and modulation of E-cadherin surface expression. Interestingly, this pinpoints a detectable occurrence of that may define a subclass indicating metastatic potential. While there are several biomarkers available to identify aggressive clusters that have already invaded, there has yet to be specific biomarkers characterized to differentiate between those that remain static and those that present with early invasive potential. Detection of this early event may be critical to diagnose those that are at risk for invasive disease and allow objective decisions for appropriate therapy.

## RESULTS

*Tumor Muscle Invasion Assay:* The initial objective of this research was to investigate the ability of the  $\alpha 6^{AA}$  to inhibit the onset of cohesive collective tumor muscle invasion and to elucidate the significance the role  $\alpha 3$  integrin loss plays in tumor invasion and extravasation through muscle. According to previous publications, tumor onset is independent of the presence of  $\alpha 3$  integrin but depletion results in reduced survival and increased tumor growth and vascularization (Ramovs *et al.*, 2019). Similar results were reported with a PCa study in Varzvand *et al.*, 2013 in which  $\alpha 3$  integrin was silenced in prostate

carcinoma cell lines. In order to facilitate a model for collective prostate cancer muscle invasion, DU145 cells were utilized. A CRISPR Cas9  $\alpha 3$  integrin gene deletion was performed to generate a DU145 cell line lacking  $\alpha 3$  integrin surface expression. In addition, a non-cleavable  $\alpha 6$  integrin ( $\alpha 6^{AA}$ ) mutant cell line was generated and transfected into DU145 cells to inhibit cleavage of the  $\alpha 6$  integrin at amino acid (aa) region 594A-595A (alanine residues). These cell lines were allowed to culture and were harvested for injection into severe combined immunodeficient (SCID) mice for tumor dissemination.

*SCID mouse xenograft models:* To demonstrate the role that the loss of  $\alpha 3$  integrin and the cleavage of  $\alpha 6$  integrin plays in the formation of tumor colonies and collective tumor muscle invasion, we injected DU145 CRISPR Cas9 prostate tumor cultured cell lines into SCID mice. According to previous testing, DU145 cells introduced into male SCID mice will readily produce tumors (Rubenstein *et al.*, 2019). The purpose was to generate invasive tumors targeting diaphragm invasion. The murine diaphragm mimics the muscle stroma of the prostate, containing an ample vascular supply, sensory and motor nerve endings, stromal fibroblasts and muscle cells and contains both smooth and skeletal muscle features (McCandless *et al.*, 1997; Rubenstein *et al.*, 2019). These mice contain a loss of function homozygous mutation on the PRKDC gene that results in absence of mature T and B lymphocytes, as well as natural killer (NK) cells, and a Null mutation in the allele of the IL2 gamma chain (ILR2 $\gamma$ ) to eliminate cytokine signaling pathways. Therefore, these mice are severely immunocompromised and



unable to mount a sufficient immune response making them a prime candidate for model tumor invasion assays.

Three tumor cell lines, along with a normal cell line, were selected for the study. The tumor cell lines were DU145  $\alpha 6$ WT, DU145  $\alpha 3$  knockout ( $\alpha 3$ KO) and the DU145  $\alpha 6^{AA}$  mutant representing the non-cleavable full-length  $\alpha 6$  integrin. Five mice from each were selected to represent the cell line category for observation. The DU145 cell cultures were administered via injection through the peritoneum. The time point for sample harvest was 8 weeks. However, some of the animals began to exhibit ascites at 5 weeks indicating distress due to tumor burden in which a fluid drain was accomplished and the subjects were allowed to continue to reach a 6-week and 8-week interval before harvest. All the cell lines demonstrated tumor colonies on the diaphragm surface at the end of the 8-week period. At each target time point, subjects from each category were sacrificed and portions of the small bowel were removed and placed into 50ml vials containing 10% Neutral Buffered Formalin (NBF) and stored for a twenty-four-hour period to allow tissue fixation. After removal of the small bowel sections, the subjects were placed with open peritoneal cavities into a container with approximately 20mls 10% NBF for twenty-four hour to allow tissue fixation.

After completion of the twenty-four-hour tissue fixation, the fixed diaphragm samples were removed from the 10% NBF and placed in laminar flow hood. The diaphragms samples were excised from the subjects and the superior (top) side was blotted with cotton tipped swabs to remove excess moisture for application of

India ink to demarcate superior from inferior (bottom) side of the diaphragm. Samples were then placed into separately labeled 50ml vials containing 70% ethanol (EtOH) for overnight incubation. For each subject, the 10% NBF fixed sections of the small bowel were removed and also placed into separately labeled 50mL vials containing 70% EtOH for potential tumor dissemination and genomic testing. Images of the sample diaphragms were captured to demonstrate the amount of tumor burden and any potential evidence of superior side dissemination. Both the DU145  $\alpha 6^{WT}$  and DU145  $\alpha 3^{KO}$  samples were observed to exhibit high amount of tumor burden throughout the peritoneal cavity whereas the DU145  $\alpha 6^{AA}$  mutant samples demonstrated a lower amount of burden (**Figure 6.1**).

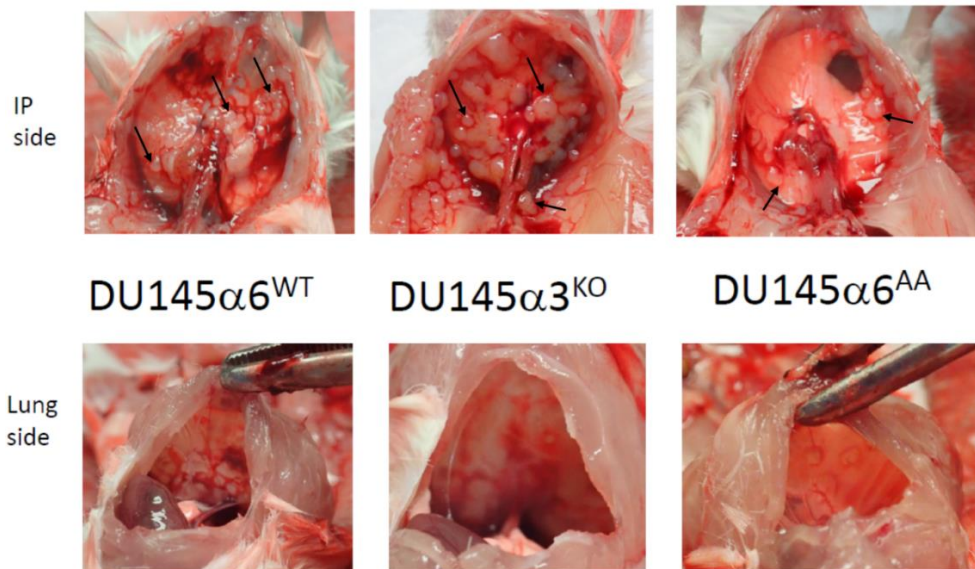


**Figure 6.1. DU145 diaphragm tumor burden.** Gross images of diaphragm sample harvest. (**IP side**) Intraperitoneal side (diaphragm side) showing tumor burden for DU145 WT,  $\alpha 3^{KO}$ , and  $\alpha 6^{AA}$ . (**Lung side**) (Superior side) evaluating tumor invasion through the diaphragm to the lung side. DU145 WT and DU145  $\alpha 3^{KO}$  demonstrate substantial amount of tumor burden (black arrows) on IP side compared to DU145  $\alpha 6^{AA}$  exhibiting minute tumor burden amount (black arrows).

After 70% EtOH storage, each sample tissue (small bowel and diaphragm) were sliced into approximately 3-4 sections (strips) and paraffin embedded for serial sectioning. The sample diaphragms were each placed on the side to orient the samples with the superior side (with India ink) in the same direction. Unstained FFPE serial section slides were prepared for immunostaining. The sectioned slides were allowed to dry in a laminar flow hood for a 24-hour period and afterwards the first slide of the series in each sample category was stained with hematoxylin and eosin (H&E). H&E stained slide images of 1x, 4x, 10x and 20x were captured to evaluate any tumor invasion through the diaphragm.

The H&E stained slides demonstrated visual evidence of tumor burden for each category of cell line with the DU145  $\alpha 6^{WT}$  and DU145  $\alpha 3^{KO}$  displaying an increased incidence of collective tumor muscle invasion with more frequency compared to the DU145  $\alpha 6^{AA}$  (**Figure 6.2**). The 6-week incidence of tumor invasion sites was counted and the total amount was tabulated for each 4mm sample diaphragm strip for each test category, both diaphragm (**Table 2**) and small bowel (**Table 3**). The 6-week sample mice tested with DU145  $\alpha 6^{WT}$  resulted in approximately forty-nine invasion sites on the diaphragm strips, this totaled to be an average of approximately four invasion sites per section of diaphragm with the maximum depth of penetration exhibited at 604 units. The DU145  $\alpha 3^{KO}$  6-week specimens resulted in an approximate thirty-nine tumor invasion sites averaging approximately three per section of diaphragm with the maximum depth of invasion presenting at 363 units. In contrast, the DU145  $\alpha 6^{AA}$  sample mutants exhibited only five invasion sites averaging less than one invasion site per section of

diaphragm with the maximum depth of penetrant muscle invasion recorded at 270 units.

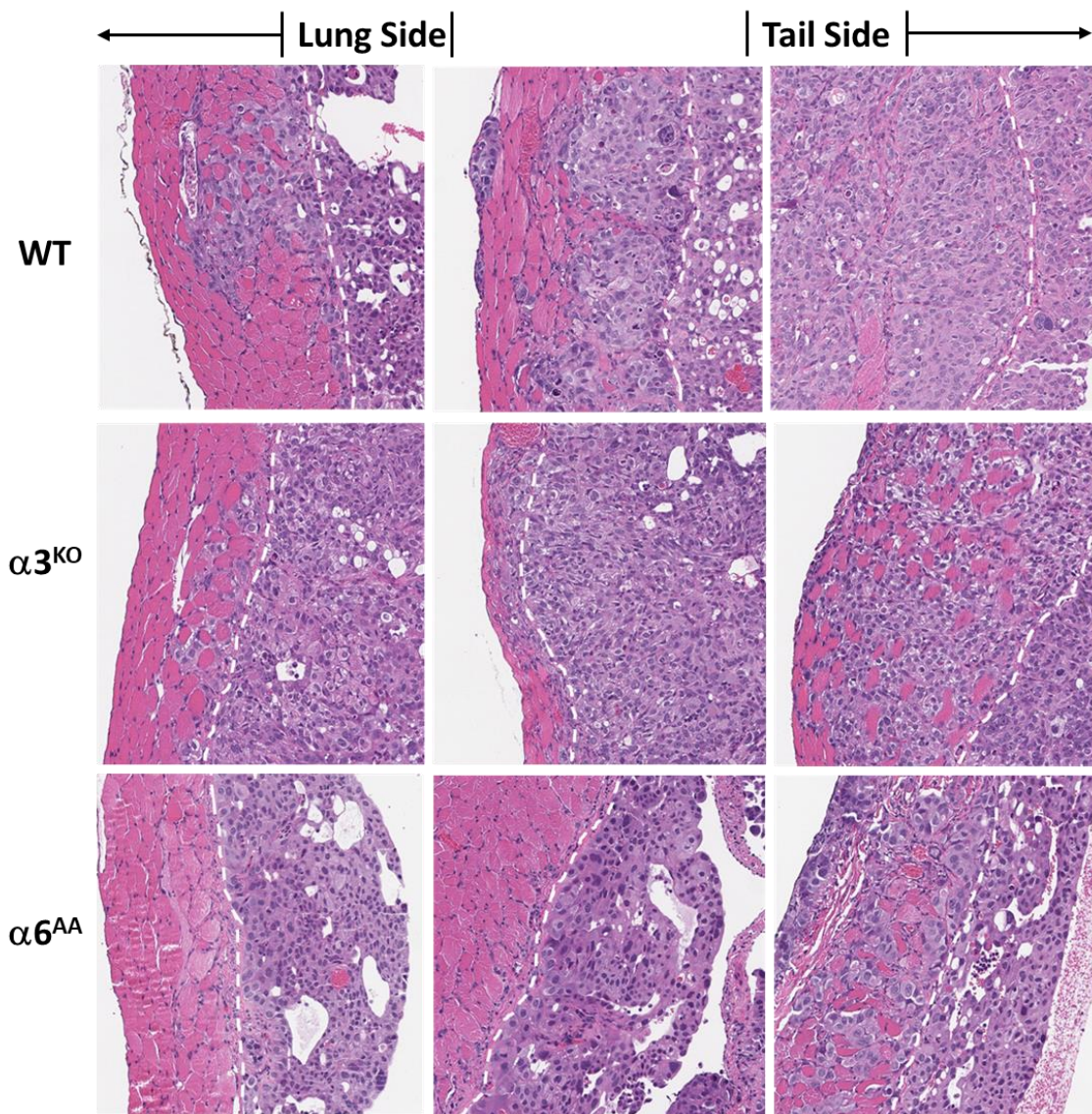
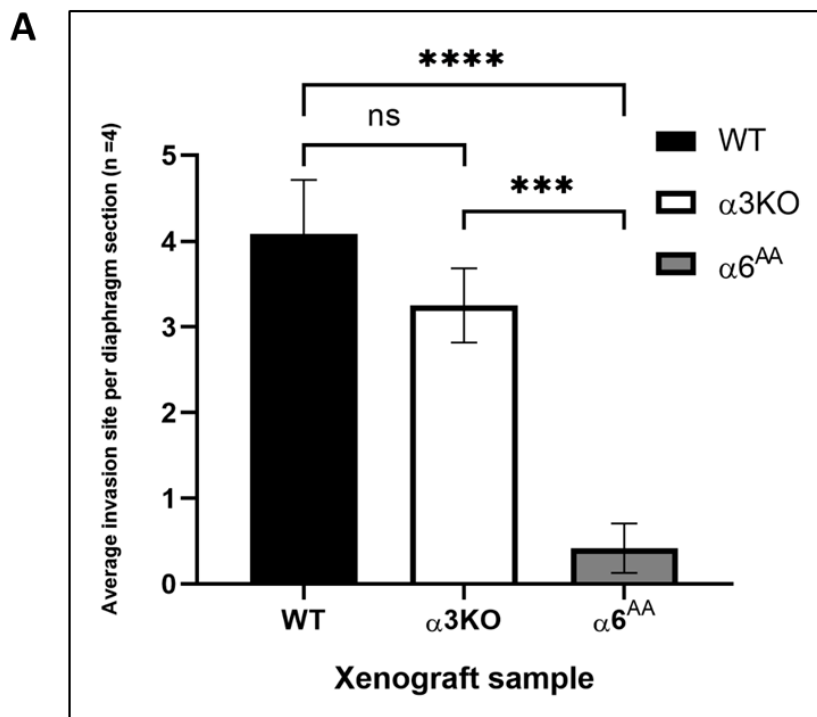


**Figure 6.2. Hematoxylin and eosin stained xenograft PCa tissue slides.** Sample slides with collective tumor invasion through muscle diaphragm indicated by dotted white line. **DU145 WT** tissue slides demonstrating collective tumor invasion through each muscle diaphragm (Top row). **DU145  $\alpha 3^{KO}$**  tissue slides demonstrating collective tumor invasion through each muscle diaphragm (middle row). **DU145  $\alpha 6^{AA}$**  tissue slides demonstrating tumor colonies remaining on the surface of muscle diaphragm (bottom left and middle panel) and tumor chord invasion through muscle diaphragm (bottom right panel). [Images, 10x magnification]

The average number of invasion sites for each cell line was tabulated and analyzed for comparisons for any significant differences or parallels. The data indicates no significant difference in amount of tumor sites between the DU145 WT and the DU145  $\alpha 3^{KO}$ , but significant difference between DU145  $\alpha 6^{AA}$  and DU145 WT and DU145  $\alpha 3^{KO}$  (**Figure 6.3**). Suggesting significant inhibition of invasion by the  $\alpha 6^{AA}$ .

The depth of tumor invasion on the H&E stained slides was measured (in  $\mu\text{m}$ ) utilizing the Aperio AT2 software and analyzed with GraphPad analysis to determine the maximum depth per each sample type. The analysis of the 6-week DU145 samples indicated that a slightly significant difference existed between the DU145 WT and  $\alpha 3^{KO}$  but did not indicate a significant difference in depth of invasion between the DU145  $\alpha 3$  and  $\alpha 6$  samples (**Figure 6.4, A and B**). However, this may be an artifact of the diaphragm size and shape since each diaphragm exhibited variable thicknesses even within each sample. It must also be noted that there were fewer sites of diaphragm invasion for the  $\alpha 6^{AA}$ , which may have also skewed the average. The DU145 WT 8-week specimen demonstrated approximately forty-five tumor invasion sites within the diaphragm sections and incurred a maximum depth of approximately 518 units (**supplemental data, Figure S1**).



**B**

Tukey's multiple comparisons test	Mean Diff.	95.00% CI of diff.	Significant ?	Summary	Adjusted P Value
WT vs. $\alpha 3$ KO	0.8333	-0.6081 to 2.275	No	ns	0.3384
WT vs. $\alpha 6^{AA}$	3.667	2.225 to 5.108	Yes	****	<0.0001
$\alpha 3$ KO vs. $\alpha 6^{AA}$	2.833	1.392 to 4.275	Yes	***	0.0001

**Figure 6.3. Inhibition of  $\alpha 6$  integrin cleavage reduces tumor invasion sites. (A)** Average number of tumor invasion sites per diaphragm section charted for DU145 WT,  $\alpha 3$ , and  $\alpha 6$  integrin xenografts. **(B)** Comparison of invasion sites across each xenograft cell line. Statistical significance calculated for mean differential between each cell line as two-way ANOVA GraphPAD analysis, (n=4).

*Loss of  $\alpha 3$  integrin results in highly metastatic phenotype.* Interestingly, at 6 weeks, the mice injected with the DU145  $\alpha 3^{\text{KO}}$  tumor cells displayed the highest incidence of tumor dissemination to the small bowel with a total of fifteen sites compared to five totaled for the DU145  $\alpha 6^{\text{WT}}$  and just one tumor incidence with mice burdened with DU145  $\alpha 6^{\text{AA}}$  mutant tumors (**Figure 6.4**). However, visual evidence suggests that the tumor clusters did not invade through the muscle of the small bowel but only colonized on the muscle surface. Nevertheless, the tumors did exhibit invasion through the pancreatic space (**Figure 6.5**). This was intriguing result and appeared similar to the results in previous experiments accomplished by other groups utilizing WT,  $\alpha 3$  integrin silenced ( $\alpha 3\text{si}$ ),  $\alpha 6$  integrin-silenced ( $\alpha 6\text{si}$ ) and  $\alpha 3$  and  $\alpha 6$  integrin silenced ( $\alpha 3/\alpha 6\text{si}$ ) GS689.Li prostate carcinoma cell lines inoculated via tail vein into SCID BALB-c mice (Varzavand *et al.*, 2013). Their bioluminescence imaging (BLI) results showed after 5 weeks, the tumor burden caused by  $\alpha 3\text{si}$  cell dissemination to the lungs appeared greater than burden caused by the WT.

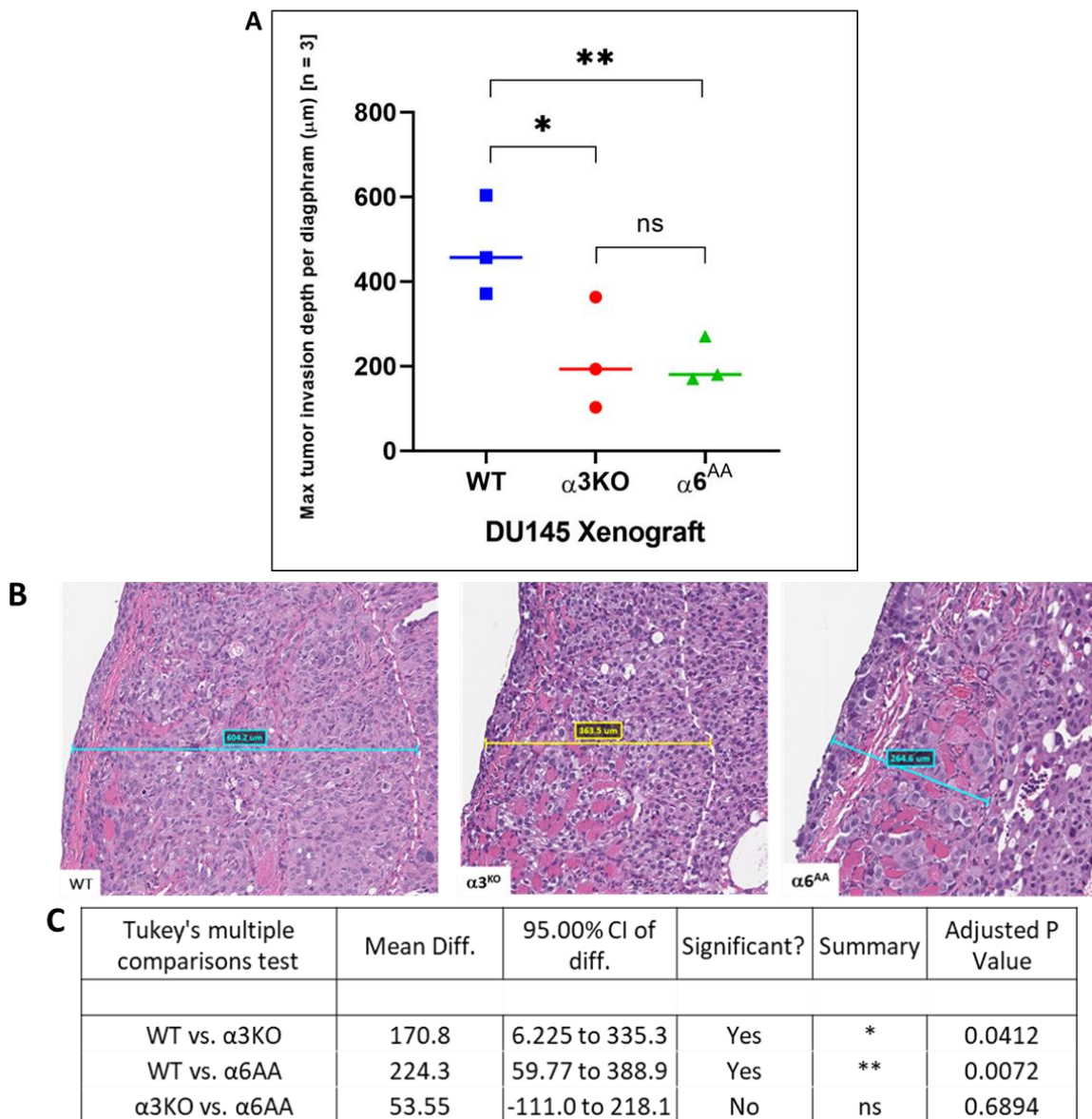


**Figure 6.4. Maximum depth of tumor invasion in mouse diaphragms. (A)** Average of maximum tumor invasion depth for observed diaphragm charted for DU145 WT,  $\alpha 3^{\text{KO}}$ ,  $\alpha 6^{\text{AA}}$  xenografts. **(B)** H&E stained slide images with maximum tumor depth measurement for DU145 WT (left panel), DU145  $\alpha 3^{\text{KO}}$  (middle panel), and DU145  $\alpha 6^{\text{AA}}$  (right panel). **(C)** Comparison of maximum tumor depths across each xenograft cell line. Statistical mean difference calculated as two-way ANOVA GraphPAD analysis, (n =3)



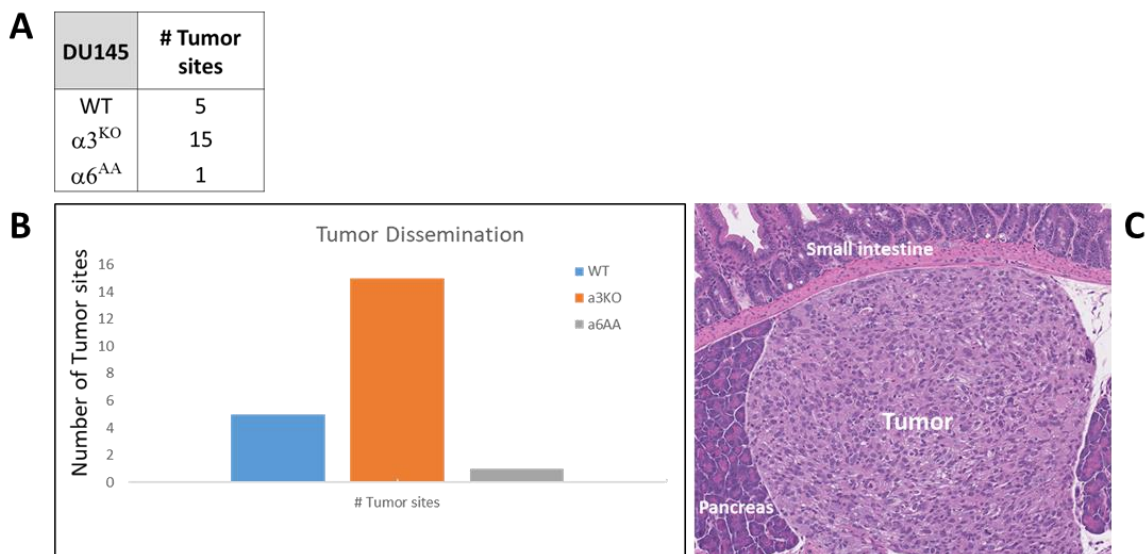


**Figure 6.5. Loss of  $\alpha 3$  integrin increases tumor dissemination to the small bowel and  $\alpha 6^{\text{AA}}$  reduces dissemination. (A)** Table containing number of tumor sites per observed disseminated to the small bowel. **(B)** Charted number of tumor sites to the small bowel per DU145 cell type. **(C)** H&E stained slide of DU145  $\alpha 3^{\text{KO}}$  collective tumor colonization on the small bowel infiltrating the pancreas. [Image, 10x magnification].

*$\alpha 6$  integrin and E-cadherin co-distribute in cohesive tumor collectives:* Immunostaining with antibodies for  $\alpha 6$  integrin and E-cadherin demonstrated specific regions in the invading tumor clusters that exhibited similar expression patterns for both proteins (**Figure 6.6, A**). However, the tumors displayed heterogeneity such that the biomarkers exhibited various localization patterns in areas of invasion. In regions indicative of migration both membrane and intracellular (cytoplasmic) localization of  $\alpha 6$  integrin and E-cadherin was observed (**Figure 6.6, B**). This observation corroborates the theory of integrin and E-cadherin crosstalk mediating tumor invasive migration through the muscle stroma.

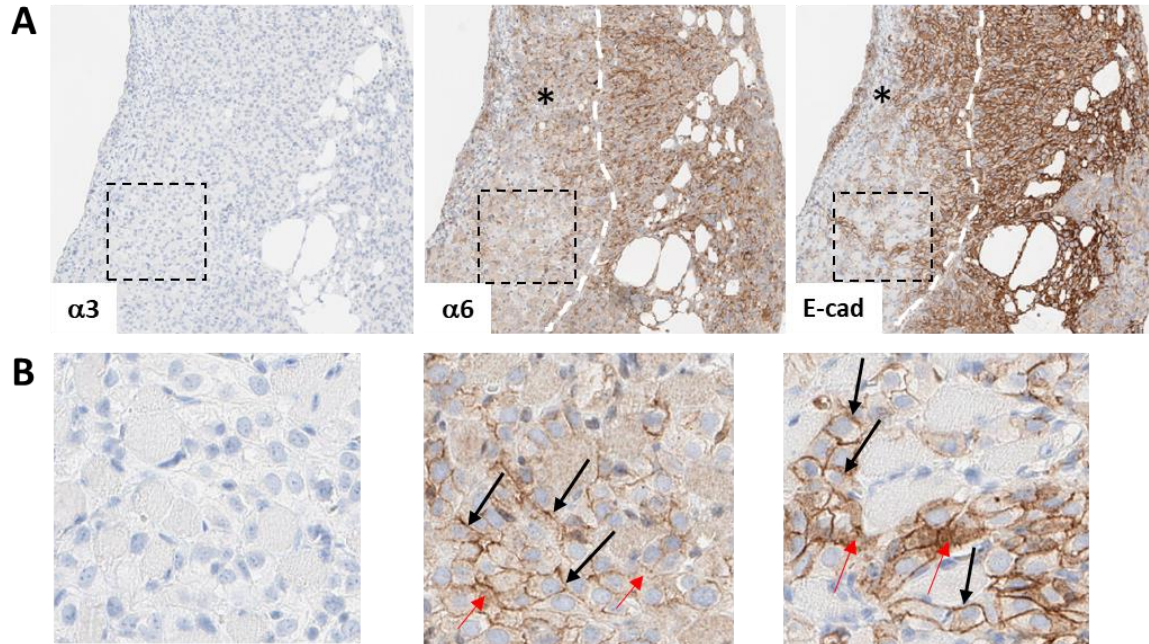


**Figure 6.6. DU145  $\alpha 3^{\text{KO}}$  xenograft  $\alpha 6$  and E-cadherin IHC expression.** Xenograft serial sections were immunostained with IHC DAB for antibodies for  $\alpha 3$  integrin,  $\alpha 6$  integrin and E-cadherin. **(A)** Images demonstrating lack of  $\alpha 3$  integrin with deletion of gene (top left panel), expression of  $\alpha 6$  integrin in tumor clusters (\*) invading through muscle diaphragm (dotted line) (top middle panel), and expression of E-cadherin in tumor clusters (\*) invading through muscle diaphragm (dotted line) top right panel). [Images 10x magnification]. **(B)** Image magnification of annotated region of tumor showing heterogeneous localization with membrane (black arrows) and cytoplasmic (red arrows) expression of  $\alpha 6$  integrin and E-cadherin in co-distributed region in which  $\alpha 3$  integrin is lost. [Magnification, 40x].

## DISCUSSION

Tumors invading as a cohesive collective have been observed in various types of aggressive cancers including prostate. Aggressive prostate cancers initiate invasion with the budding of clusters of cohesive cells from pre-malignant HGPIN lesions (as seen in chapter 2). These observations challenge the prevalent theory that invasion into the surrounding stromal environment primarily occurs as single tumor cells. We have demonstrated earlier that aberrant events leading the loss of  $\beta 4$  and  $\alpha 3$  integrins indicate the early stages of oncogenesis. We further demonstrated that the absence of the  $\alpha 3$  integrin expression increases both production of the tumor specific cleavage form of  $\alpha 6$  integrin, ( $\alpha 6p$ ), and results in decreased cell surface expression of E-cadherin.

The tumor burden with the loss of  $\alpha 3$  integrin was comparable to the WT, but interestingly resulted in a 3-fold increase in collective tumor dissemination sites to distant tissue compared to the WT. We suggest that loss of the  $\alpha 3$  integrin promotes a phenotypic switch to a subclass of tumor with a more aggressive migratory capability with the potential to metastasize. This may be a direct result of the increase in  $\alpha 6p$  production in conjunction with the downregulation of the surface expression of E-cadherin, which exacerbates the pliability of the tumor collective through the stroma.

The IHC detection with antibodies specific for  $\alpha 6$  integrin and E-cadherin demonstrated similar regions of localization in the DU145  $\alpha 3^{KO}$  sample diaphragm invasion but also exhibited areas on heterogenous expression in which the E-

cadherin demonstrated cytoplasmic localization. The co-distribution of these proteins in specific regions would support previous studies that indicate an  $\alpha 6$ /E-cadherin complex in association with aggressive tumor dissemination (Marchio et al., 2012). This would also suggest that  $\alpha 6$  integrin crosstalk with E-cadherin plays a role in regulating the cell surface or cytoplasmic expression.

Also as expected, the inhibition of the  $\alpha 6$  integrin cleavage (with  $\alpha 6^{AA}$ ) proved a benefit with a reduction of invasive cohesive tumor collectives in almost 60% (7/12) of DU145  $\alpha 6^{AA}$  sample diaphragms at the 6-week time period. Although it did not completely mitigate the formation of tumors, it reduced the number of invasive sites and dramatically inhibited cohesive dissemination to distant tissue (one site) compared to the DU145 WT (five sites) and DU145  $\alpha 3^{KO}$  (fifteen sites). The most intriguing result observed was the increased E-cadherin total protein expression as a result of the cleavage inhibition by the  $\alpha 6^{AA}$ . We demonstrated the increase in total protein expression corresponded to an increase in E-cadherin membrane localization and thus increase in tight cell-cell junctions creating cohesive clusters. It is possible that the abrogation of the  $\alpha 6$  integrin cleavage induces a constitutive activation state in the  $\alpha 6$  integrin that enacts signal transduction to a positive transcription pathway for E-cadherin upregulation. This result may indicate that a specific switch in phenotypic functionality may occur leading to decreased plasticity and therefore reduced migratory capability. Future testing to identify the specific factors or pathways that are directly involved in upregulating E-cadherin will be an important endeavor to possibly designing therapeutics possibly targeting tumor clusters before they invade.

## VII. $\alpha 6$ integrin correlative localization with PTEN and ERG expression

### ABSTRACT

The phosphatase and tensin homolog (PTEN) tumor suppressor is frequently found mutated or deregulated in various cancers. The inhibition of the PI3K/AKT pathway by PTEN modulates downstream cellular signaling molecules that have roles in regulating the cell cycle, cell survival and invasion such as mammalian target of rapamycin (mTOR). Over the past decade, the loss of PTEN expression has been an indicator of prostate cancers associated with poor prognosis and high-risk metastatic disease. In human prostate cancers PTEN loss is also associated with increased intracellular expression of  $\alpha 6$  integrin. Recently, there has also been increased correlation of aggressive prostatic disease with extracapsular escape relating to PTEN status with the ETS-related gene (ERG) overexpression. This chapter investigates the potential to correlate  $\alpha 6$  integrin membrane or cytoplasmic localization to PTEN/ERG positive or negative expression in aggressive prostate cancer. Here, we immunostained FFPE human prostate core needle biopsies (CNBs) with anti-HMWCK+p63 antibody to identify normal regions of prostate and anti-PTEN, anti-ERG and anti- $\alpha 6$  for assessment of aggressive disease. We utilized an innovative image capture platform to develop a novel quantitative algorithm by employing the QuPATH image analysis tool to evaluate and quantify immunostain localization patterns to correlate with aggressiveness. In the CNBs tested, we establish a relationship in which a shift in  $\alpha 6$  integrin localization, identified within samples evaluated for PTEN and ERG status, could allow categorization of tumors as aggressive or non-aggressive.

## INTRODUCTION

PTEN loss has been shown to be a critical pathway involved to disease progression in specific tumor types (Hollander *et al.*, 2011). Multiple studies have concluded that PTEN loss is a major contributing event in prostate cancer progression. For instance, PTEN is demonstrated to be lost in 40% of metastatic prostate cancer (Suzuki *et al.*, 1998, Han *et al.*, 2009; Taylor *et al.*, 2010), and is critical in progression to castration-resistant prostate cancer (CRPC) (Jamaspishvili *et al.*, 2018). PTEN acts as a lipid phosphatase converting phosphatidylinositol 3, 4, 5-triphosphate (PtdIns 3, 4, 5 or PIP<sub>3</sub>) into phosphatidylinositol 4, 5-biphosphate (PIP<sub>2</sub>) regulating membrane phosphoinositide composition (Sun *et al.*, 1999). This function occurs by antagonizing PI3K activity by dephosphorylating FAK and Shc adaptor proteins involved in integrin-mediated signaling. Both FAK and Shc are involved in integrin clustering in focal adhesions during cellular migration (Gillmore and Romer., 1996). In epithelial cells, E-cadherin-mediated cell-cell interaction (and possibly integrin-mediated cell-matrix interaction) lead to PIP<sub>3</sub> production, which involve downstream Rho GTPases, actin rearrangements and changes in membrane traffic (Gassama-Diagne *et al.*, 2006).

PTEN can facilitate direct interaction with these adaptors resulting in their dephosphorylation suppressing downstream effectors that mitigate the cell cycle, apoptosis, differentiation, cellular architecture and invasion (Gu *et al.*, 1998; Tamura *et al.*, 1998; Tamura *et al.*, 1999; Lee *et al.*, 1999; Yamada and Araki., 2001; Song *et al.*, 2012; Nagle *et al.*, 2013; Jamasphili *et al.*, 2018) (**Figure 7.1**). In polarized cells, PTEN localizes to the apical membrane where the function as a phosphatase prevents PIP<sub>3</sub> accumulation by converting it to PIP<sub>2</sub> (Martin-Belmonte *et al.*, 2007). By restricting PIP<sub>3</sub> localization to the basolateral membrane, PTEN plays a role in regulating cellular polarity (Gassama-Diagne *et al.*, 2006).

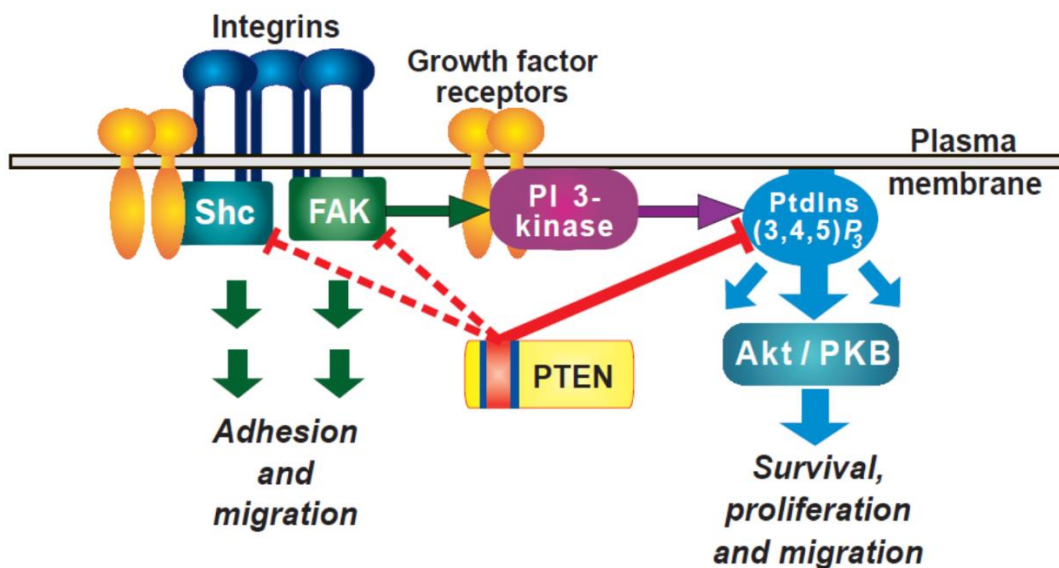


**Figure 7.1. PTEN regulates PIP<sub>3</sub>, FAK and Shc.** Schematic representation of PTEN regulation of cellular survival, proliferation and migration through inhibition of PIP<sub>3</sub> activation of the Akt pathway. In addition, PTEN phosphatase domain (red) dephosphorylates and inhibits Shc and FAK which may mediate integrin membrane expression modulating adhesion and migration (Adapted from Yamada and Araki., 2001).

The Rab11 family of small GTPases play a role in directing lipid, receptor and transporter traffic from endocytic vesicles to the plasma membrane (Lindsey and McCaffery., 2004; Campa and Hirsh., 2017). A Rab11 family of interacting proteins (FIPs) contain a C2 phospholipid-binding domain that serves as a docking site to target phosphoinositide in the cell membrane for membrane translocation (Lindsey and McCaffery., 2017). In theory, the PTEN regulation of PIP<sub>3</sub> may influence the trafficking  $\alpha$ 6 integrin to cell surface and thus impact the capability of tumor aggressiveness and mobility. Integrin trafficking to the surface promotes tumor cell invasion and metastasis through laminin-rich matrices (Bridgewater *et al.*, 2012), and this may be mediated by PTEN and Rab11 function.



The TMPRSS2/ERG fusion gene (which is associated with the protein expression of ERG) is shown to be present in approximately 50% of PCa and promotes progression *in vivo* (Ayala *et al.*, 2015). It is hypothesized that PCa negative for these gene fusions may still harbor rearrangements of other ETS family members (Tomilins *et al.*, 2006). Studies have demonstrated the TMPRSS2/ERG fusion gene can enhance prostate epithelial cell proliferation, motility and invasion (Wang *et al.*, 2008). Multiple proteins and pathways involved in prostate oncogenesis are activated in response to ERG expression including SOX2, EZH2, TGF $\beta$ , Wnt pathway and SOX9 (Tomilins *et al.*, 2008; Brase *et al.*, 2011., Wu *et al.*, 2013; Ayala *et al.*, 2015). This links ERG to pathways mediating invasive properties (Becker-Santos *et al.*, 2012). Interestingly, in human prostate cancer development, TMPRSS/ERG fusions are stated to occur in context of early lesions such as with the loss of single NKX3-1 and/or PTEN alleles (Tomilins *et al.*, 2008). In theory, this could mean the presence of ERG in prostate cancer development, indicates invasive potential.

The presence of ERG along with PTEN expression status (positive or negative), has been demonstrated in various types of aggressive cancers. The overexpression of the ERG protein in prostate tumors is considered by some a hallmark of advanced disease and relates to poor prognosis (Yoshimoto *et al.*, 2008; King *et al.*, 2009; Nagle *et al.*, 2011; Leinonen *et al.* 2013; Ayala *et al.*, 2015). However, some found that ERG expression associates with prostate cancers that demonstrate lower stage and longer progression free survival (Petrovics *et al.*, 2005; Saramaki *et al.*, 2008). Other studies measuring biochemical recurrence demonstrated that regardless of ERG status the patients did poorly when PTEN was lost (Khron *et al.*, 2012; Lotan *et al.*, 2016). The variability of results shown by different groups highlight the difficulty that the heterogeneity of aggressive PCa poses in determination of aggressive phenotypes.

The heterogeneity within these tumors results in shifting phenotypes that contribute to diverse patterns and mechanisms (Geraschenko *et al.*, 2019). These phenotypes present with variable expression of cell surface molecules that make it problematic to identify molecules that may be utilized as predictive biomarkers. This uncertainty creates an obstacle in the identification and treatment of patients at risk for tumors capable of invasion and metastatic dissemination. Previous chapters showed the ability to quantitate the  $\alpha 6$  integrin co-distribution with uPAR and E-cadherin in human prostate tissues to the categorize tumors with invasive and aggressive potential. The hypothesis tested in this chapter is that the membrane and cytoplasmic localization status of  $\alpha 6$  integrin correlates with PTEN and ERG expression in human prostate characterizations.

This chapter investigates if  $\alpha 6$  integrin localization (membrane, cytoplasmic or both) correlates with PTEN and ERG expression status in prostate tumor cells and could be quantified with an image analysis algorithm. The combination of IHC along with a quantitative image analysis was used in the identification and stratification of aggressive PCa. The results reported here indicate the ability to associate the  $\alpha 6$  integrin expression with PTEN and ERG status in human prostate FFPE tissue samples.

## RESULTS

*$\alpha 6$  integrin localizes to the membrane with PTEN loss and ERG expression:*

Human prostate cancer FFPE tissue CNBs (~435) were serial sectioned and immunostained with antibodies specific for PTEN, ERG,  $\alpha 6$  integrin and HMWCK + p63. H&E stained slides were prepared with the first slides of the series. The H&E stained slides were then evaluated by a board-certified pathologist (RBN) for tissue morphology, architecture, normal elements and tumor content (**Figure 7.2, A**). Serial sections of evaluated CNB samples were immunostained with the specified antibodies previously mentioned and assessed for positive or negative, Gleason grades, and localization of  $\alpha 6$  integrin (membrane, cytoplasmic or both). Sample observations revealed very interesting protein localization patterns of expression. The first observation occurred with samples containing tumors with the loss of basal cells (identified by the lack of HMWCK+p63 expression) (**Figure 7.2, B and C, lower right panel**). Region of tumor with negative PTEN expression demonstrated ERG positive expression within the identical region of the sequential slide, even at the cellular level (**Figure 7.2, B and C, left and right top panels**). Secondly, PTEN negative and ERG positive cancer exhibited  $\alpha 6$  integrin membrane expression in a cell-cell membranous pattern resembling a “fish net” (**Figure 7.2, B and C, left bottom panels**). Interestingly this was repeated in specific tumor regions in five samples demonstrating this specific pattern (PTEN negative and ERG positive) (**supplemental data, Figure S2-S4**). PTEN positive and ERG negative tumors demonstrated either cytoplasmic  $\alpha 6$  integrin localization or a combination of cytoplasmic and membranous expression (**supplemental**

data, Figure S2-S4).

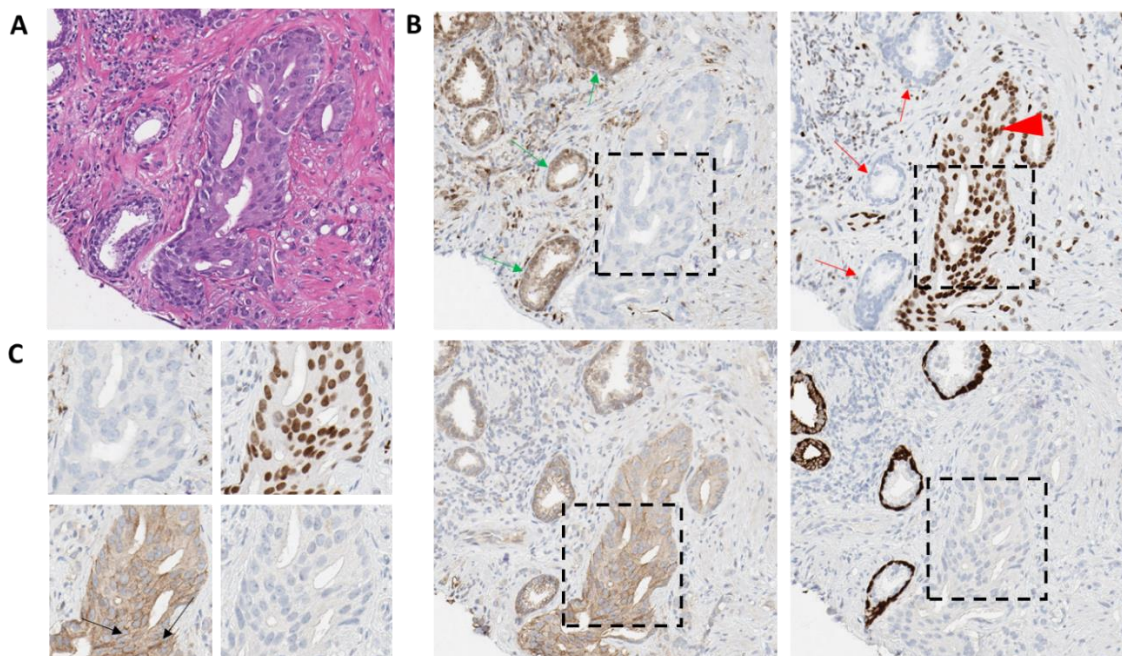


**Figure 7.2. PTEN, ERG,  $\alpha 6$  integrin and HMWCK+p63 protein expression in prostate cancer.** Serial sections of human prostate cancer CNBs were immunostained for PTEN, ERG,  $\alpha 6$  integrin and HMWCK+p63 (n=435). **(A)** H&E stained slide of FFPE prostate tissue. **(B)** FFPE IHC DAB detection with antibodies for PTEN (top left panel), ERG (top right panel),  $\alpha 6$  integrin (left bottom panel), and HMWCK+p63 (right bottom panel). Regions with positive PTEN expression (green arrows) with identical region in sequential slides with negative ERG result (red arrows). PTEN negative tumor (\*\*), demonstrates positive ERG expression (red arrowhead). The  $\alpha 6$  Integrin in PTEN negative/ERG positive region demonstrates membrane expression (black arrows) (Images are 10x magnification). **(C)** Enlarged images of indicated immunostained regions (20x magnification).

*Quantitative analysis of  $\alpha 6$  integrin expression:* To evaluate if a correlation between  $\alpha 6$  integrin localization with PTEN and ERG expression status could determine sample category (benign, low grade or high grade), a quantitative machine-learning algorithm was applied to the scanned images of  $\alpha 6$  integrin immunostained slides using QuPATH™ image analysis tool. The algorithm employed a classifier to detect cells positive or negative for DAB immunostaining. A set of measurements were made for each detected cell and a filter is incorporated that allowed selection of positive DAB immunostained cells from negative cells. The algorithm differentiated between cytoplasmic and membrane immunostaining by utilizing an arbitrary distance ratio (2 $\mu$ m) from the nuclei of each cell detected to annotate individual cells. The results ratios were obtained by calculating the cytoplasmic optical density (OD) mean divided by membrane OD mean of the 4656 positive DAB cells detected from the annotated region of interest (ROI) (**Figure 7.3, A**). The ratios were plotted on a histogram with membrane OD mean of 0.823 and cytoplasmic OD mean of 0.659 calculated (**Figure 7.3, B**). The OD mean ratios plotted indicated the initial ROI tested contained a more membrane expression of  $\alpha 6$  integrin. The determination of cytoplasmic vs membrane distribution status depended on how far the mean ratio shifts from the standard of one (**Figure 7.3, C**).

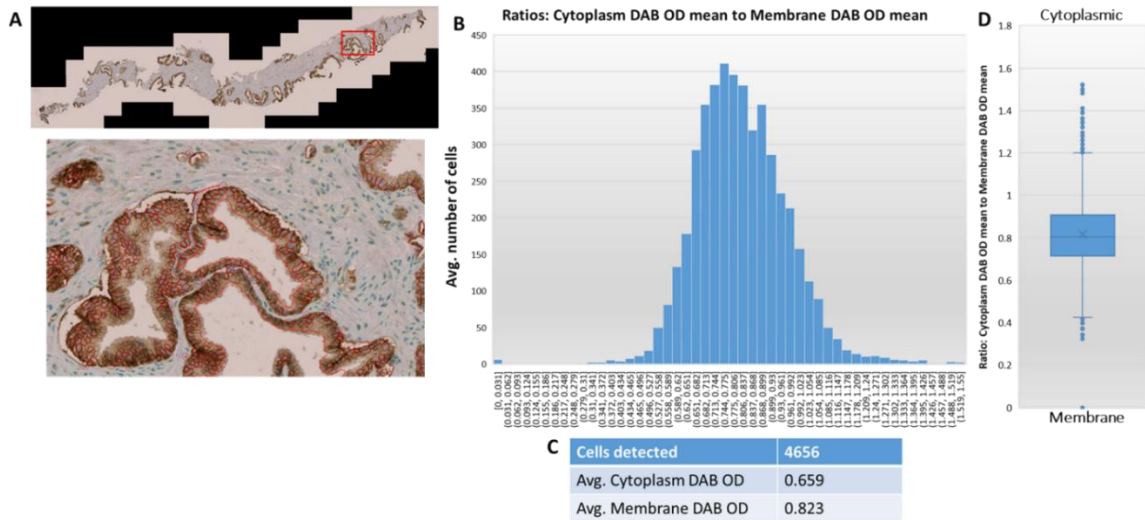


**Figure 7.3.**  $\alpha 6$  integrin localization is quantifiable on immunostained human prostate FFPE slides. **A** scanned prostate CNB IHC DAB slide immunostained with anti- $\alpha 6$  antibody was quantified with QuPATH image analysis. **(A)** Image of annotated prostate CNB (top panel) and magnified ROI with individual cells identified by algorithm (bottom panel). **(B)** Histogram plot of calculated ratios cytoplasmic DAB OD mean to membrane DAB OD mean in total cells detected in ROI. **(C)** Table of cells detected with positive DAB immunostaining in ROI and total averages OD mean of cells with cytoplasmic and membrane expression of  $\alpha 6$  integrin. **(D)** Box and whisker plot of cellular distribution in the ROI with cytoplasmic OD mean over membrane OD mean (dots are outliers that are more than 1.5 standard deviations from the mean).

*$\alpha 6$  integrin membrane and cytoplasmic staining correlates with aggressive tumors:*

After the preliminary evaluation of the algorithm on the test sample, we next analyzed nine prostate samples immunostained with anti- $\alpha 6$  representing two PNI samples, two high-grade tumor (Gleason 3+4), three low grade (Gleason 3+3) and one PIN lesion. To accomplish this testing, one core from each CNB was selected for annotation and analysis of the entire core. The results with the two high-grade tumors demonstrating cytoplasmic to membrane OD mean (C/M OD mean) of 0.92 showed a distribution shift to membranous. One sample exhibited PTEN negative tumor with positive ERG expression and the other with PTEN and ERG negative expression. The three Gleason 3+3 tumor samples demonstrated slight variability in PTEN and ERG expression and C/M OD mean. One tested core presented tumor with negative PTEN and ERG expression with C/M OD mean of 0.91. Another sample exhibited both PTEN and ERG positive immunostaining with C/M OD mean of 0.86 (rounded). The final Gleason 3+3 sample demonstrated positive PTEN immunostaining and had negative expression of ERG with C/M OD mean of 0.90. Interestingly, the samples with PNI displayed variable PTEN expression. One sample expressed positive PTEN and negative ERG intensity with PNI (**Figure 7.4, A**) and demonstrated a C/M OD mean of 0.91 (rounded) (**Figure 7.4, D, left panel**), while the other exhibited a lack of PTEN expression and displayed weak ERG positive expression (**Figure 7.4, B**) demonstrating a C/M OD mean of 0.80 (**Figure 7.4, D, middle panel**). This result would suggest the distribution indicated a shift to membranous expression while showing some cytoplasmic expression in this sample. The sample with PIN lesion that demonstrated positive



PTEN expression and negative ERG expression. (**Figure 7.4, B**) As expected, PIN sample displayed a C/M OD mean of 0.84 (**Figure 7.4, C, right panel**). The distribution results from the PIN sample would indicate more cells exhibited membrane staining.

Overall, these results suggest that  $\alpha 6$  integrin membrane localization in aggressive cancers is associated with the loss or mutation of PTEN in concert with overexpression of ERG. Prostate cancer presenting with positive PTEN expression and negative ERG appears to result in cytoplasmic with some membrane expression of  $\alpha 6$  integrin, whereas prostate tumors with both PTEN and ERG Negative expression displays  $\alpha 6$  integrin cytoplasmic localization.

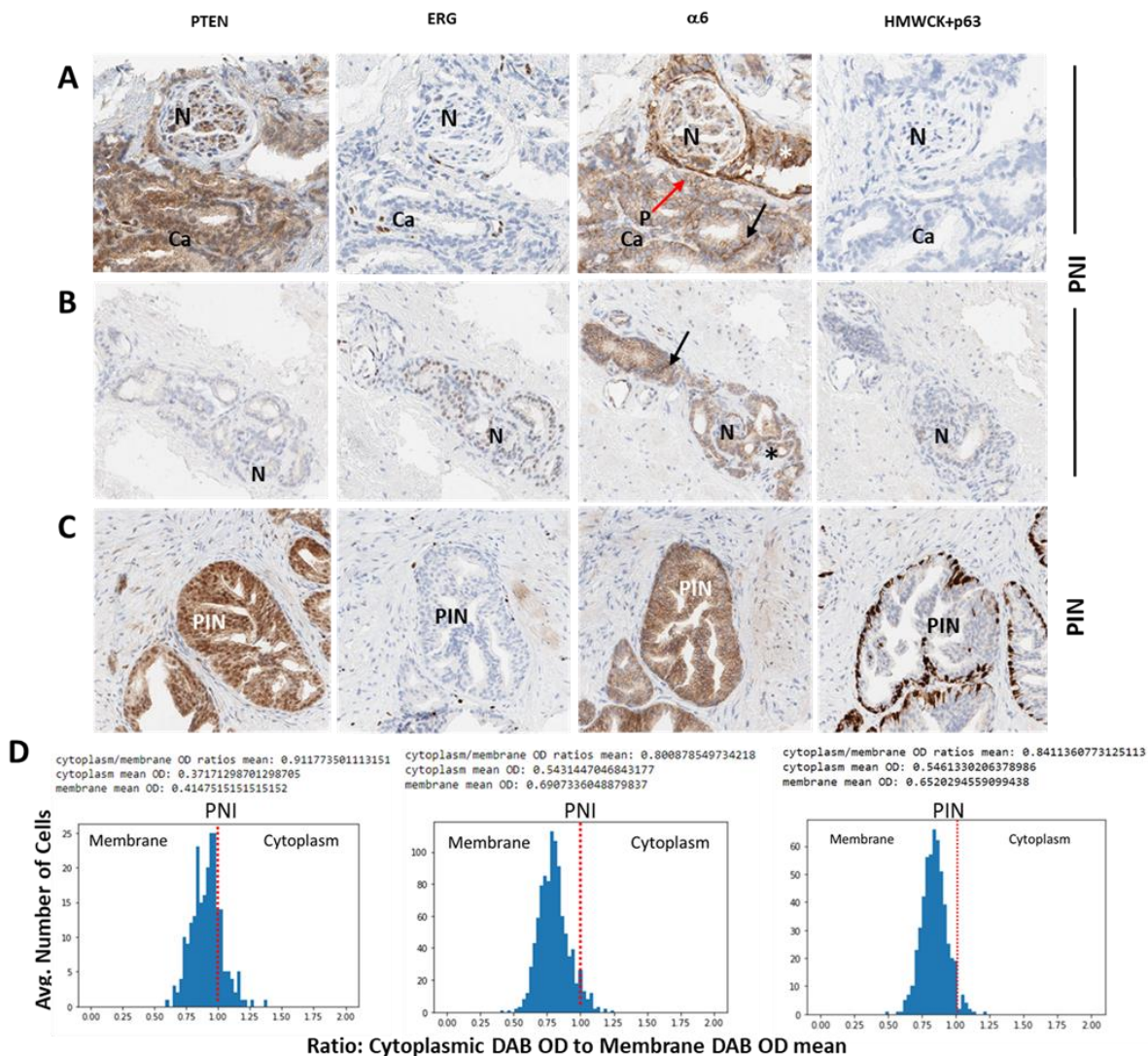


**Figure 7.4.  $\alpha 6$  integrin cytoplasmic and membrane IHC expression in PNI and PIN.** Human prostate CNB serial sections were immunostained with antibodies specific for PTEN, ERG,  $\alpha 6$  integrin for presence of tumor and HMWCK+p63 for normal element comparison. **(A)**  $\alpha 6$  integrin exhibits cytoplasmic (\*) and membrane expression (black arrow) in cancer cells (Ca) invading the perineurium (P and red arrow) of nerves (N) in PNI sample with positive PTEN and negative ERG and HMWCK+p63 expression. **(B)** Membrane expression of  $\alpha 6$  integrin (black arrow) and cytoplasmic (\*) observed in PNI sample with negative PTEN and HMWCK+p63 intensity and weak ERG expression. **(C)**  $\alpha 6$  integrin demonstrates mostly membrane and some cytoplasmic expression in PIN lesion with positive PTEN, negative ERG and discontinuous HMWCK+p63 expression. **(D)** Histogram plots of QuPATH algorithm ratio analysis of cytoplasmic to membrane OD mean in PNI (left panel), (middle panel) and PIN lesion (right panel). (Images are 10x Magnification).

## DISCUSSION

The detection of PTEN with ERG expression status in prostate cancers has become an intriguing discussion in the attempt to investigate reliable biomarkers to identify tumors with propensity for invasion. These tumors express a high degree of variability in protein expression associated with aggressive potential. Although our understanding of the downstream effector pathways directly or indirectly related to PTEN function has improved, it still has not definitively led to a signature of invasive potential. This current chapter associates the localization of  $\alpha 6$  integrin with PTEN and ERG protein expression status to identify prostate cancers with aggressive capacity.

Human prostate cancers demonstrate multiple proteins that display upregulated or downregulated expression status, variable localization pattern within the tumor cells and variable co-distribution patterns, even within one tumor. Many of the observed prostate cancers and some PIN lesions with PTEN loss and ERG expression presented with an  $\alpha 6$  integrin membranous “fish net” immunostaining pattern. Tumors with PTEN positive and ERG negative expression displayed mostly cytoplasmic but some membrane  $\alpha 6$  integrin immunostaining. Tumors with both PTEN and ERG positive expression (although rare) exhibited slightly more membrane localization of  $\alpha 6$  integrin. Prostate cancer demonstrating a lack of PTEN and ERG expression presented with mostly diffuse cytoplasmic localization.

Studies have shown that PTEN can inhibit cellular invasion, migration and growth by negatively regulating integrin function (Gu *et al.*, 1998; Tamura *et al.*, 1998; Tamura *et al.*, 1999). Although the PTEN phosphatase function modulates PIP<sub>3</sub>/PI3K pathway activity and phosphoinositide composition regulating vesicular membrane trafficking, the activation of other kinase mediated effector proteins may also be able to perform this function. For instance, other groups have shown that PTEN negatively regulates ERK1/2 signaling (although indirectly) in prostate cancer (Bouali *et al.*, 2008; Chetram *et al.*, 2011; Chetram and Hinton., 2012). Studies have shown ERG as a specific target of ERK for phosphorylation and activation in prostate cancers (Selvaraj *et al.*, 2015; Kedage *et al.*, 2017). This may explain the specific membrane localization patterns with  $\alpha 6$  integrin with PTEN loss and ERG expression. This also suggests that further investigation of non-canonical pathways influenced by alterations in PTEN/PI3K status associated  $\alpha 6$  integrin regulation is critical in assessing tumor aggressiveness.

Prostate cancer is an extremely heterogeneous type of cancer that displays an indolent and aggressive phenotype. During progression, these tumors exhibit phenotypic transitions that enhances cellular plasticity and exacerbates the inability to identify tumors that will acquire invasive capability. Alterations and mutations in specific gene and proteins have long been designated as focal points for initiation of oncogenesis; here the alterations in PTEN with respect ERG functionality have come to the forefront.

PTEN loss and ERG status in relevance to aggressive PCa behavior has been a debate for some time. The variable expression for both (or either) within PCa tumors is an evident display of tumor intratumoral heterogeneity. The fact that these tumors can exhibit varying status of these protein expressions indicates the potential existence of subclasses of tumor within just one primary region. Here, we have determined a relevance in the detection of specific  $\alpha 6$  integrin localization in PCa tissues in correlation with PTEN and ERG expression status. The patterns displayed have indicated a potential connection with deregulation of PTEN and increased expression of  $\alpha 6$  integrin. The membrane presence of  $\alpha 6$  integrin in concert with PTEN negative and ERG positive expression may indicate a transition to an aggressive tumor subtype. Previous chapters have established the upregulation of  $\alpha 6$  integrin (specifically to the cell-cell region) results in interaction with uPAR and PTM to the tumor specific variant form associated with invasion. In addition, our results demonstrate inhibition of the  $\alpha 6$  integrin cleavage activates unknown pathways to upregulate E-cadherin expression and mitigate tumor cell migration. It will be critical to determine if inhibition of the PTM of  $\alpha 6$  integrin will also activate pathways re-establishing PTEN expression in tumor with mutation of inactivation.

### **VIII. Method to reuse archived H&E stained slides**

**PMID: 31731599**

**James P. Hinton**, Katerina Dvorak, Esteban Roberts, Wendy J. French, Jon C. Grubbs, Anne E. Cress, Hina-Arif Tawari, Raymond B. Nagle. "A Method to Reuse Archived H&E Stained Histology Slides for a Multiplex Protein Biomarker Analysis." *Methods and Protocols*. (2019); 2: 4, 86.

#### **ABSTRACT**

The potential to reuse archived Hematoxylin and Eosin (H&E) stained slides with various immunostaining detection strategies present a unique opportunity for not only for interrogating past tissues with new biomarkers but also as an alternative for samples with limited tissue availability. Archived Hematoxylin and Eosin (H&E) stained pathology slides are routinely stored to index FFPE sample tissue blocks. The FFPE blocks are clinically annotated human tumor specimens that can be valuable in studies decades after the tissue was collected. If stored properly they have the potential to yield a valuable number of serial sectioned slides for diagnostic or research purposes. However, some retrospective studies are limited in scope because the tissue samples have been depleted or not enough material is available in stored blocks for serial sections. The goal of these studies was to determine if archived H&E-stained slides can be directly reutilized by optimizing methods to de-stain and then re-stain the H&E stained slides to allow detection of several biomarkers of interest using a conjugated antibody with chromogen multiplex immunohistochemistry procedure. This simple but innovative procedure, combined with image analysis techniques, demonstrates the ability to perform

precise detection of relevant markers correlated to disease progression in initially identified tumor regions in tissue. This may add clinical value in retaining H&E slides for further use.

## **INTRODUCTION**

In immunohistochemistry several types of tissue immunostains are utilized to analyze morphological features, cellular structures, cell type, and presence or absence of microorganisms. The most popular of the staining methods for diagnostic potential is the utilization of hematoxylin and eosin (H&E) staining (Bancroft and Layton., 2013). H&E stains reveal structural information, with specific functional implications. H&E staining of tissue is used to assess cellular and morphological structures, identify type of tissue, morphological variability, cell type, and pathological changes. The use of H&E staining has been the most effective and utilized procedure for pathological diagnosis of patient neoplasia for over a century (Fischer *et al.*, 2008; Chan., 2014) It has allowed pathologists to pinpoint focal areas of a specimen containing aggressive tissue and foster a proper diagnosis (Titford., 2005). Therefore, developing procedures to re-utilize these archived samples to determine individual biomarker expression levels (and potential protein-protein association) could assist in determining disease progression and directions for appropriate treatments.

H&E staining is used in conjunction with a variety of tissue fixatives and allows the display of various cellular and tissue components including the extracellular matrix, the cellular cytoplasm, and the nuclear structures (Fischer *et al.*, 2008). The

hematoxylin is converted into its oxidization product hematein, which is a basic dye that stains acidic (basophilic) tissue components (ribosomes, nuclei, and rough endoplasmic reticulum) a darker purple color while the acidic eosin dye stains other protein structures of the tissue (stroma, cytoplasm, muscle fibers) a pink color (Chan., 2014; Titford., 2005; Feldman and Wolfe., 2014). They are also valuable in distinguishing normal structural components from neoplastic regions. However, with current procedures, H&E staining is utilized along with sequential sections stained with antibody. Serial sectioning may cut through the region of interest and may result in loss of regions necessary for critical diagnosis. This is particularly an issue with smaller core needle biopsies (CNBs), that are of limited size and number. These samples are considered “precious” in regard to availability and require the utmost accuracy in testing procedures to result in proper diagnoses.

A major advantage of a method that allows reuse of the H&E-stained slide is that it will alleviate the need for additional sequentially-sectioned slides, particularly with the diminutive CNBs. Due to the small size of CNBs, they are also subject to tissue sample exhaustion with loss of the diagnostic lesion. This method would present a major practicality when a particular region of interest is no longer available in the sample block due to sequential cuts. The ability to reuse the initial H&E containing the lesion could be critical. De-staining these H&E-stained tissue slides could also potentially reduce the need for re-biopsy.

Another advantage for retaining archived H&E-stained slides is due to the rapidly expanding use of whole-slide imaging (WSI), also known as digital pathology (DP) or virtual pathology. DP is a technology that involves high-speed, high-resolution



digital acquisition of images representing entire stained tissue sections from glass slides in a format that allows them to be viewed by a pathologist on a computer monitor (Mukhopadhyay *et al.*, 2018). This streamlines the ability of surgical pathologist to make a primary diagnosis utilizing digitized images of the H&E-stained slide, allowing digital preservation while the H&E and other stains are fresh (Zarella *et al.*, 2018). As the validation of this technology becomes widespread, the method reported here could be used for analysis of stored H&E-stained slides for subsequent diagnosis of tumor subtypes within a patient sample or future discovery of novel target proteins.

For our research, prostate cancer was initially chosen due to frequent limitations of tissue in sample biopsies and the requirement for biomarker study. PCa is also known to express variable levels of several markers associated with disease progression, such as PTEN ERG, making it a viable target for testing this procedure. A link between the PTEN pathway and ERG protein expression has previously been evaluated in previous chapters and various prostate cancer studies [Yoshimoto *et al.*, 2008; Han *et al.*, 2009; Leinonen *et al.*, 2013; Nagle *et al.*, 2013; Ayala *et al.*, 2015; Jamaspishvili *et al.*, 2018). In studies investigating the trend of PTEN loss in tumors of prostatectomies and locally recurring castrate-resistant prostate cancers (CRCPs) with ERG overexpression, the data showed that the loss of PTEN was significantly associated with ERG positivity (Leinonen *et al.*, 2013). Another study indicated that the combination of ERG overexpression and PTEN deletion is common in aggressive capsular penetrating lesions (Ports

*et al.*, 2009). Therefore, we decided that using antibodies targeting PTEN and ERG would be the validated markers in this study.

## RESULTS

Archived H&E stained slides from PCa resections or CNBs stored for at least one year (with film coverslips) were initially used to demonstrate proof that the H&Es could be reutilized for biomarker stain using an H&E de-staining procedure with standard equipment and reagents. De-identified patient tissue samples were provided with no link to information that can be used to identify patients. FFPE prostate tissue multi-array (TMA), adenocarcinoma, lung, colon, and skin tissue slide samples were used (**Table 5**). The initial antibodies chosen for the proof-of-concept testing were ready to use products from Ventana/RTD such as anti-p40 (B28) mouse monoclonal antibody (data not shown), anti-cytokeratin 5/14 (CK5/14) (EP1601Y/LL002) rabbit and mouse monoclonal antibody cocktail from Cell Marque (**Figure 8.1**). In addition, the rabbit polyclonal antibody against the laminin-binding extracellular domain of  $\alpha 6$  integrin (CD49f) was also tested.

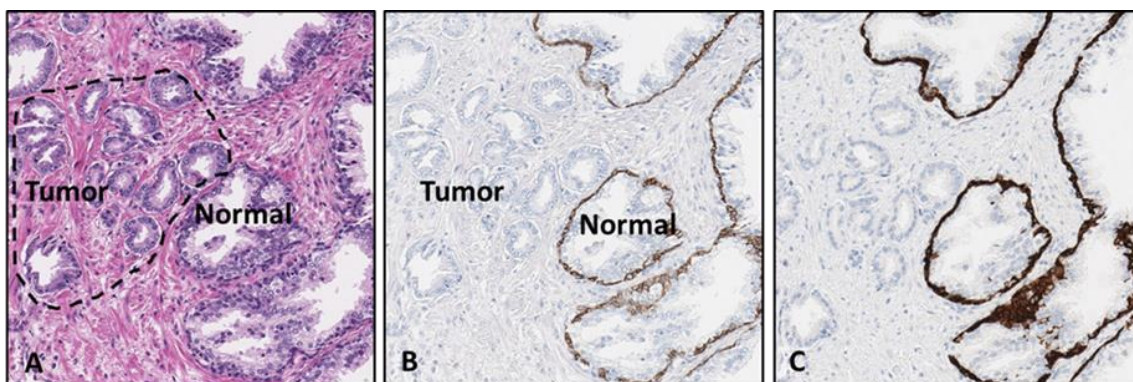


**Figure 8.1. Malignant primary prostate adenocarcinoma tissue sample.** The first image shows the prostate tissue stained with H&E **(A)**. The areas with tumor and normal prostate gland tissue are labeled. The H&E stained tissue slide was de-stained and anti-CK5/14 mouse monoclonal antibody cocktail was applied to determine feasibility of the proposed protocol **(B)**. A sequential sample slide was stained with the same anti-CK5/14 marker using a standard protocol procedure (right panel), for comparison of stain intensity to initial de-stain/re-stain procedure results **(C)**. [10x magnification]

The method described in this study utilized forty-nine sample H&E-stained resection and CNB slides that were analyzed and commented on by a board-certified pathologist (Dr. Ray Nagle) for normal or neoplastic status, Gleason grade, preservation status, and any distinguishing features for categorization of potential aggressiveness **(Table 4)**. The initial testing was accomplished using DAB IHC detection kits to determine retention of marker stain intensity. During the initial stages of this study, multiple test samples demonstrated lower intensities as a result of utilizing an un-optimized protocol (data not shown). However, continued editing and updates to the initial procedure on re-utilized H&E index slides resulted in viable stain intensity demonstrating the feasibility of the procedure and potential for optimization to culminate in stain intensity comparable to that of sequential slides utilizing standard procedures **(Figure 8.2)**.

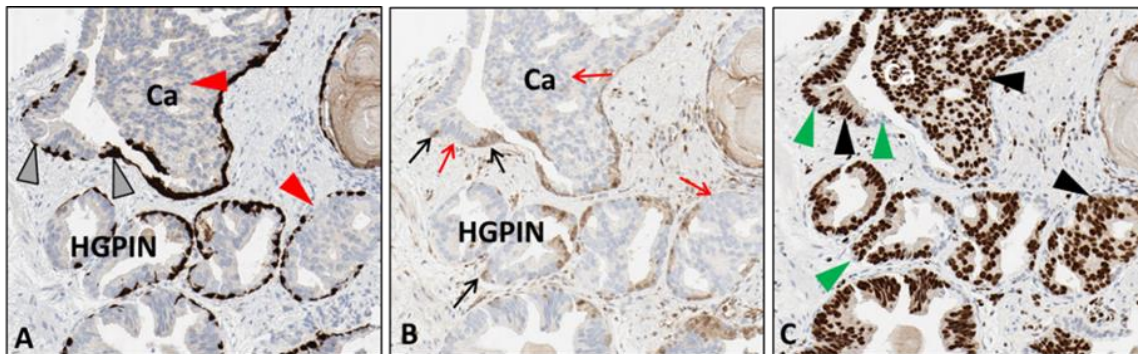


**Figure 8.2. Sequential slides of human prostate tissue exhibiting cancer (Ca) invading into normal glands and high-grade prostatic intraepithelial neoplasia (HG PIN).** There is an aggressive carcinoma invading glandular structures that have retained normal basal cells. The retained basal cells are positive for HMWCK + p63 (A) [grey arrowheads], positive for PTEN (B) [black arrows], and negative for ERG (C) [green arrowheads]. The cancer is negative for HMWCK + p63 (A) [red arrowheads], PTEN (B) [red arrows], but positive for ERG (C) [black arrowheads]. [Images, 10x magnification].

The initial testing procedures resulted in moderate but visible stain intensity providing proof-of-concept. At this stage, further optimization and repeat testing was warranted to increase the stain intensity to comparable levels of those occurring using the standard antibody staining methods and to ensure reproducibility. The procedure methods were improved by four steps: 1. Applying timed reagent rinse procedures at the xylene, ethanol (EtOH), and Ventana/RTD proprietary reaction buffer steps (1-minute rinse times between each hold); 2. Increasing EtOH and reaction buffer reagent rinses from 1 rinse to 5-6 and 3-4 manual rinses respectively for optimal efficiency; 3. Including an approximate 5-minute drying step after the reaction buffer rinse to limit residual excess reagent interference in the online application of biomarkers; and 4. Editing online cell conditioning steps (for heat induced antigen retrieval) to reduce potential epitope destruction.

This procedure optimization was considered the standard when applied to any H&E-stained slide stored up to 2 years but needed further optimization for tissues stored for periods 2 years or longer. The subsequent experimentation steps employed the use of antibodies targeting PTEN and ERG biomarkers, VENTANA anti-PTEN (SP218) mouse monoclonal antibody, and anti-ERG (EPR3864) rabbit monoclonal antibody respectively. These validated markers were used since they demonstrate 1. the heterogeneous variability of aggressive prostate cancer and 2. the comparative expression of PTEN loss and ERG expression in aggressive tumors. In this procedure, steps (1-8) represent the optimized H&E de-staining procedures. However, during the testing, unforeseen scheduling resulted in slight deviations (extended reagent HOLD times) in steps 4 and 7 that lead to determination that certain steps, which were the xylene and reaction buffer HOLD times, could be amended without incurring damage to samples. The updated procedure, which only involved an extended xylene hold time and is essentially the same optimized procedure, resulted in comparable stain intensity to the standard protocol and allowed the ability of distinct determination of aggressive tumor areas (**Figure 8.3**). After the successful completion of a sequential round of experimentation using IHC DAB, we tested if antibodies targeting multiple biomarkers could be applied for detection with the use of chromogenic detection reagents. Again, prostate adenocarcinoma CNBs were used as experimental specimens for the de-stain and re-stain procedure. The antibodies chosen were specific for the  $\alpha 6$  integrin laminin-binding domain and HMWCK + p63. These markers were chosen due to known membranous expression levels (CD49f) and

cytoplasmic and nuclear (HMWCK + p63 respectively) positive expression levels in non-neoplastic basal cells of prostate tissue. In PCa,  $\alpha 6$  integrin expression is membranous and aggressive and invasive disease exhibits an intracellular expression pattern (Ports *et al.*, 2009; Sroka *et al.*, 2010; Sroka *et al.*, 2016; Harryman *et al.*, 2016; Das *et al.*, 2017). It is also associated with poor patient prognosis, reduced survival, and increased metastasis (Friedrichs *et al.*, 1995; Landowski *et al.*, 2014; Stewart *et al.*, 2016). These markers were not expected to colocalize but to demonstrate the expression pattern of both non-neoplastic and neoplastic structures and focal areas in tissue after marker application, following the de-stain procedure.

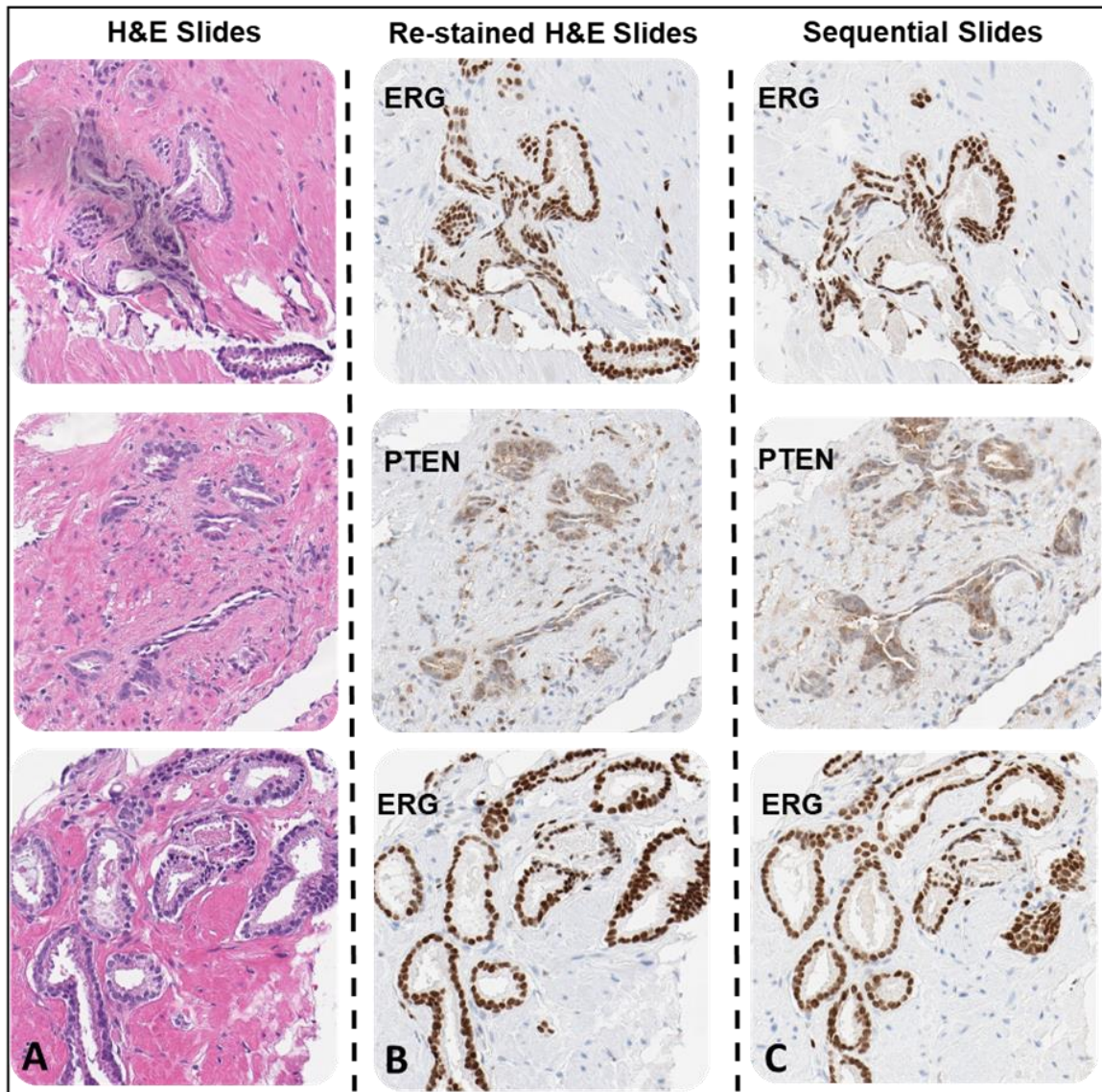


**Figure 8.3. Prostate cancer CNBs sample H&E slides with PTEN and ERG IHC DAB stained slides.** The first slide for each sample was H&E-stained **(A)** Each sample H&E was de-stained and re-stained with either PTEN or ERG antibody depending on the pathologist analysis for biomarker loss or positivity to demonstrate tumor heterogeneity **(B)** The additional sequential slides for each sample were stained with anti-PTEN antibody or anti-ERG antibody **(C)** Each sample H&E was de-stained and re-stained with either PTEN or ERG antibody depending on the pathologist analysis for biomarker loss or positivity to demonstrate tumor heterogeneity [10x magnification].

The expected outcome was to demonstrate definitive areas of non-neoplastic vs. tumor regions with the application of antibodies and chromogen detection. This would allow the simultaneous detection of normal and aggressive structures in one tissue sample after pathologist analysis of the H&E-stained slide, allowing for the potential utilization of one slide. The results demonstrated strong stain intensities for both targets and well-defined areas of demarcation of non-neoplastic vs tumor structures. As expected, both markers are visible in normal basal cells of normal prostate glands (although the HMWCK + p63 stain intensity primarily masks the  $\alpha 6$  integrin signal in those areas), but anti- $\alpha 6$  antibody displays an intracellular and cytoplasmic expression in the areas of budding tumor (**Figure 4**).

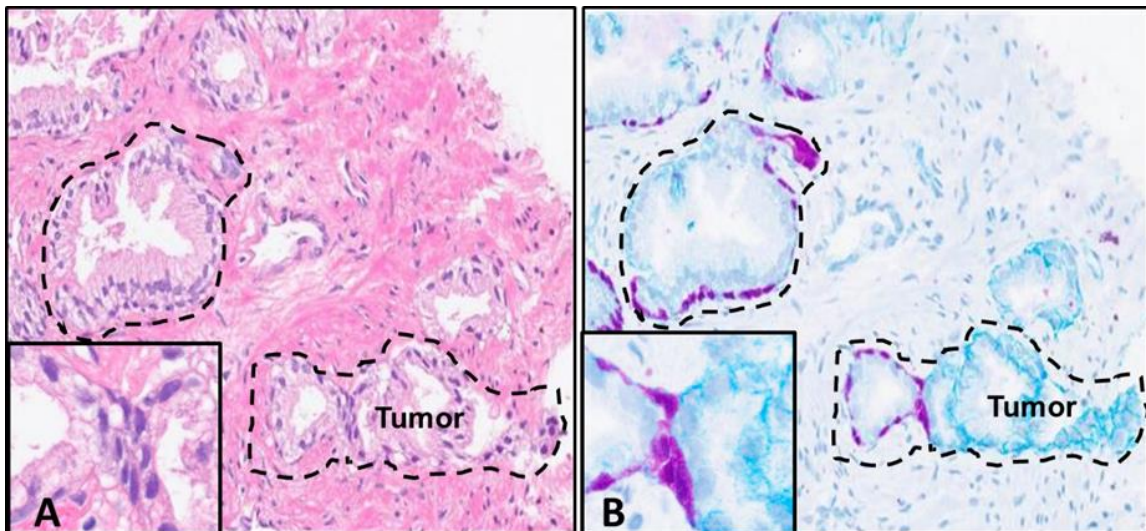


**Figure 8.4. Prostate adenocarcinoma sample CNB H&E and Chromogen IHC.** The initial H&E-stained slide with dotted line indicating prostatic intraepithelial neoplasia (PIN) lesion and tumor area (left panel) **(A)** The de-stained H&E that was stained with HMWCK + p63 mouse monoclonal antibody cocktail and anti-CD49f rabbit polyclonal antibodies using Dual Chromogen detection (right panel) **(B)** The anti-HMWCK + p63 antibody cocktail (purple) stains the basal cells of normal prostatic glands, and the anti-CD49f (teal) antibody stains normal basal cell membranes (masked by the HMWCK + p63) but demonstrates an intracellular and



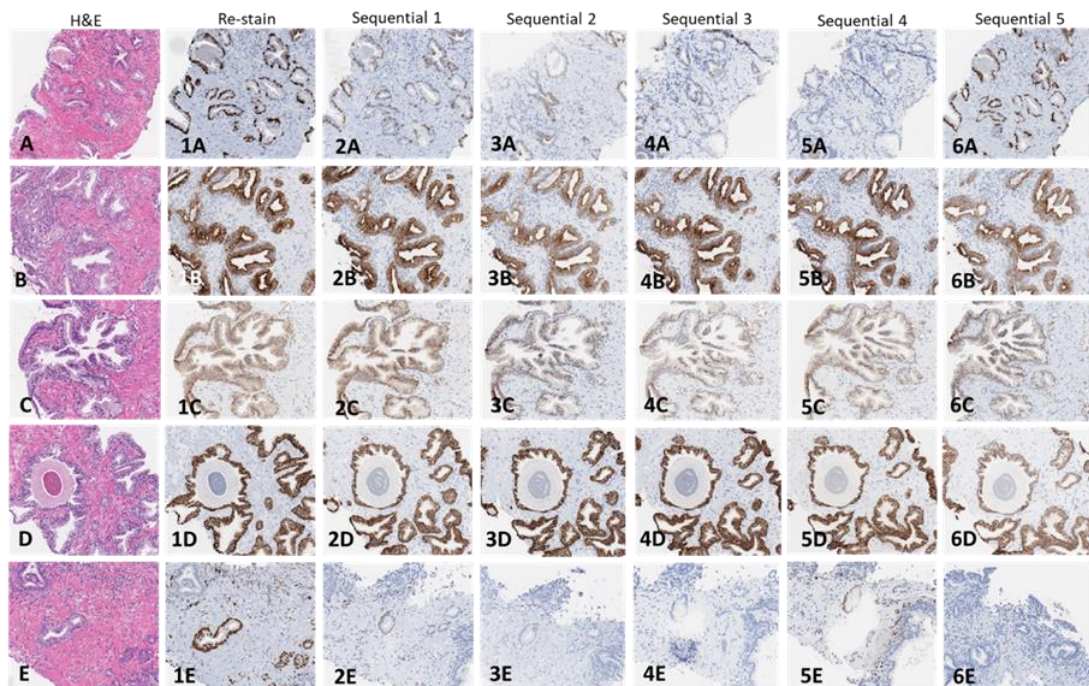
cytoplasmic expression in aggressive tumors (area demonstrating budding tumor outlined in H&E-stained slide in left panel and right panel). [Images, 20x magnification with 60x inset].

These positive results from testing samples archived up to 2 years warranted the evaluation of the potential ability of this procedure to be utilized with other tissue types, for H&E stained slides archived 2 years or more, and samples archived utilizing glass coverslips. Therefore, five archived PCa CNBs (2 years 11 months), a normal colon (2 years 1 month), liver and lung samples (4 years) along with 4-plus year (4+) PCa resection (4 years 11 months) H&E stained sample slides sealed with thin film coverslip were tested. For the testing of H&E stained slides sealed with glass coverslips, archived PCa CNBs (2 years 11 months), skin samples (5 years) and a PCa TMA sample (12 years) were tested. During the execution of this procedure the removal of the coverslip was determined to be a limiting factor therefore the parameters involved with the removal was tracked and recorded in this report (**Table 5**). After the removal of the H&E stain, the sample slides were re-stained with selected antibodies utilizing optimized protocols adapted for IHC on de-stained H&E slides (**Table 6**).

The testing of the H&E stained slide samples archived 2 years or more involved extended coverslip removal and reagent rinse times (2+, 4, 4+, 5, and 12-year archived samples) which indicated that archival time, storage condition and coverslip type may play a factor in slide processing with the procedure. The processing of 2-year archived H&E stained slides sealed with thin film (all PCa CNBs) only required minimal extension time of coverslip removal (to ~ 60 minutes) but resulted in H&E stain removal and comparable antibody immunostaining intensities compared to the corresponding sequential slides (**Figure 8.5, A-6E**). The reused H&E and corresponding sequential slides were evaluated by a board-certified pathologist in a side by side comparison for immunostaining intensity (**Table 7**). The histopathologic analysis focused on any present tumor or normal regions for intensity. The data analysis indicates that there was a significant matching in the immunostaining intensities between the reused H&E stained slides and sequential comparator slides immunostained with the various antibodies (**Figure 8.5, F**).

The processing of the 4 and 4+ year archived H&E stained slides (PCa resections) sealed with thin film coverslip required extended time of coverslip removal (~38 and 47 hours) but resulted in H&E stain removal. The archived H&E stained slides sealed with glass coverslip for 2+, 5 and 12-year (PCa resection, two skin and PCa TMA) required 1-2 days and 4-5 days for coverslip removal. The 4+ year archived sample resulted in comparable intensity (CK 8 & 18) to the sequential comparator slide (**Figure 6**). The reused 12-year archived PCa TMA H&E stained slide immunostained with Ventana anti-ERG resulted in immunostaining but intensity

was variable across different cores but demonstrated feasibility (data not shown). The reused 5-year archived H&E stained slides (skin resections) sealed with glass coverslips also required extended time for coverslip removal and reagent rinses. The resulting H&E stain removal exhibited residual H&E stain on the slides resulting in incomplete immunostaining (ERG) (data not shown). The resulting retention of the hematoxylin and eosin on the slides may have potentially impacted the results and will need further inquiry on storage conditions to ascertain steps to mitigate any issue. We have found that storage conditions of older H&E stained slides (particularly with glass coverslips) causes extensive adhesion of the coverslip to the tissue slide due to the extended time in storage, requiring a slight extension of extraction procedures. Also, we observed that pre-analytics will impact H&E removal resulting in some residual retention. Unfortunately, due to age of the slide, pre-analytical data was not available.



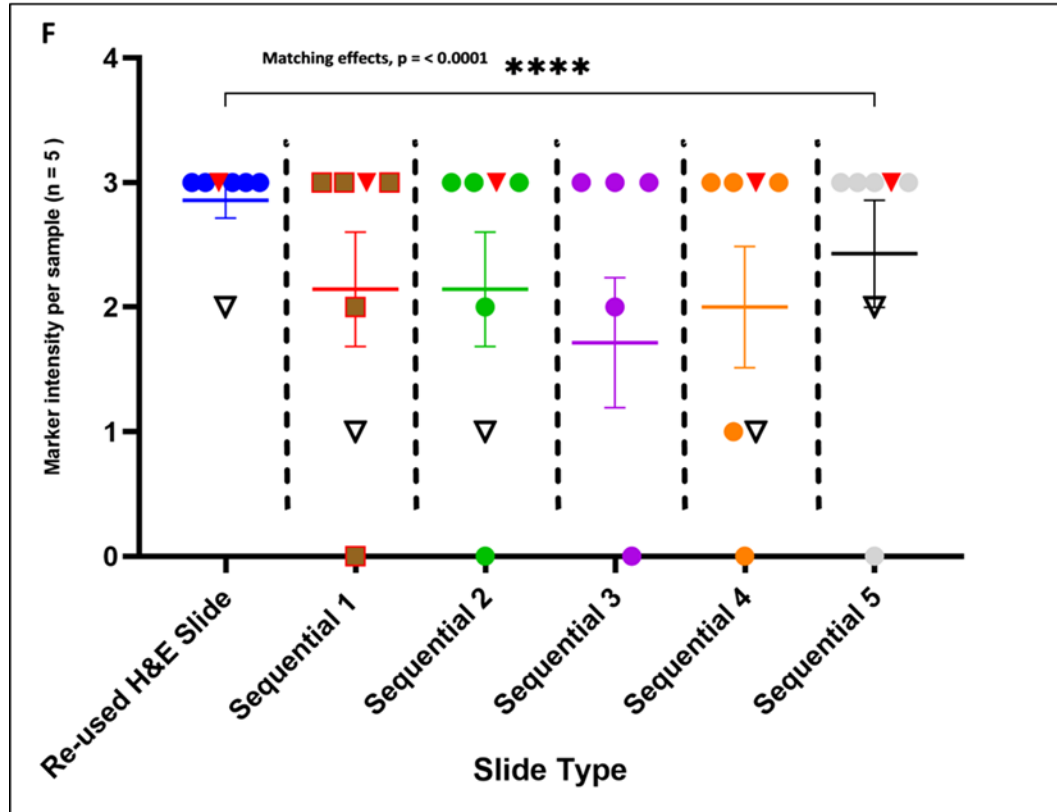


**Figure 8.5. H&E stained slide image and reused H&E slide selected antibody immunostain comparison with sequential slides in PCa CNBs. (A through 6E). H&E stained Slides. (A-E) Antibodies: HMWCK+p63 (1A-5A), [Note: uneven data points for Sequential slide 5 due to lack of immunostain for HMWCK+p63]; CK 8 & 18 (1B-6B); CD49f (1C-6C); E-cadherin (1D-6D); ERG (1E-6E). Scatter plot assessment of side by side comparison of pathologist analysis scores and comments for sequential slide and reused H&E antibody immunostaining. Note: red inverted triangles represent ERG internal controls and open inverted triangles with black outline represent CD49f internal controls (F). Data presented as SEM with Chi square, df (18,12, 1). The results determined by RM one-way ANOVA matching across rows (see Table 5) showing significant matching with p value (<0.0001). Analysis performed using GraphPad Prism version 8.2.1. [Images 4x Magnification]**

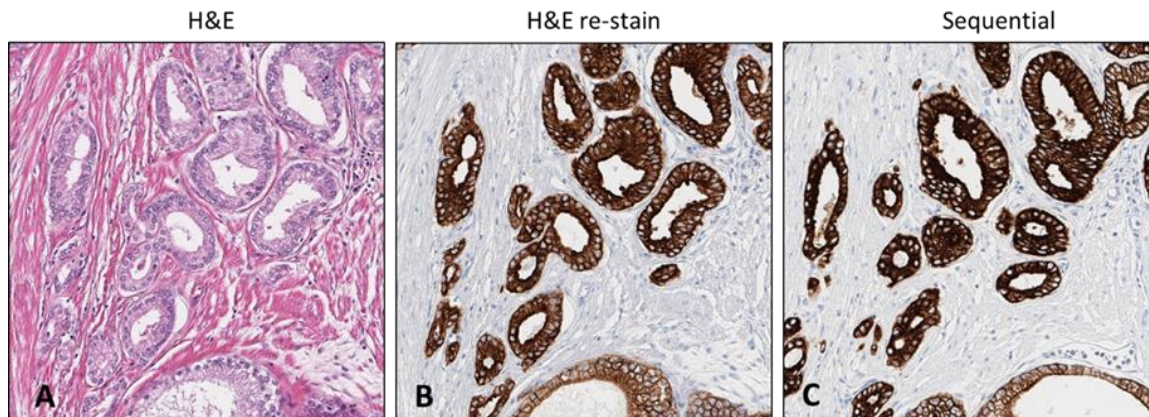


**Figure 8.6. H&E stained slide archived 4+ years subjected to de-stain and re-stain procedure compared to sequential sample slide.** Initial H&E stained slide containing region of tumor (**A**). CK 8 & 18 antibody re-stained slide retaining region of interest and exact architecture (**B**). Sequential slide comparison immunostain with CK 8 & 18 exhibiting comparable stain intensity. [Images, 10x Magnification].

## DISCUSSION

When patients are suspected of having PCa, a tissue sample is required for diagnosis. The sampling of the potentially neoplastic area may be assisted through means of ultrasound (US) or multiparametric magnetic resonance imaging (mpMRI) guided techniques. Sample resections and needle biopsies are routinely formalin-fixed and processed and embedded for histological sampling then stained for H&E and IHC, allowing pathologists to analyze an excised patient tissue sample from the affected area after diagnosis to differentiate between cancer and non-neoplastic events, such as benign prostatic hyperplasia. The H&E-stained slide plays a critical role in assisting the diagnosis of the pathologist in corroborating the initial findings with MRI and US procedures. Traditionally, after pathologist analysis and diagnosis, the samples can then be processed with biomarkers targeting detection of epitopes that are overexpressed in aggressive tumors. Currently this

is the standard procedure deployed in companion diagnostics that allows for the stratification of patients who may benefit from a specific therapeutic intervention.

The accurate evaluation of biomarkers with these samples is critical for patient diagnosis, particularly with smaller samples, such as CNBs, fine needle aspirates, and potentially transurethral resection of prostate samples (TURPS). The smaller size of these tissue samples limits tissue availability and requires precise testing for important results. Loss of available tissue slides is a risk that could be mitigated with the use of H&E slide de-stain and re-stain procedures. The potential to detect multiple markers using chromogenic multiplexing on a single indexed tissue slide that had been analyzed and diagnosed by a pathologist to definitively contain aggressive tumor, leaves open the possibility of predictive companion diagnostics with minimal sampling. This may provide the opportunity for a one sample/one result diagnosis limiting the invasive nature of tissue specimen collection, which benefits the patient greatly.

There are few reports that provide instructions for removal of the H&E staining that leaves the target epitopes intact for potential reuse of the slide for selective biomarkers. Current existing protocols (and forums) only discuss de-stain procedures for slides that have stained inadequately, or have been stained with excessive hematoxylin and have lengthy protocol steps that may extend the procedure hours to days. Others may require the use of more corrosive reagents (% HCL solutions). Procedures utilizing either beta-mercaptoethanol/sodium dodecyl sulfate (2ME/SDS), 6 guanidinium hydrochloride (GnHCL) or 6 M Urea have been demonstrated to elute antibodies from immunostained tissues on

positively charged glass slides (or glass coverslips) for sequential antibody re-stain (Gendusa *et al.*, 2014; Bolognesi *et al.*, 2017). However, these methods focused on the removal of the bound primary antibody and the reagents used were not intended to remove the H&E stain. For this report, an innovative method utilizing non-corrosive reagents was created and applied in a particular procedure using these reagents in sequence that optimized the H&E slide de-stain. This procedure removed the majority of the visible stain while retaining tissue integrity and morphology and allowed preparation of specified IHC protocol to restain the sample sides. The primary tissue sample used for initial testing was prostate adenocarcinoma, however, this will translate to other tissues.

This study utilized liver, colon, skin and PCa resections and CNB samples for procedure testing. The study included the addition of antibodies detecting clinically relevant biomarkers such as PTEN, ERG, E-cadherin, Racemase (p504s), cytokeratin 8 & 18 and the CD49f protein for potential indication of aggressiveness and antibodies against HMWCK cocktailed with a p63 marker (a p53 homologue containing the N-terminal transactivation domain) as well as the variant p40 marker (lacking the N-terminal domain), that will detect the presence of normal basal cells of prostatic glands. These antibodies were critical in detection of differentiating prostatic adenocarcinomas vs detection of non-neoplastic prostatic tissue, as well as determination of intracellular marker activity and basal cell attenuation, respectively. Also, during this study the positive outcome from testing various tissue samples archived beyond 4 years utilizing thin film and 12 years with glass coverslips yielded promising results indicating tissue epitopes remain stable on

H&E stained slides archived at a minimum of 4 years. This indicates that the procedure may be useful for interrogating other clinically relevant proteins in tissues other than prostate and for H&E-stained slides stored for longer periods of time. However, the conditions of the slide storage and the type of adhesives applied to seal the slide may have an impact on results. Another factor may be the specific antibody selected for each specific study. The antibodies used for this study yielded promising results but each antibody demonstrates various qualities, therefore continued optimization may be warranted for this procedure.

Further experimentation will be repeated involving archived specimen slides utilizing film coverslips that have been stored for 4 years and more, as well as continued interrogation of samples sealed with glass coverslips. This will determine the robustness of the procedure to encompass reproducible testing of samples from decades past to incorporate newly discovered targets to test protein expression that may offer answers to questions that may have remained unsolved. Also, with the development of newer chromogen dyes, the possibility of utilizing one slide for multiple markers may now become a distinct possibility saving valuable time and resources. The results demonstrated in this report can be considered the first step towards a more extensive study incorporating much larger cohorts that may ultimately utilize this procedure as a viable tool in cancer diagnosis and treatments.



## IX. Concluding statements and future research

Prostate cancer (PCa) progression to metastatic disease involves a complex process of cascading steps. The first steps begin with development of premalignant PIN lesions with continuity gaps in basal cell layer. Next, a malignant cluster of tumor cells invade through continuity gaps into surrounding tissues. These clusters then escape via laminin-expressing peripheral nerves, migrate into and survive the circulatory system, enter and colonize distant tissue causing death. The cleavage of  $\alpha 6$  integrin by the uPA facilitates the altered adhesive status, increasing the cellular rate of migration on laminin. This uPA-mediated cleavage of  $\alpha 6$  integrin is regulated by the uPA receptor (uPAR) through direct co-distributive interaction as confirmed in previous co-immunoprecipitation experiments (Rubenstein *et al.*, 2019). The co-distribution of  $\alpha 6$  integrin with uPAR was found to be dependent on the expression of  $\alpha 3$  integrin. A deletion of the  $\alpha 3$  integrin gene produced increased levels of the cleavage product  $\alpha 6p$ . This result indicates the loss of  $\alpha 3$  integrin is a critical event that occurs in early PCa and promotes progression to aggressive disease. In addition to influencing the cleavage of  $\alpha 6$  integrin, the loss of  $\alpha 3$  integrin also promoted the reduced expression of the cell-cell adhesion protein E-cadherin. The lost surface expression of E-cadherin reduces stable connectivity and promotes cellular plasticity. Taken in concert with the  $\alpha 6$  integrin cleavage, this creates progressive tumors with the ability to disseminate as highly motile collectives. The ability to detect these cascading

events early in disease progression could potentially lead to a preventative measure that would prove beneficial to patients at risk for aggressive cancer.

Advancements in diagnostic strategies and early screening for detection of aggressive disease have lowered the prostate cancer mortality rate 40% and increased the 5-year survival rate for confined disease to nearly 100%. The primary tests are direct rectal examination and PSA serum tests for evidence of cancer. Current tests target newer molecular and protein biomarkers, such as PTEN and ERG, for expression status in patient samples relevant to aggressive disease. However, multiple proteins and other molecular determinants are involved in processes that occur simultaneously that promote progression from low risk to aggressive tumors. This results in patient misdiagnosis and overtreatment of low risk cancers that lack invasive capability and has still yet to curtail the <30% 5-year survival rate of patients with tumors presenting extracapsular invasion.

Consequently, the characterization of more a reliable detection signature indicating the early transition to invasive disease will provide the crucial information for objective decisions for patients truly at risk. Therefore, this research aimed to develop and utilize multiple strategies to characterize various protein associations related to early invasive disease transition. Based on the detection and quantitative analysis of human PCa tissues, it can be concluded that when the loss of  $\alpha 3$  integrin is observed, the increased production of  $\alpha 6$ p associated with enhanced migration. In addition, there is increased coincidence of  $\alpha 6$  integrin with E-cadherin and a correlation to PTEN and ERG status that is an important signature

determining early invasiveness. The results suggest that together, the associations of these surface protein molecules indicate a signature of phenotypical aggressive tumors that are initiating the first steps of invasion.

The research here utilized primary antibody detection strategies on patient tissues and cell lines to target proteins of interest relating to disease progression. The use of antibodies to detect proteins involved in early stage progression of prostate cancer has been a problematic due to the unique and heterogeneous nature of tumors. During different stages of cancer progression, proteins will demonstrate variable expression within a tumor. Furthermore, proteins will also show variable expression within the same focal regions of the same tumors. This means that a cancer can exhibit different subtypes and demonstrate the ability to perform a phenotypic switch from non-aggressive to invasive. It is within this switch to invasive cancer that protein localization patterns and associations can determine a precursor to metastatic potential. Another issue is that tumor regions of interest can be lost due to serial sampling. A viable method to reuse H&E stained slides was developed and tested to mitigate this. The resulting data indicated that the method demonstrated comparable intensities to standard IHC and can be used with multiple targets and allow quantitation.

The optimization of multiplex IHC antibody assays for multiple biomarkers in patient tissue samples resulted in observable patterns of protein localizations indicative of such associations. First, the dual chromogenic detection of  $\alpha 6$  integrin and uPAR exhibited increased co-distribution in increasing Gleason grade tumor samples compared to normal and aggressive. In theory, the resulting pattern would be an early signature of potential invasion. However, discontinuation of the uPAR antibody did not allow further testing. Therefore, E-cadherin became a viable option to test co-distribution. Additional chromogen multiplex detection demonstrated distinct co-distribution patterns of  $\alpha 6$  integrin and E-cadherin with focal loss of  $\alpha 3$  integrin. Furthermore, a quantitative analysis of separate nodes expressing  $\alpha 6$  integrin and E-cadherin co-distribution exhibited distinct ratios percentages that could coincide with potential invasive capability. Although the analysis of the  $\alpha 6$  and E-cadherin co-distribution was accomplished by comparing mappings of chromogen expression in unmixed images, the analysis of the pixels relative to the chromogen intensities were an approximation of protein expression.

The process of PCa cell invasion and migration is a co-opted embryonic developmental process that incorporates cell-matrix and cell-cell adhesion. Cohesive collective migration is a mechanism of cellular mobilization utilized in differentiation of tissues and tissue repair. Adhesive interactions among cells, between cells and the ECM are important during this morphogenetic process (Burdal *et al.*, 1993).  $\alpha 6$  Integrin and E-cadherin are key cell-matrix and cell-cell factors (respectively) involved in collective cell migration. They are also necessary for the dynamic dissemination of these cohesive clusters through adjacent tissues.

The co-association of these two receptors in early cancer progression and migrating clusters indicate the coordination of signaling pathways that control cytoskeletal dynamics in tumor cells regulating the turnover of cell-cell and cell-matrix adhesions allowing tumor plasticity throughout migration. In previous work, we have shown that inhibition of  $\alpha 6$  integrin cleavage prevents invasive cord networks and cellular migration (Rubenstein *et al.*, 2019). However, it was unknown how the inhibition promoted adhesion and what specific pathway was mediated by the loss of  $\alpha 3$  integrin that promoted the invasive process.

Results described in Chapter VI showed that tumor cells expressing a deletion in  $\alpha 3$  integrin demonstrated significant collective migration through muscle and greatly increased dissemination to distant tissue. The collective migration was slightly comparable to the tumor cells expressing endogenous wild type receptors but the dissemination was increased 3-fold. In addition, this exhibited stark contrast with tumor cells expressing an uncleavable full-length  $\alpha 6$  integrin, which demonstrated reduced collective invasion sites and minor dissemination. Interestingly, the results indicate that deletion of  $\alpha 3$  integrin not only promotes the production of the tumor variant  $\alpha 6p$ , but also increases E-cadherin cell membrane localization. This would play a significant role in the regulating the plasticity of invading tumor collectives through tissues. The most profound discovery was that the inhibition of  $\alpha 6$  integrin cleavage not only mitigated production of  $\alpha 6p$ , but also significantly increased E-cadherin protein expression and cell membrane localization on tumor cell pellets. Proximity detection assay confirmed the formation of  $\alpha 6$  integrin an E-cadherin dynamic complexes in human prostate

tissues. The comparison between normal tissues and aggressive PNI lesions demonstrated differential localization patterns that would indicate the  $\alpha 6$  integrin cleavage event in aggressive samples and stable, intact  $\alpha 6$  integrin, complexes in normal. Therefore, inhibiting the  $\alpha 6$  integrin PTM has revealed a pathway regulating a phenotypic switch to inhibit tumor migration by promoting E-cadherin surface expression. Future experiments to elucidate the unknown activated factors promoting E-cadherin expression will provide a promising development for potential intervention of metastatic disease.

The localization of  $\alpha 6$  integrin was also associated with status of PTEN and ERG in human PCa specimens. PTEN is a regulator of intracellular vesicular trafficking that inhibits integrin mediated cell migration. ERG, which is associated with the TMPRSS2: ERG gene fusion, is expressed in ~50% of prostate cancers and correlates with prostate cancer progression. Correlative studies have shown a relationship between PTEN loss and ERG expression in promoting prostate cancer progression (Yoshimoto *et al.*, 2008; King *et al.*, 2009; Carver *et al.* 2009; Guedes *et al.*, 2017). Integrins internalize and sort through the intracellular pathway system and then recycle to the surface membrane in focal adhesions for cellular migration. The results in this research showed that a number of tumor sample specimens with focal PTEN loss and ERG expression demonstrated membrane expression of  $\alpha 6$  integrin. This suggested that loss of PTEN promotes increased recycling of the  $\alpha 6$  integrin to the surface in more aggressive tumors. This notion was tested with the development of a quantitative algorithm to determine if the membrane or cytoplasmic positive localization of  $\alpha 6$  integrin in PCa CNB samples (n=9)

correlated to aggressiveness. The results showed that tumors with negative PTEN and positive ERG expression exhibited shift to more membranous localization of  $\alpha 6$  integrin whereas cytoplasmic localization was observed in samples PTEN negative and ERG negative.

Overall, the results observed in this research demonstrate the heterogenous nature of tumor progression. While relying on the detection of relevant proteins to identify tumors initiating aggressive events, it does elucidate the genomic causal determinants of invasive transition. This research demonstrates several protein associations either mediate or are indicative of transition from non-aggressive to aggressive disease. The expression of  $\alpha 3$  integrin regulates the expression and cleavage of  $\alpha 6$  integrin and the expression of E-cadherin. The status of PTEN and ERG correlate with low risk or aggressive disease. Hence, either the loss or co-occurrence of these in association with  $\alpha 6$  integrin localization in a sample can be predictive of tumor invasiveness in patients. Our ability to detect these protein associations in patient tissue samples have given the capability to stratify tumors with aggressive potential. Therefore, it has predictive value and brings further insight into evaluating other protein associations in other aggressive cancers for interventional means of therapeutics. Further evaluations of cellular adhesion factors, such as these described in this study, may lead to understanding how these factors relate to clinical progression of disease and metastasis across various cancer types including prostate, colorectal and breast cancers.

## X. Tables

Table 1. List of antibody diluents

Diluent	Buffer, pH
95119	Tris, 7.7
90039	
95028	Phosphate, 7.3
90040	
90103	Tris, 7.5

Table 2. 6-week diaphragm invasion sites

DU145 Diaphragm ID	Tumor invasion sites-strip number					Overall total
	1	2	3	4	Total	
WT Diaphragm 1	1	6	3	6	16	49
WT Diaphragm 2	4	5	3	2	14	
WT Diaphragm 3	3	5	7	4	19	
$\alpha 3^{\text{KO}}$ Diaphragm 1	1	3	5	3	12	39
$\alpha 3^{\text{KO}}$ Diaphragm 2	1	4	5	5	15	
$\alpha 3^{\text{KO}}$ Diaphragm 3	4	3	3	2	12	
$\alpha 6^{\text{AA}}$ Diaphragm 1	1	1	1	0	3	5
$\alpha 6^{\text{AA}}$ Diaphragm 2	1	0	0	0	1	
$\alpha 6^{\text{AA}}$ Diaphragm 3	0	0	0	1	1	



**Table 3. 6-week small bowel tumor incidence**

Small Bowel DU145 ID	Tumor incidence-specimen number				Overall Total
	1	2	3	Total	
WT Sm. Bowel 1	0	0	0	0	
WT Sm. Bowel 2	0	0	0	0	
WT Sm. Bowel 3	0	0	0	0	5
WT Sm. Bowel 4	0	1	2	3	
WT Sm. Bowel 5	1	0	1	2	
$\alpha 3^{KO}$ Sm. Bowel 1	0	2	1	3	
$\alpha 3^{KO}$ Sm. Bowel 2	0	1	1	2	
$\alpha 3^{KO}$ Sm. Bowel 3	1	0	0	1	15
$\alpha 3^{KO}$ Sm. Bowel 4	1	6	0	7	
$\alpha 3^{KO}$ Sm. Bowel 5	1	1	0	2	
$\alpha 6^{AA}$ Sm. Bowel 1	0	0	0	0	
$\alpha 6^{AA}$ Sm. Bowel 2	0	0	0	0	
$\alpha 6^{AA}$ Sm. Bowel 3	0	0	0	0	1
$\alpha 6^{AA}$ Sm. Bowel 4	0	0	0	0	
$\alpha 6^{AA}$ Sm. Bowel 5	0	0	1	1	

**Table 4. List of initially assessed sample H&E stained slides with specimen parameters, de-stain results and antibodies tested.**

Tissue	Specimen	H&E De-stain result	Antibodies used	Initial H&E Analysis
Prostate	Resection	+	p40	Malignant Primary_Adenocarcinoma, Gleason 3+3 = 6
Prostate	Resection <sup>a</sup>	+	CK5/14: PTEN	NA
Prostate	Resection <sup>a</sup>	+	CK5/14: p504s	Malignant Primary_Adenocarcinoma, Gleason 3+3 = 6
Liver (Pancreas Met)*	CNB <sup>a</sup>	+	PTEN/p504s/CK5/14	Mock CNBs (due to the cut)
Liver	Resection	+/-	HMWCK+p63	NA
Lung	Resection	+/-	HMWCK+p63	NA
N. colon	Resection	+	HMWCK+p63	NA
Skin	Resection	-	E-cadherin	NA
Skin	Resection	-	E-cadherin	NA
Prostate	TMA	+	ERG	NA
Prostate	CNB	+	CD49f	3+3
Prostate	CNB	+	CD49f	no cancer
Prostate	CNB	+	CD49f	no cancer
Prostate	CNB	+	PTEN/ERG <sup>b</sup>	High grade growing into normal glands 3+3
Prostate	CNB	+	PTEN/ERG <sup>b</sup>	little bit of tumor grade 3+3
Prostate	CNB	+	PTEN/ERG <sup>b</sup>	3+3, area of tumor, fragmented tumor
Prostate	CNB	+	PTEN/ERG <sup>b</sup>	no tumor
Prostate	CNB	+	PTEN/ERG <sup>b</sup>	grade 4 and 5 cancer, High grade
Prostate	CNB	+	PTEN/ERG <sup>b</sup>	low grade 3, Lot of PIN
Prostate	CNB	+	PTEN/ERG <sup>b</sup>	atrophy, inflammation
Prostate	CNB	+	PTEN/ERG <sup>b</sup>	no cancer, small nerve area
Prostate	CNB	+	PTEN/ERG <sup>b</sup>	a little fragment tumor
Prostate	CNB	+	PTEN/ERG <sup>b</sup>	HGPIN, few basal cells left, some cancer
Prostate	CNB	+	PTEN/ERG <sup>b</sup>	Atypical adenomatous hyperplasia and atrophic glands, Central zone lesion
Prostate	CNB	+	PTEN/ERG <sup>b</sup>	1 mm grade 3 tumor
Prostate	CNB	+	PTEN/ERG <sup>b</sup>	small tumor area
Prostate	CNB	+	PTEN/ERG <sup>b</sup>	small tumor area
Prostate	CNB	+	CD49f/HMWCK <sup>b</sup>	high grade cancer 4 and 5 trying to make glands invading into norm glands
Prostate	CNB	+	CD49f/HMWCK <sup>b</sup>	grade 5 cancer (high grade), PIN
Prostate	CNB	+	CD49f/HMWCK <sup>b</sup>	small amount of tumor no basal cells
Prostate	Resection	+	CK 8 & 18	NA
Prostate	CNB	+	CD49f	little bit of tumor grade 3+3
Prostate	CNB	+	HMWCK+p63	grade 4 and 5 cancer, High grade
Prostate	CNB	+	p504s	low grade 3, Lot of PIN
Prostate	CNB	+	CK 8 & 18	cancer (3+3 with normal)
Prostate	CNB	+	PTEN	3+3 ERG positive, tumor folded over
Prostate	CNB	+	CD49f	3+3 lesion: 3 cores
Prostate	CNB	+	ERG	3+3 involving 2/2 cores
Prostate	CNB	+	CD49f	2 cores: 3+3 involving 2/2 cores
Prostate	CNB	+	CK 8 & 18	3+3 lesion in one frag 1mm heterogeneous chromatin
Prostate	CNB	+	HMWCK+p63	tumor 3+3 Atrophic glands, edge normal
Prostate	CNB	+	HMWCK+p63	no tumor
Prostate	CNB	+	HMWCK+p63	atrophy inflammation
Prostate	CNB	+	CK 8&18	atrophy, inflammation
Prostate	CNB	+	CD49f	no cancer
Prostate	CNB	+	ERG	3+3 fragmented tumor lost basal cells

Abbreviations: Met, Metastasis; CNB, Core needle biopsy; NA, Not applicable: a Multiple H&Es prepared. b Dual chromogen immunostaining. \*Mock needle cores: Appropriate H&E de-stain, (+); Moderate de-stain, (+/-); retention of H&E, (-).

**Table 5. Time tracking and coverslip parameters**

Sample Archive time	Coverslip removal time	Type of Coverslip
1 month	10 min	Thin film
1 year	10 min	Thin film
2 year	10 min-60min	Thin film
4 year	~38 hrs	Thin film
4+ year**	~47 hrs	Thin film
2+ year#	1-2 days	Glass
5 year	4-5 days	Glass
5 year	4-5 days	Glass
12 year	4-5 days	Glass

Abbreviations: hrs, hours; \*\* Sample Archived 4 years 11 months; # Samples Archived 2 years 11 months ~Approximation due to time at removal

**Table 6. Immunohistochemistry (IHC) Antibodies and Adapted Staining Protocols**

Antibody (clone)	HMWCK+p63 (34 $\beta$ E12)	p504s (SP116)	CK 8 & 18 (B22.1 & B23.1)	PTEN (SP218)	E-cadherin (36)	CD49f	ERG (EPR3864)
Species	mouse monoclonal	rabbit monoclonal	mouse monoclonal	rabbit monoclonal	mouse monoclonal	rabbit polyclonal	rabbit monoclonal
Antibody Vendor	Ventana Medical Systems, Inc., Tucson, Arizona	Cell-Marque, Rocklin, California	Ventana Medical Systems, Inc., Tucson, Arizona			N/A	Ventana Medical Systems, Inc., Tucson, Arizona

**De-stained H&E slide Immunohistochemistry adapted protocol**

IHC platform	Ventana Benchmark ULTRA						
Detection Kit	Ventana OptiView DAB IHC		Ventana UltraView DAB IHC		Ventana OptiView DAB IHC		
Deparaffin				none			
HIER	64 min CC1 (pH 8.5)	32 min CC1 (pH 8.5)	36 min CC1 (pH 8.5)	56 min CC1 (pH 8.5)	63 min CC1 (pH 8.5)	64 min CC1 (pH 8.5)	32 min CC1 (pH 8.5)
Blocking Ab incubation parameters	36°C, 16 min	36°C, 32 min	37°C, 16 min	37°C, 16 min	36°C, 24 min	36°C, 24 min	36°C, 32 min

Abbreviations: Ab, antibody; CC, cell conditioning; DAB, 3, 3'- diaminobenzidine HIER, heat-induced epitope retrieval; min, minutes, N/A, Not Applicable.

**Table 7. Comparison of H&E re-used and sequential comparator immunostaining intensity scores**

Marker	Re-used H&E stain intensity	Sequential stain intensity: 0-3 (int ctrl)					Initial H&E assessment
HMWCK+p63	3	2	2	2	0	3	atrophy inflammation
CK8&18	3	3	3	3	3	3	Atrophy + inflammation: whole glands
CD49f	3(2)	3 (1)	3 (1)	3 (1)	3 (1)	3 (2)	no cancer, int ctrls
E-cadherin	3	3	3	3	3	3	not much cancer but weird well differentiated lots of infiltrating lymphocytes, grade 3+3
ERG	3 (3)	0 (3)	0 (3)	0 (0)	1 (3)	0 (3)	fragmented tumor lost basal cells, int ctrls

Abbreviation: int ctrls, internal controls.

## XI. Materials and methods

**Cell culture:** A human prostate DU145 cell line was obtained from the American Tissue Type Collection (ATCC, Manassas, VA). The cell line was cultured in Iscove's modified Dulbecco's medium (IMDM) from Invitrogen (Grand Island, NY) supplemented with 10% fetal bovine serum (FBS) Hyclone Laboratories (Novato, CA) and incubated at 37° in a 5% CO<sub>2</sub> humidified chamber. Non-enzymatic Cellstripper (CelGro, Manassas, VA) was used for cell harvesting.

**Whole cell lysate and cell pellet preparation.** The DU145 cell lines were washed in a saline buffer and cell lysis was performed with CHAPS lysis buffer (50 mmol/L Tris HCL, 110 mmol/NaCl, 5 mmol L EDTA, 1% CHAPS) with a complete mini protease inhibitor and phosphatase 1 and 2 inhibitor additives from Roche and Sigma, respectively.

**Gene editing.** Homozygous knock-out cell lines for ITGA6 gene ( $\alpha 6$ KO), ITGA3 gene (DU145  $\alpha 3$ KO) and homozygous amino acid substitutions for the ITGA6 R594A and 596A (DU145  $\alpha 6^{AA}$ ) were created using CRISPR/Cas9 technologies in the University of Arizona Cancer Center (UACC) Genome Editing Facility. For the production of DU145  $\alpha 6^{AA}$  the facility produced double strand breaks on either side of exon 4 of *ITGA6* transcription unit at predicted sites 2: 172,466,252 and 2: 172,468,987 with the guide RNAs corresponding to the sequences 5'-TAGACCGAACATATCAAACG-3' and 5'-ATATTTGCTGGTCTGGGATC-3'.

Colonies were screened by an AA-specific polymerase chain reaction (PCR) primer and agarose gel electrophoresis. Clones positive for the AA amplification were sent for sequencing.

Parental prostate cancer cells DU145 were transfected with Cas 9 protein, crRNAs, and tracrRNA (Integrated DNA Technologies) using the Lipofectamine RNAiMAX reagent (Thermo Fisher Scientific). Two days after transfection, cutting efficiency was estimated based on DNA prepared from a portion of the transfected cell population using a T7 endonuclease assay (New England BioLabs) employing PCR primers flanking the predicted ligation-junction product (5'-GTTCTGCAGGAGGTTGTGGA-3' and 5'-TCGCCCATCACAAAAGCTCC-3'). Single cells were deposited in ten 96-well plates by UACC Flow Cytometry Shared Resource. Colonies were expanded and screened by PCR and agarose gel electrophoresis. Clones that were negative for fragment internal to the targeted deletion (5'-ACTCAGAGTCGAGGCCATTTG-3') and 5'-TAGGTTGTGTGATTGCTTCTAAGT-3') but positive for ligation-junction fragment were potentially homozygous for the deletion. Absence of  $\alpha 6$  integrin or presence of  $\alpha 6$  integrin AA mutant was confirmed by flow cytometry and western-blot analysis. All cells were authenticated by the University of Arizona Genetics Core (UAGC).

**SCID Mouse Muscle Invasion Model.** For the mouse xenograft muscle invasion assay, NOD.Cg-*Prkdc*<sup>scid</sup> *Il2rg*<sup>tm1Wjl</sup>/SzJ mice (or NOD-*scid* IL2Rgamma) (3 mice per group) from Dr. Leonard D. Shultz from The Jackson Laboratory, were

interperitoneally (IP) implanted with human DU145 wildtype (WT),  $\alpha 3^{KO}$ ,  $\alpha 6^{KO}$  or  $\alpha 6^{AA}$  tumor cells ( $1 \times 10^7$ ). Tumor colonies were allowed to grow on the diaphragm and within the peritoneal cavity for 6 and 8 weeks (formation of ascites dictated harvest at 6 weeks). Diaphragm samples from each subject was harvested, fixed and embedded in a lateral manner to orient the tumor colony on top of the muscle. Sequential transverse sectioning will demonstrate tumor displacement of the myoepithelium and invasion into and through the muscle to the superior side of the diaphragm.

The experimental mouse studies were reviewed and approved by the Institutional Animal Care and Use Committee (IACUC), Protocol Number: 07029. The protocol was conducted in accordance with all applicable federal and institutional policies, procedures and regulations, including PHS policy on Human Care and Use of Laboratory Animals, USDA regulations (9 CFR parts 1, 2, 3), the Federal Animal Welfare Act (7 USC 2131 et Seq.), the Guide for the Care and Use of Laboratory Animals, and all institutional regulations and policies regarding animal care and use at the University of Arizona. The mice were anesthetized by placement into a CO<sub>2</sub> chamber.

**Advanced staining and detection platforms:** Processing of FFPE tissue sample slides was performed on either the Roche Tissue Diagnostics/ Ventana BenchMark ULTRA (BenchMark ULTRA) IHC/ISH system or DISCOVERY Ultra (DISCOVERY) automated system platform. The optimization of initial antibody protocols was accomplished on the BenchMark ULTRA. The migration of these procedures for antibody Chromogenic Multiplex, and protein biomarker proximity detection assays was performed using the DISCOVERY platform.

**Reagent Detection Kits:** The reagent detection kits utilized for these studies were all acquired from Roche Tissue Diagnostics. The kits used were Ventana OptiView DAB IHC Detection Kit, *ultraView* IHC DAB Detection Kit and DISCOVERY Chromomap Detection kits. The proximity detection assay is a research use only, in research development detection system applied to samples on the DISCOVERY ULTRA platform for interrogation of protein co-distribution.

**Ready to use Antibodies.** The ready to use antibodies used for this study included anti-high molecular weight cytokeratin (HMWCK) + p63 mouse monoclonal Basal Cell Cocktail (Ventana, clone 34 $\beta$ E12+4A4), anti-E-cadherin mouse monoclonal antibody (mAb) (0.314 $\mu$ g/mL, Ventana, clone 36), anti-E-cadherin rabbit mAb (Cell-Marque, EP700Y), anti-p120 Catenin mouse mAb (Ventana, clone 98), anti-PTEN rabbit mAb (1:300, Ventana, clone SP218), anti-ERG mouse mAb (Ventana, clone EPR3864). The ready to use antibodies used sparingly in this study were anti-p40 (BC28), CK 5/14 and anti-Desmin mouse mAb (DER). These antibodies were used primarily for IHC of de-identified archived FFPE tissues.



*E-cadherin antibody titration:* It had been determined the antibody dilution of ready to use anti-E-cadherin resulted in saturated immunostaining intensity. Therefore, it was decided to formulate dilution titers of E-cadherin from a ready to use dispenser. The standard concentration of ready to use dispensers is 0.314 µg/ml. A 1:10 dilution of the standard dispenser concentration was optimal and also utilized in chromogen multiplex IHC and protein gels.

***Experimental Research Antibodies:*** The anti- $\alpha$ 6 (CD49f) or AA6NT rabbit polyclonal antibody (pAb) was characterized by our lab and used at a dilution of 1:800. The anti- $\alpha$ 3 (CD49c) rabbit pAb (Sigma Aldrich, clone HPA008572) was used at 1:200. The anti- $\beta$ 4 integrin rat monoclonal antibody (BD Pharmingen, clone 439.9B) was used at 1:100. The anti-uPAR mouse monoclonal (Sekisui Diagnostics, clone ABG3937) was used at 1:100. Each of these were used in the analysis of protein expression in FFPE tissues and the AA6NT was also used in western blot. Each primary antibody was initially formulated at 1:100 dilution in various RTD proprietary Tris or Phosphate based antibody diluents (**Table 1**) to determine specificity of epitope binding, non-specific binding of endogenous proteins and background deposition. A dilution “guard-banding” was performed to determine the appropriate antibody dilution for optimal immunostaining intensity. Two titrations above and below the 1:100 dilution was tested with each research antibody and the dilution exhibiting appropriate immunostaining intensity was selected.

**Human Prostate Tissue Immunohistochemistry.** Prostate tissue resections from various vendors that had been formalin fixed and embedded in paraffin were acquired from Ventana Medical Systems, Inc. / Roche Tissue Diagnostics (RTD). In addition, ~435 prostate core needle biopsies (CNBs) were obtained from the University of Arizona Medical Imaging Department with permission from Dr. Hina-Arif Tawari. Prostate resection samples slides were micro-sectioned at 4 $\mu$ m thickness and mounted to positively charged Matsunami TOMO® or superfrost (Thermo Fischer Scientific) glass slides for hematoxylin and eosin staining (H&E) and immunohistochemistry by RTD integrated (iCORE) services histotechnologists. The University of Arizona TACMASR department prepared the prostate CNB sample slide sections. H&E stained slides were prepared from the initial sectioning of each sample tissues and evaluated for content by a pathologist (Dr. Ray Nagle). Immunohistochemical (IHC) staining was conducted manually or with automated protocols on the VENTANA BenchMark ULTRA or DISCOVERY ULTRA platforms following antibody package insert protocols for publicly released (on market) antibodies or optimized protocols for experimental antibodies. The IHC staining protocols performed for each antibody used is listed in **Table 5**.

**Chromogen Multiplex Assays:** To perform chromogen multiplex IHC (cmIHC) using brightfield microscopy, anti-species secondary and tertiary antibodies conjugated with hydroxy quinazoline (HQ), horseradish peroxidase (HRP), nitroprazole (NP) and alkaline phosphatase (AP) were acquired from RTD. All chromogen multiplex IHC assays were performed on the DISCOVERY ULTRA platform.

**Proximity Detection Assay:** The Proximity Detection Assay (PDA) is a proprietary, in research development detection system of RTD. Execution of the PDA was performed on the DISCOVERY ULTRA. Antibodies for  $\alpha 6$  integrin and E-cadherin were utilized with the PDA for the proximal detection of protein complexes.

**Imaging Platforms and Image Analysis:** Tissue slide imaging was performed using the following imaging platforms: the Aperio AT2 slide scanner (Leica Biosystems), VENTANA DP200 slide scanner, a hyperspectral research imager (HRI) and Axio Scan 2.1™ (Axio™) slide scanner. The Aperio AT2 and DP200 imagers were utilized for IHC DAB and chromogen multiplex IHC detection. The HRI was utilized for image un-mixing and quantitative image analysis of individual chromogen intensities and protein co-distribution quantitative values after chromogenic multiplexing. The Aperio AT2 image software was used for image analysis for measurements of tumor invasion depth. The Axio™ was used with QuPath™ image analysis software for quantitative analysis of  $\alpha 6$  integrin protein localization on slide images.

**Statistical Analysis:** GraphPad Prism 8.2.1 was utilized to perform Two-way ANOVA and RM one-way ANOVA analysis throughout. MATLAB analysis software was used to develop a quantitative image analysis for HRI imaging. QuPath™ image analysis software was used in development of membrane/ cytoplasmic localization algorithm with the Axio™ scanner. For muscle invasion assays, two-way ANOVA statistical significance was tested for differences in number of tumor sites and invasion depth. For H&E de-stain and re-stain, RM one-way ANOVA statistical significance was tested for differences in matching intensities assuming equal variance. P-values lower than 0.05 were considered statistically significant.

## XII. Supplemental figures

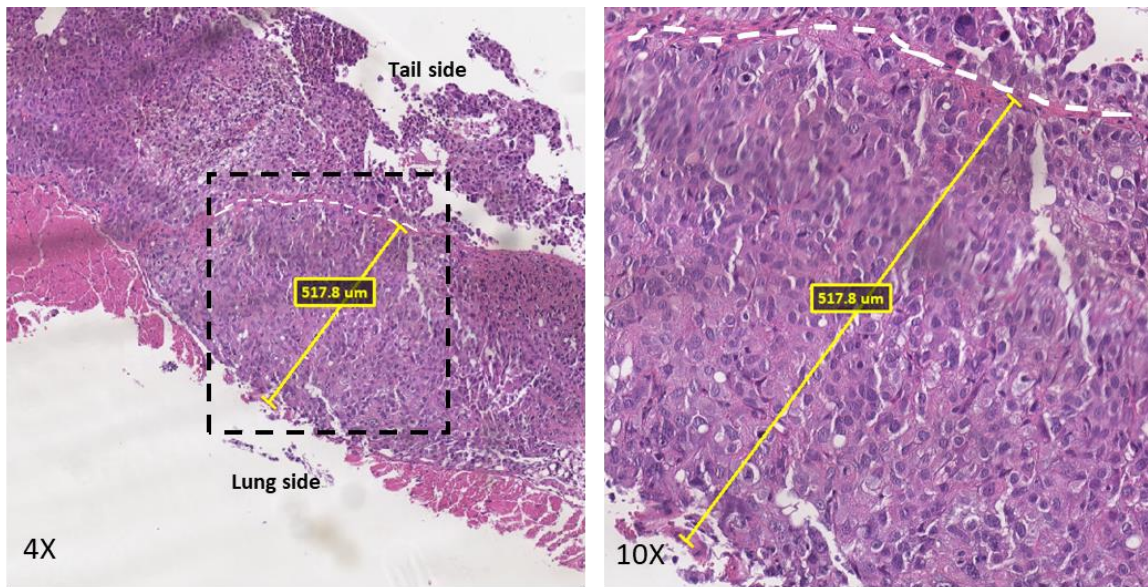


**Figure S1. H&E stained slide of DU145 WT 8-week mouse diaphragm.** Sample slide images with maximum tumor cluster depth measurement showing invasion to the lung side (left panel, 4x). Image magnification of the annotated region (right panel, 10x).

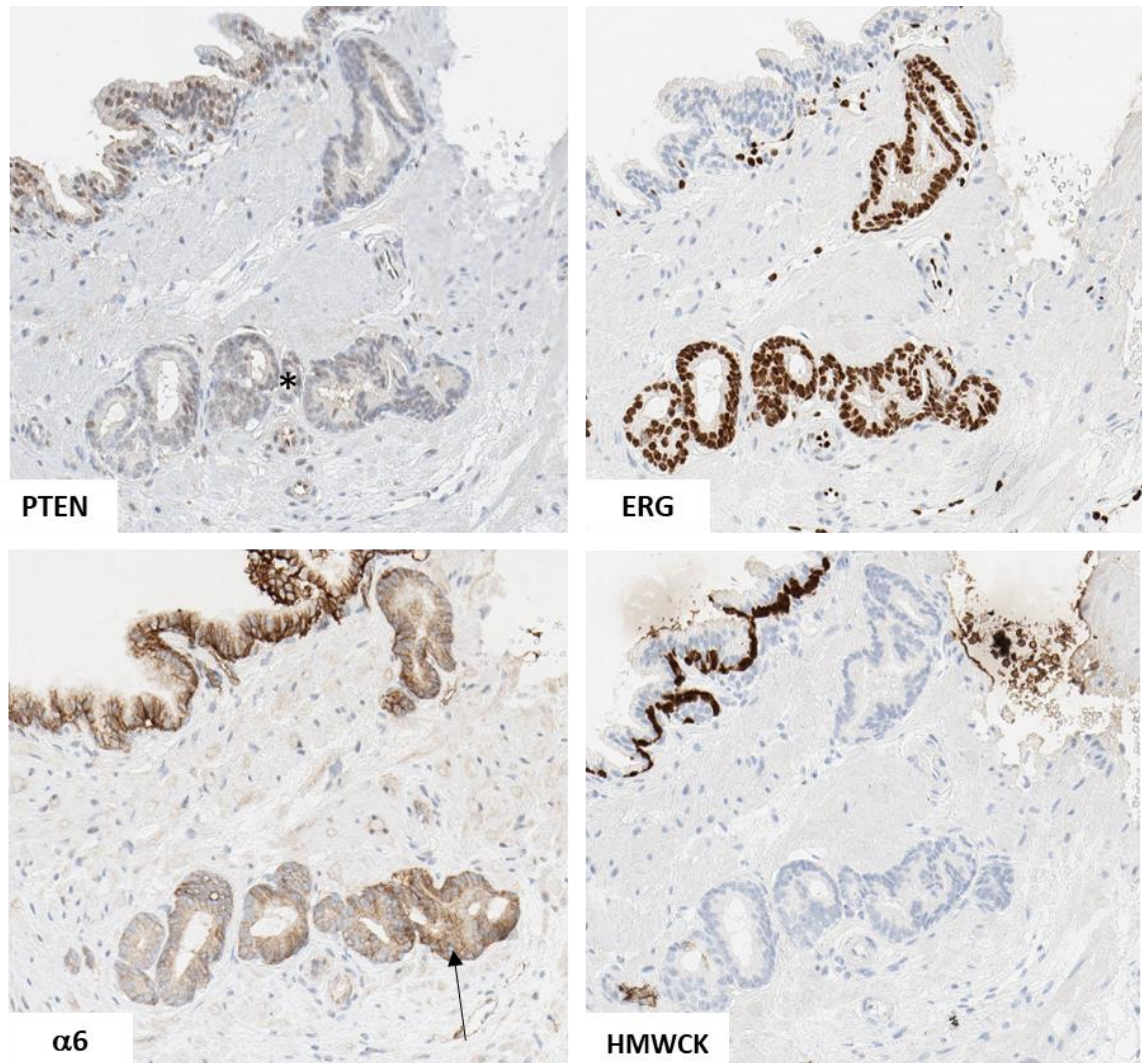


**Figure S2.  $\alpha 6$  integrin localization with PTEN and ERG expression.** Prostate cancer immunostained with antibodies for PTEN, ERG,  $\alpha 6$  integrin and HMWCK+p63 (HMWCK). Cancer region with PTEN loss (\*) (top left panel). ERG positive (top right panel),  $\alpha 6$  integrin membrane expression (black arrow) (bottom left panel) and lack of HMWCK intensity (bottom right panel).

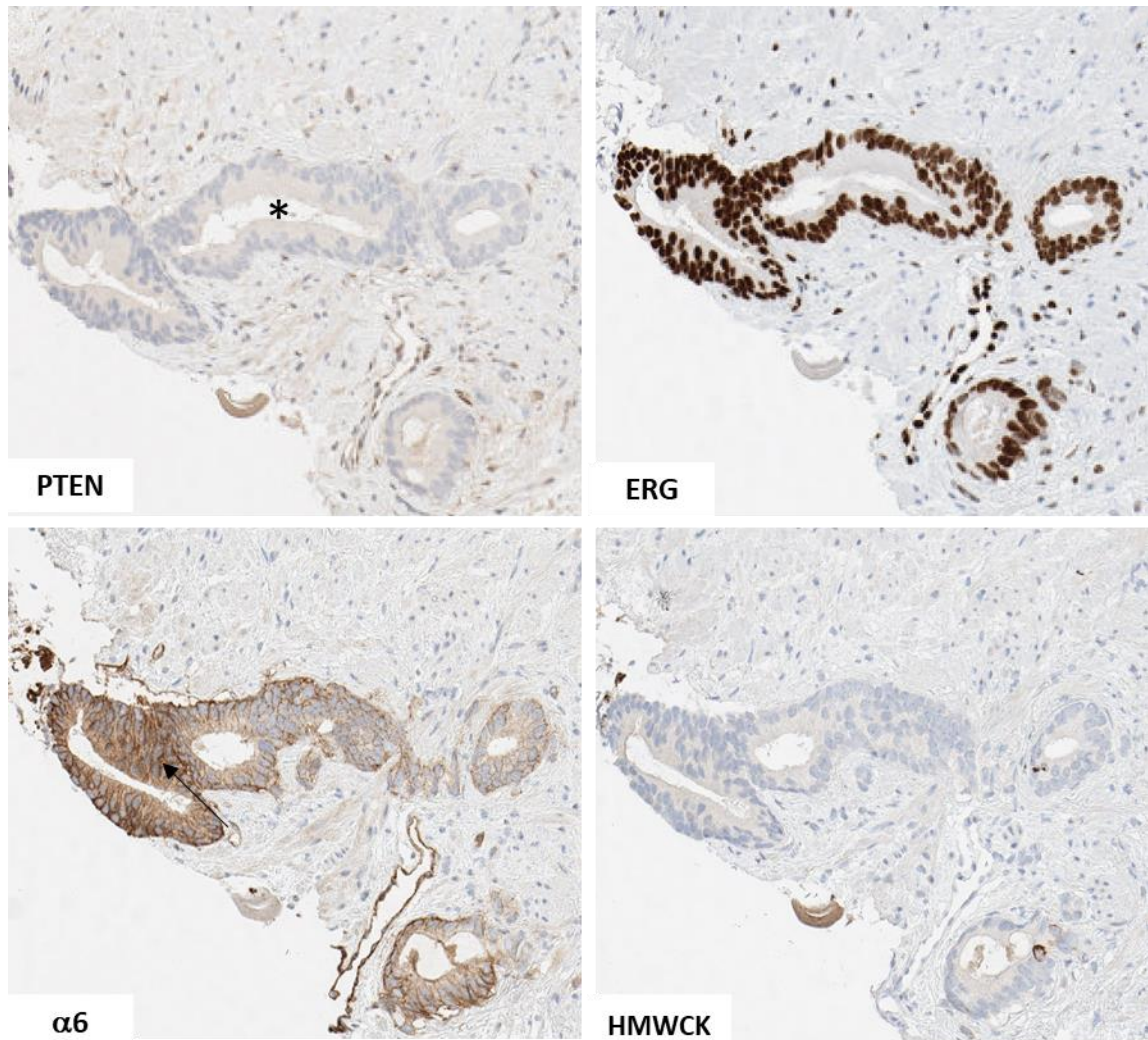


**Figure S3.  $\alpha 6$  integrin localization with PTEN and ERG expression.** Prostate cancer immunostained with antibodies for PTEN, ERG,  $\alpha 6$  integrin and HMWCK+p63 (HMWCK). Cancer region with PTEN loss (\*) (top left panel), ERG positive (top right panel),  $\alpha 6$  integrin membrane expression (black arrow) (bottom left panel) and lack of HMWCK intensity (bottom right panel).

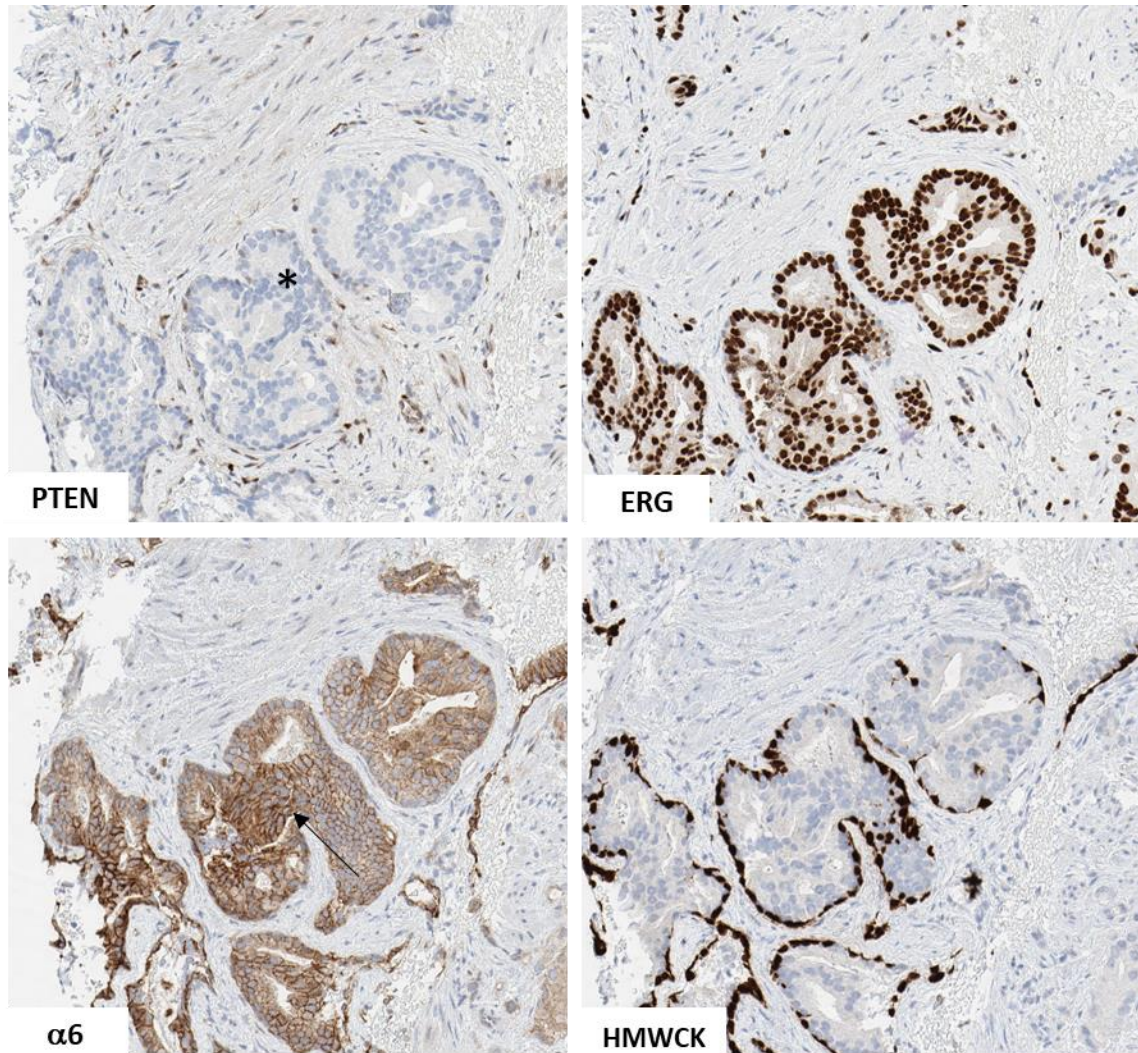


**Figure S4.  $\alpha 6$  integrin localization with PTEN and ERG expression.** Prostate cancer immunostained with antibodies for PTEN, ERG,  $\alpha 6$  integrin and HMWCK+p63 (HMWCK). Tumor invading into normal glands with PTEN loss (\*) (top left panel), ERG positive (top right panel),  $\alpha 6$  integrin membrane expression (black arrow) (bottom left panel) and positive expression of HMWCK in normal basal cells of the glands (bottom right panel).



## Appendix A: Manuscripts

1. William L. Harryman, **James P. Hinton**, Cynthia P. Rubenstein, Parminder Singh, M.D., Raymond B. Nagle, M.D., Ph.D., Sarah J. Parker, Ph.D., Beatrice S. Knudsen, M.D., Ph.D., Anne E. Cress, Ph.D. “The Cohesive Metastasis Phenotype in Human Prostate Cancer.” *Biochimica et Biophysica Acta (BBA) – Reviews on Cancer* 1866 (2016): 221-31.
2. Cynthia S. Rubenstein, Jamie M.C. Gard, Mengdie Wang, Julei E. McGrath, Nadia Ingabire, **James P. Hinton**, Kendra D. Marr, Skyler J. Simpson, Raymond B. Nagle, Cindy K. Miranti, Noel A. Warfel, Joe G.N. Garcia, Hina Arif-Tiwari and Cress, Anne E. Cress. “Gene Editing of  $\alpha 6$  Integrin Inhibits Muscle Invasive Networks and Increases Cell-Cell Biophysical Properties in Prostate Cancer.” *Cancer Research* (2019); 79: 4703-14.
3. Mengdie Wang, **James P. Hinton**, Joe G.N. Garcia, Beatrice S. Knudsen, Raymond B. Nagle, and Anne E. Cress. “Integrin  $\alpha 6\beta 4$  variant is associated with actin and CD9 structures and modifies the biophysical properties of cell-cell and cell-extracellular matrix interactions.” *Molecular Biology of the Cell* (2019): 838-850.
4. **James P. Hinton**, Katerina Dvorak, Esteban Roberts, Wendy J. French, Jon C. Grubbs, Anne E. Cress, Hina-Arif Tawari, Raymond B. Nagle. “A Method to Reuse Archived H&E Stained Histology Slides for a Multiplex Protein Biomarker Analysis.” *Methods and Protocols*. (2019); 2: 4, 86.

## REFERENCES

- A. Sakr, Wael, David J. Grignon, Gabriel P. Haas, Lance K. Heilbrun, J. Edson Pontes, and John D. Crissmana. 1996. "Age and Racial Distribution of Prostatic Intraepithelial Neoplasia." *European Urology* 30 (2): 138–44. <https://doi.org/10.1159/000474163>.
- Ayala, Gustavo, Anna Frolov, Deyali Chatterjee, Dandan He, Susan Hilsenbeck, and Michael Ittmann. 2015. "Expression of ERG Protein in Prostate Cancer: Variability and Biological Correlates." *Endocrine-Related Cancer* 22 (3): 277–87. <https://doi.org/10.1530/ERC-14-0586>.
- Barczyk, Malgorzata, Sergio Carracedo, and Donald Gullberg. 2010. "Integrins." *Cell and Tissue Research* 339 (1): 269–80. <https://doi.org/10.1007/s00441-009-0834-6>.
- Becker-Santos, Daiana D, Yubin Guo, Mazyar Ghaffari, Elaine D Vickers, Melanie Lehman, Manuel Altamirano-Dimas, Arusha Oloumi, *et al.* 2012. "Integrin-Linked Kinase as a Target for ERG-Mediated Invasive Properties in Prostate Cancer Models." *Carcinogenesis* 33 (12): 2558-67. <https://doi.org/10.1093/carcin/bgs285>.
- Berx, G., and F. van Roy. 2009. "Involvement of Members of the Cadherin Superfamily in Cancer." *Cold Spring Harbor Perspectives in Biology* 1 (6): a003129–a003129. <https://doi.org/10.1101/cshperspect.a003129>.
- Birchmeier, W, and J Behrens. 1994. "Cadherin Expression in Carcinomas: Role in the Formation of Cell Junctions and the Prevention of Invasiveness." *Biochimica et Biophysica Acta (BBA) - Reviews on Cancer* 1198 (1): 11–26. [https://doi.org/10.1016/0304-419X\(94\)90003-5](https://doi.org/10.1016/0304-419X(94)90003-5).
- Bolognesi, Maddalena Maria, Marco Manzoni, Carla Rossana Scalia, Stefano Zannella, Francesca Maria Bosisio, Mario Faretta, and Giorgio Cattoretti. 2017. "Multiplex Staining by Sequential Immunostaining and Antibody Removal on Routine Tissue Sections." *The Journal of Histochemistry and Cytochemistry: Official Journal of the Histochemistry Society* 65 (8): 431–44. <https://doi.org/10.1369/0022155417719419>.
- Bonkhoff, H., and K. Remberger. 1995. "Morphogenetic Aspects of Normal and Abnormal Prostatic Growth,." *Pathology - Research and Practice* 191 (9): 833-35. [https://doi.org/10.1016/S0344-0338\(11\)80963-5](https://doi.org/10.1016/S0344-0338(11)80963-5).
- Borghì, N., M. Lowndes, V. Maruthamuthu, M. L. Gardel, and W. J. Nelson. 2010. "Regulation of Cell Motile Behavior by Crosstalk between Cadherin- and Integrin-Mediated Adhesions." *Proceedings of the National Academy of Sciences* 107 (30): 13324–29. <https://doi.org/10.1073/pnas.1002662107>.
- Bostwick, David G., and Joseph W. Aquilina. 1996. "Prostatic Intraepithelial Neoplasia (PIN) and Other Prostatic Lesions as Risk Factors and Surrogate Endpoints for Cancer Chemoprevention Trials." *Journal of Cellular Biochemistry* 63 (S25): 156–64. [https://doi.org/10.1002/\(SICI\)1097-4644\(1996\)25+<156](https://doi.org/10.1002/(SICI)1097-4644(1996)25+<156).
- Bostwick, David G, Lina Liu, Michael K Brawer, and Junqi Qian. 2004. "High-Grade Prostatic Intraepithelial Neoplasia." *Reviews in Urology* 6 (4): 171–79.

- Bouali, S., Chrétien, A., Ramacci, C., Rouyer, M., Becuwe, P., Merlin, J. "PTEN expression controls cellular response to cetuximab by mediating PI3K/AKT and RAS/RAF/MAPK downstream signaling in KRAS wild-type, hormone refractory prostate cancer cells". *Oncology Reports* 21, no. 3 (2009): 731-735. [https://doi.org/10.3892/or\\_00000278](https://doi.org/10.3892/or_00000278)
- Brase, Jan C, Marc Johannes, Heiko Mannsperger, Maria Fälth, Jennifer Metzger, Lukasz A Kacprzyk, Tatjana Andrasiuk, *et al.* 2011. "TMPRSS2-ERG - Specific Transcriptional Modulation Is Associated with Prostate Cancer Biomarkers and TGF- $\beta$  Signaling." *BMC Cancer* 11 (1). <https://doi.org/10.1186/1471-2407-11-507>.
- Bridgewater, R. E., J. C. Norman, and P. T. Caswell. 2012. "Integrin Trafficking at a Glance." *Journal of Cell Science* 125 (16): 3695-3701. <https://doi.org/10.1242/jcs.095810>.
- Bronsert, P, K Enderle-Ammour, M Bader, S Timme, M Kuehs, A Csanadi, G Kayser, *et al.* 2014. "Cancer Cell Invasion and EMT Marker Expression: A Three-Dimensional Study of the Human Cancer-Host Interface: 3D Cancer-Host Interface." *The Journal of Pathology* 234 (3): 410-22. <https://doi.org/10.1002/path.4416>.
- Burdsal, C.A., C.H. Damsky, and R.A. Pedersen. 1993. "The Role of E-Cadherin and Integrins in Mesoderm Differentiation and Migration at the Mammalian Primitive Streak." *Development* 118 (3): 829.
- Busso, N. 1994. "Induction of Cell Migration by Pro-Urokinase Binding to Its Receptor: Possible Mechanism for Signal Transduction in Human Epithelial Cells." *The Journal of Cell Biology* 126 (1): 259-70. <https://doi.org/10.1083/jcb.126.1.259>.
- Campa, Carlo Cosimo, and Emilio Hirsch. 2017. "Rab11 and Phosphoinositides: A Synergy of Signal Transducers in the Control of Vesicular Trafficking." *Advances in Biological Regulation* 63 (January): 132-39. <https://doi.org/10.1016/j.jbior.2016.09.002>.
- Canel, M., A. Serrels, M. C. Frame, and V. G. Brunton. 2013. "E-Cadherin-Integrin Crosstalk in Cancer Invasion and Metastasis." *Journal of Cell Science* 126 (2): 393–401. <https://doi.org/10.1242/jcs.100115>.
- Carter, W G, P Kaur, S G Gil, P J Gahr, and E A Wayner. 1990. "Distinct Functions for Integrins Alpha 3 Beta 1 in Focal Adhesions and Alpha 6 Beta 4/Bullous Pemphigoid Antigen in a New Stable Anchoring Contact (SAC) of Keratinocytes: Relation to Hemidesmosomes." *The Journal of Cell Biology* 111 (6 Pt 2): 3141–54. <https://doi.org/10.1083/jcb.111.6.3141>.
- Carver, Brett S, Jennifer Tran, Anuradha Gopalan, Zhenbang Chen, Safa Shaikh, Arkaitz Carracedo, Andrea Alimonti, *et al.* 2009. "Aberrant ERG Expression Cooperates with Loss of PTEN to Promote Cancer Progression in the Prostate." *Nature Genetics* 41 (5): 619–24. <https://doi.org/10.1038/ng.370>.
- Chaffer, C. L., J. P. Brennan, J. L. Slavin, T. Blick, E. W. Thompson, and E. D. Williams. 2006. "Mesenchymal-to-Epithelial Transition Facilitates Bladder Cancer Metastasis: Role of Fibroblast Growth Factor Receptor-2." *Cancer Research* 66 (23): 11271–78. <https://doi.org/10.1158/0008-5472.CAN-06-2044>.

- Chan, John K. C. 2014. "The Wonderful Colors of the Hematoxylin–Eosin Stain in Diagnostic Surgical Pathology." *International Journal of Surgical Pathology* 22 (1): 12–32. <https://doi.org/10.1177/1066896913517939>.
- Chang, A C, D R Salomon, S Wadsworth, M J Hong, C F Mojcik, S Otto, E M Shevach, and J E Coligan. 1995. "Alpha 3 Beta 1 and Alpha 6 Beta 1 Integrins Mediate Laminin/Merosin Binding and Function as Costimulatory Molecules for Human Thymocyte Proliferation." *The Journal of Immunology* 154 (2): 500.
- Chartier, N. T. 2006. "Laminin-5-Integrin Interaction Signals through PI 3-Kinase and Rac1b to Promote Assembly of Adherens Junctions in HT-29 Cells." *Journal of Cell Science* 119 (1): 31–46. <https://doi.org/10.1242/jcs.02698>.
- Chattopadhyay, Nibedita, Zemin Wang, Leonie K. Ashman, Susann M. Brady-Kalnay, and Jordan A. Kreidberg. 2003. "A3 $\beta$ 1 Integrin–CD151, a Component of the Cadherin–Catenin Complex, Regulates PTP $\mu$  Expression and Cell–Cell Adhesion." *The Journal of Cell Biology* 163 (6): 1351–62. <https://doi.org/10.1083/jcb.200306067>.
- Chen, Yih-Tai, Daniel B Stewart, and W James Nelson. 1999. "Coupling Assembly of the E-Cadherin/ $\beta$ -Catenin Complex to Efficient Endoplasmic Reticulum Exit and Basal-Lateral Membrane Targeting of E-Cadherin in Polarized MDCK Cells." *The Journal of Cell Biology* 144: 13.
- Chetram, M. A., V. Odero-Marah, and C. V. Hinton. 2011. "Loss of PTEN Permits CXCR4-Mediated Tumorigenesis through ERK1/2 in Prostate Cancer Cells." *Molecular Cancer Research* 9 (1): 90-102. <https://doi.org/10.1158/1541-7786.MCR-10-0235>.
- Chetram, Mahandranauth A., and Cimona V. Hinton. 2012. "PTEN Regulation of ERK1/2 Signaling in Cancer." *Journal of Receptors and Signal Transduction* 32 (4): 190–95. <https://doi.org/10.3109/10799893.2012.695798>.
- Cheung, K. J., and A. J. Ewald. 2016. "A Collective Route to Metastasis: Seeding by Tumor Cell Clusters." *Science* 352 (6282):167-69 <https://doi.org/10.1126/science.aaf6546>.
- Cousin, H el ene. 2017. "Cadherins Function during the Collective Cell Migration of Xenopus Cranial Neural Crest Cells: Revisiting the Role of E-Cadherin." *Mechanisms of Development* 148 (December): 79–88. <https://doi.org/10.1016/j.mod.2017.04.006>.
- Cox, Elisabeth A, Sarita K Sastry, and Anna Huttenlocher. 2001. "Integrin-Mediated Adhesion Regulates Cell Polarity and Membrane Protrusion through the Rho Family of GTPases." *Molecular Biology of the Cell* 12: 13.
- Cress, Anne E., Manolis C. Demetriou, Kevin A. Kwei, Marianne B. Powell, Raymond B. Nagle, and G. Tim Bowden. 2008a. "Integrin A6 Cleavage in Mouse Skin Tumors." *The Open Cancer Journal* 2 (1): 1-4. <https://doi.org/10.2174/1874079000802010001>.
- . 2008b. "Integrin A6 Cleavage in Mouse Skin Tumors." *The Open Cancer Journal* 2 (1): 1–4. <https://doi.org/10.2174/1874079000802010001>.

- Cress, Anne E., Isaac Rabinovitz, Weiguo Zhu, and Ray B. Nagle. 1995. "The A6 $\beta$ 1 and A6 $\beta$ 4 Integrins in Human Prostate Cancer Progression." *Cancer and Metastasis Reviews* 14 (3): 219-28. <https://doi.org/10.1007/BF00690293>.
- Cunningham, O. 2003. "Dimerization Controls the Lipid Raft Partitioning of UPAR/CD87 and Regulates Its Biological Functions." *The EMBO Journal* 22 (22): 5994–6003. <https://doi.org/10.1093/emboj/cdg588>.
- Das, Lipsa, Todd A. Anderson, Jaime M.C. Gard, Isis C. Sroka, Stephanie R. Strautman, Raymond B. Nagle, Colm Morrissey, Beatrice S. Knudsen, and Anne E. Cress. 2017. "Characterization of Laminin Binding Integrin Internalization in Prostate Cancer Cells: LAMININ BINDING INTEGRIN INTERNALIZATION." *Journal of Cellular Biochemistry* 118 (5): 1038–49. <https://doi.org/10.1002/jcb.25673>.
- Davis, Michael A., Renee C. Ireton, and Albert B. Reynolds. 2003. "A Core Function for P120-Catenin in Cadherin Turnover." *The Journal of Cell Biology* 163 (3): 525–34. <https://doi.org/10.1083/jcb.200307111>.
- Davis, Tracy L., Isaac Rabinovitz, Bernard W. Futscher, Martina Schnölzer, Friederike Burger, Yuangang Liu, Molly Kulesz-Martin, and Anne E. Cress. 2001. "Identification of a Novel Structural Variant of the  $\alpha_6$  Integrin." *Journal of Biological Chemistry* 276 (28): 26099-106. <https://doi.org/10.1074/jbc.M102811200>.
- De Calisto, J. 2005. "Essential Role of Non-Canonical Wnt Signalling in Neural Crest Migration." *Development* 132 (11): 2587–97. <https://doi.org/10.1242/dev.01857>.
- De Melker, A. Annemieke, Duco Kramer, Ingrid Kuikman, and Arnoud Sonnenberg. 1997. "The Two Phenylalanines in the GFFKR Motif of the Integrin A6A Subunit Are Essential for Heterodimerization." *Biochemical Journal* 328 (2): 529–37. <https://doi.org/10.1042/bj3280529>.
- Dedhar, Shoukat, Ronald Saulnier, Raymond Nagle, and Christopher M. Overall. 1993. "Specific Alterations in the Expression of A3 $\beta$ 1 and A6 $\beta$ 4 Integrins in Highly Invasive and Metastatic Variants of Human Prostate Carcinoma Cells Selected by in Vitro Invasion through Reconstituted Basement Membrane." *Clinical & Experimental Metastasis* 11 (5): 391-400. <https://doi.org/10.1007/BF00132982>.
- Delwel, Gepke O., Ingrid Kuikman, and Arnoud Sonnenberg. 1995. "An Alternatively Spliced Exon in the Extracellular Domain of the Human A6 Integrin Subunit-Functional Analysis of the A6 Integrin Variants." *Cell Adhesion and Communication* 3 (2): 143-61. <https://doi.org/10.3109/15419069509081283>.
- Demetriou, Manolis C., and Anne E. Cress. 2004. "Integrin Clipping: A Novel Adhesion Switch?" *Journal of Cellular Biochemistry* 91 (1): 26-35. <https://doi.org/10.1002/jcb.10675>.
- Demetriou, Manolis C, Michael E Pennington, Raymond B Nagle, and Anne E Cress. 2004. "Extracellular Alpha 6 Integrin Cleavage by Urokinase-Type Plasminogen Activator in Human Prostate Cancer." *Experimental Cell Research* 294 (2): 550–58. <https://doi.org/10.1016/j.yexcr.2003.11.023>.

- Desgrosellier, Jay S., and David A. Cheresh. 2010. "Integrins in Cancer: Biological Implications and Therapeutic Opportunities." *Nature Reviews Cancer* 10 (1): 9–22. <https://doi.org/10.1038/nrc2748>.
- DiPersio, C. Michael, Kairbaan M. Hodivala-Dilke, Rudolf Jaenisch, Jordan A. Kreidberg, and Richard O. Hynes. 1997. "A3 $\beta$ 1 Integrin Is Required for Normal Development of the Epidermal Basement Membrane." *The Journal of Cell Biology* 137 (3): 729–42. <https://doi.org/10.1083/jcb.137.3.729>.
- DiPersio, C.M., S. Shah, and R.O. Hynes. 1995. "Alpha 3A Beta 1 Integrin Localizes to Focal Contacts in Response to Diverse Extracellular Matrix Proteins." *Journal of Cell Science* 108 (6): 2321.
- Drake, Justin M., J. Matthew Barnes, Joshua M. Madsen, Frederick E. Domann, Christopher S. Stipp, and Michael D. Henry. 2010. "ZEB1 Coordinately Regulates Laminin-332 and B4 Integrin Expression Altering the Invasive Phenotype of Prostate Cancer Cells." *Journal of Biological Chemistry* 285 (44): 33940–48. <https://doi.org/10.1074/jbc.M110.136044>.
- D'Souza-Schorey, Crislyn. 2005. "Disassembling Adherens Junctions: Breaking up Is Hard to Do." *Trends in Cell Biology* 15 (1): 19-26. <https://doi.org/10.1016/j.tcb.2004.11.002>.
- Durbeej, Madeleine. 2010. "Laminins." *Cell and Tissue Research* 339 (1): 259–68. <https://doi.org/10.1007/s00441-009-0838-2>.
- Etienne-Manneville, Sandrine, and Alan Hall. 2002. "Rho GTPases in Cell Biology." *Nature* 420 (6916): 629–35. <https://doi.org/10.1038/nature01148>.
- Felding-Habermann, Brunhilde. 2003. "Integrin Adhesion Receptors in Tumor Metastasis." *Clinical & Experimental Metastasis* 20 (3): 203-13. <https://doi.org/10.1023/A:1022983000355>.
- Fitter, S, P M Sincock, C N Jolliffe, and L K Ashman. 1999. "Transmembrane 4 Superfamily Protein CD151 (PETA-3) Associates with Beta 1 and Alpha IIb Beta 3 Integrins in Haemopoietic Cell Lines and Modulates Cell-Cell Adhesion." *The Biochemical Journal* 338 (Pt 1) (Pt 1): 61–70.
- Fischer, A. H., K. A. Jacobson, J. Rose, and R. Zeller. 2008. "Hematoxylin and Eosin Staining of Tissue and Cell Sections." *Cold Spring Harbor Protocols* 2008 (6): pdb.prot4986-pdb.prot4986. <https://doi.org/10.1101/pdb.prot4986>.
- Fleshner, Katherine, Melissa Assel, Nicole Benfante, Justin Lee, Andrew Vickers, Samson Fine, Sigrid Carlsson, and James Eastham. 2016. "Clinical Findings and Treatment Outcomes in Patients with Extraprostatic Extension Identified on Prostate Biopsy." *Journal of Urology* 196 (3): 703-8. <https://doi.org/10.1016/j.juro.2016.03.152>.
- Flier, Arjan van der, and Arnoud Sonnenberg. 2001. "Function and Interactions of Integrins." *Cell and Tissue Research* 305 (3): 285-98. <https://doi.org/10.1007/s004410100417>.
- Fornaro, Mara, Thomas Manes, and Lucia R. Languino. 2002. "Integrins and Prostate Cancer Metastases." In *Prostate Cancer: New Horizons in Research and Treatment*, edited by Michael L. Cher, Avraham Raz, and Kenneth V. Honn, 81:185–95. Boston: Kluwer Academic Publishers. [https://doi.org/10.1007/0-306-48143-X\\_12](https://doi.org/10.1007/0-306-48143-X_12).

- Friedl, Peter. 2004. "Prespecification and Plasticity: Shifting Mechanisms of Cell Migration." *Current Opinion in Cell Biology* 16 (1): 14-23.  
<https://doi.org/10.1016/j.ceb.2003.11.001>.
- Friedl, Peter, and Stephanie Alexander. 2011. "Cancer Invasion and the Microenvironment: Plasticity and Reciprocity." *Cell* 147 (5): 992-1009.  
<https://doi.org/10.1016/j.cell.2011.11.016>.
- Friedl, Peter, and Darren Gilmour. 2009. "Collective Cell Migration in Morphogenesis, Regeneration and Cancer." *Nature Reviews Molecular Cell Biology* 10 (7): 445-57. <https://doi.org/10.1038/nrm2720>.
- Friedl, Peter, Yael Hegerfeldt, and Miriam Tusch. 2004. "Collective Cell Migration in Morphogenesis and Cancer." *The International Journal of Developmental Biology* 48 (5-6): 441-49. <https://doi.org/10.1387/ijdb.041821pf>.
- Friedl, Peter, and Katarina Wolf. 2010. "Plasticity of Cell Migration: A Multiscale Tuning Model." *The Journal of Cell Biology* 188 (1): 11-19.  
<https://doi.org/10.1083/jcb.200909003>.
- Friedrichs, Kay, Patricia Ruiz, Folker Franke, Ingbert Gille, Hans-Joachim Terpe, and Beat A. Imhof. 1995. "High Expression Level of A6 Integrin in Human Breast Carcinoma Is Correlated with Reduced Survival." *Cancer Research* 55 (4): 901.
- Gassama-Diagne, Ama, Wei Yu, Martin ter Beest, Fernando Martin-Belmonte, Arlinet Kierbel, Joanne Engel, and Keith Mostov. 2006  
 "Phosphatidylinositol-3,4,5-Trisphosphate Regulates the Formation of the Basolateral Plasma Membrane in Epithelial Cells." *Nature Cell Biology* 8 (9): 963-70. <https://doi.org/10.1038/ncb1461>.
- Gendusa, Rossella, Carla Rossana Scalia, Serena Buscone, and Giorgio Cattoretti. 2014. "Elution of High-Affinity ( $>10^{-9} K_D$ ) Antibodies from Tissue Sections: Clues to the Molecular Mechanism and Use in Sequential Immunostaining." *Journal of Histochemistry & Cytochemistry* 62 (7): 519-31. <https://doi.org/10.1369/0022155414536732>
- Gerashchenko, Tatiana S., Nikita M. Novikov, Nadezhda V. Krakhmal, Sofia Y. Zolotaryova, Marina V. Zavyalova, Nadezhda V. Cherdyntseva, Evgeny V. Denisov, and Vladimir M. Perelmuter. 2019. "Markers of Cancer Cell Invasion: Are They Good Enough?" *Journal of Clinical Medicine* 8 (8): 1092.  
<https://doi.org/10.3390/jcm8081092>.
- Ghadimi, B.M, J Behrens, I Hoffmann, W Haensch, W Birchmeier, and P.M Schlag. 1999. "Immunohistological Analysis of E-Cadherin,  $\alpha$ -,  $\beta$ - and  $\gamma$ -Catenin Expression in Colorectal Cancer: Implications for Cell Adhesion and Signaling." *European Journal of Cancer* 35 (1): 60-65.  
[https://doi.org/10.1016/S0959-8049\(98\)00344-X](https://doi.org/10.1016/S0959-8049(98)00344-X).
- Giehl, Klaudia. 2008. "Microenvironmental Regulation of E-Cadherin-Mediated Adherens Junctions." *Frontiers in Bioscience* Volume (13): 3975.  
<https://doi.org/10.2741/2985>.
- Gilmore, A P, and L H Romer. 1996. "Inhibition of Focal Adhesion Kinase (FAK) Signaling in Focal Adhesions Decreases Cell Motility and Proliferation." *Molecular Biology of the Cell* 7 (8): 1209-24.  
<https://doi.org/10.1091/mbc.7.8.1209>.

- Goel, H. L., J. Li, S. Kogan, and L. R Languino. 2008. "Integrins in Prostate Cancer Progression." *Endocrine Related Cancer* 15 (3): 657-64. <https://doi.org/10.1677/ERC-08-0019>.
- Goel, Hira Lal, Naved Alam, Isaac N S Johnson, and Lucia R Languino. 2009. "Integrin Signaling Aberrations in Prostate Cancer." *American Journal of Translational Research* 1 (3): 211–20.
- Gorris, Mark A. J., Altuna Halilovic, Katrin Rabold, Anne van Duffelen, Iresha N. Wickramasinghe, Dagmar Verweij, Inge M. N. Wortel, Johannes C. Textor, I. Jolanda M. de Vries, and Carl G. Figdor. 2018. "Eight-Color Multiplex Immunohistochemistry for Simultaneous Detection of Multiple Immune Checkpoint Molecules within the Tumor Microenvironment." *The Journal of Immunology* 200 (1): 347–54. <https://doi.org/10.4049/jimmunol.1701262>.
- Grignon, David J. 2018. "Prostate Cancer Reporting and Staging: Needle Biopsy and Radical Prostatectomy Specimens." *Modern Pathology* 31 (S1): 96-109. <https://doi.org/10.1038/modpathol.2017.167>.
- Gu, Jianguo, Masahito Tamura, and Kenneth M. Yamada. 1998. "Tumor Suppressor PTEN Inhibits Integrin- and Growth Factor–Mediated Mitogen-Activated Protein (MAP) Kinase Signaling Pathways." *The Journal of Cell Biology* 143 (5): 1375–83. <https://doi.org/10.1083/jcb.143.5.1375>.
- Guedes, Liana B., Jeffrey J. Tosoian, Jessica Hicks, Ashley E. Ross, and Tamara L. Lotan. 2017. "PTEN Loss in Gleason Score 3 + 4 = 7 Prostate Biopsies Is Associated with Nonorgan Confined Disease at Radical Prostatectomy." *Journal of Urology* 197 (4): 1054–59. <https://doi.org/10.1016/j.juro.2016.09.084>.
- Han, Bo, Rohit Mehra, Robert J Lonigro, Lei Wang, Khalid Suleman, Anjana Menon, Nallasivam Palanisamy, Scott A Tomlins, Arul M Chinnaiyan, and Rajal B Shah. 2009. "Fluorescence in Situ Hybridization Study Shows Association of PTEN Deletion with ERG Rearrangement during Prostate Cancer Progression." *Modern Pathology* 22 (8): 1083-93. <https://doi.org/10.1038/modpathol.2009.69>.
- Harryman, William L., James P. Hinton, Cynthia P. Rubenstein, Parminder Singh, Raymond B. Nagle, Sarah J. Parker, Beatrice S. Knudsen, and Anne E. Cress. 2016. "The Cohesive Metastasis Phenotype in Human Prostate Cancer." *Biochimica et Biophysica Acta (BBA) - Reviews on Cancer* 1866 (2): 221–31. <https://doi.org/10.1016/j.bbcan.2016.09.005>.
- Harryman, William L., Noel A. Warfel, Raymond B. Nagle, and Anne E. Cress. 2019. "Tumor Microenvironments of Lethal Prostate Cancer." In *Advances in Experimental Medicine and Biology* edited by Scott M. Dehm and Donald J. Tindall, 978-030-32655-5. Cham, Switzerland: Springer International Publishing, 2<sup>nd</sup> ed. 2019. <https://doi.org/10.1007/978-3-030-32656-2>.
- Hegerfeldt, Yael, Miriam Tusch, Eva-B. Bröcker, and Peter Friedl. 2002. "Collective Cell Movement in Primary Melanoma Explants." *Cancer Research* 62 (7): 2125.



- Hintermann, Edith, and Vito Quaranta. 2004. "Epithelial Cell Motility on Laminin-5: Regulation by Matrix Assembly, Proteolysis, Integrins and ErbB Receptors." *Matrix Biology* 23 (2): 75–85. <https://doi.org/10.1016/j.matbio.2004.03.001>.
- Hintermann, Edith, Neng Yang, Deirdre O'Sullivan, Jonathan M. G. Higgins, and Vito Quaranta. 2005. "Integrin A $\beta$ 4-ErbB2 Complex Inhibits Haptotaxis by Up-Regulating E-Cadherin Cell-Cell Junctions in Keratinocytes." *Journal of Biological Chemistry* 280 (9): 8004-15. <https://doi.org/10.1074/jbc.M406301200>.
- Hogervorst, F, L G Admiraal, C Niessen, I Kuikman, H Janssen, H Daams, and A Sonnenberg. 1993. "Biochemical Characterization and Tissue Distribution of the A and B Variants of the Integrin Alpha 6 Subunit." *The Journal of Cell Biology* 121 (1): 179–91. <https://doi.org/10.1083/jcb.121.1.179>.
- Hogervorst, Frans, Ingrid Kuikman, Ad Geurts Kessel, and Arnoud Sonnenberg. 1991. "Molecular Cloning of the Human Alpha6 Integrin Subunit. Alternative Splicing of Alpha6 mRNA and Chromosomal Localization of the Alpha6 and Beta4 Genes." *European Journal of Biochemistry* 199 (2): 425-33. <https://doi.org/10.1111/j.1432-1033.1991.tb16140.x>.
- Hollander, M. Christine, Gideon M. Blumenthal, and Phillip A. Dennis. 2011. "PTEN Loss in the Continuum of Common Cancers, Rare Syndromes and Mouse Models." *Nature Reviews Cancer* 11 (4): 289–301. <https://doi.org/10.1038/nrc3037>.
- Huang, Chaolie, Marie-Claire Kratzer, Doris Wedlich, and Jubin Kashef. 2016. "E-Cadherin Is Required for Cranial Neural Crest Migration in *Xenopus Laevis*." *Developmental Biology* 411 (2): 159-71. <https://doi.org/10.1016/j.ydbio.2016.02.007>.
- Hugo, Honor, M. Leigh Ackland, Tony Blick, Mitchell G. Lawrence, Judith A. Clements, Elizabeth D. Williams, and Erik W. Thompson. 2007. "Epithelial—Mesenchymal and Mesenchymal—Epithelial Transitions in Carcinoma Progression." *Journal of Cellular Physiology* 213 (2): 374–83. <https://doi.org/10.1002/jcp.21223>.
- Hurst, Douglas R., and Danny R. Welch. 2011. "Metastasis Suppressor Genes." In *International Review of Cell and Molecular Biology*, 286:107–80. Elsevier. <https://doi.org/10.1016/B978-0-12-385859-7.00003-3>.
- Hwang, Soonyean, Noah P. Zimmerman, Kimberle A. Agle, Jerrold R. Turner, Suresh N. Kumar, and Michael B. Dwinell. 2012. "E-Cadherin Is Critical for Collective Sheet Migration and Is Regulated by the Chemokine CXCL12 Protein During Restitution." *Journal of Biological Chemistry* 287 (26): 22227-40. <https://doi.org/10.1074/jbc.M112.367979>.
- Hynes, Richard O. 2002. "Integrins: Bidirectional, Allosteric Signaling Machines." *Cell* 110 (6): 673–87. [https://doi.org/10.1016/S0092-8674\(02\)00971-6](https://doi.org/10.1016/S0092-8674(02)00971-6).
- Ireton, René C., Michael A. Davis, Jolanda van Hengel, Deborah J. Mariner, Kirk Barnes, Molly A. Thoreson, Panos Z. Anastasiadis, *et al.* 2002. "A Novel Role for P120 Catenin in E-Cadherin Function." *The Journal of Cell Biology* 159 (3): 465–76. <https://doi.org/10.1083/jcb.200205115>.

- Itoh, M, A Nagafuchi, S Moroi, and S Tsukita. 1997. "Involvement of ZO-1 in Cadherin-Based Cell Adhesion through Its Direct Binding to Alpha Catenin and Actin Filaments." *The Journal of Cell Biology* 138 (1): 181-92. <https://doi.org/10.1083/jcb.138.1.181>.
- Jamaspishvili, Tamara, David M. Berman, Ashley E. Ross, Howard I. Scher, Angelo M. De Marzo, Jeremy A. Squire, and Tamara L. Lotan. 2018. "Clinical Implications of PTEN Loss in Prostate Cancer." *Nature Reviews Urology* 15 (4): 222–34. <https://doi.org/10.1038/nrurol.2018.9>.
- Johnson, Randy, and Georg Halder. 2014. "The Two Faces of Hippo: Targeting the Hippo Pathway for Regenerative Medicine and Cancer Treatment." *Nature Reviews Drug Discovery* 13 (1): 63–79. <https://doi.org/10.1038/nrd4161>.
- Jones, J C, M A Kurpakus, H M Cooper, and V Quaranta. 1991. "A Function for the Integrin Alpha 6 Beta 4 in the Hemidesmosome." *Cell Regulation* 2 (6): 427–38. <https://doi.org/10.1091/mbc.2.6.427>.
- Kacsinta, Apollo D., Cynthia S. Rubenstein, Isis C. Sroka, Sangita Pawar, Jaime M. Gard, Raymond B. Nagle, and Anne E. Cress. 2014. "Intracellular Modifiers of Integrin Alpha 6p Production in Aggressive Prostate and Breast Cancer Cell Lines." *Biochemical and Biophysical Research Communications* 454 (2): 335-40. 335–40. <https://doi.org/10.1016/j.bbrc.2014.10.073>.
- Kalluri, Raghu, and Robert A. Weinberg. 2009. "The Basics of Epithelial-Mesenchymal Transition." *Journal of Clinical Investigation* 119 (6): 1420-28. <https://doi.org/10.1172/JCI39104>.
- Karantanos, T, P G Corn, and T C Thompson. 2013. "Prostate Cancer Progression after Androgen Deprivation Therapy: Mechanisms of Castrate Resistance and Novel Therapeutic Approaches." *Oncogene* 32 (49): 5501-11. <https://doi.org/10.1038/onc.2013.206>.
- Kedage, Vivekananda, Brady G. Strittmatter, Paige B. Dausinas, and Peter C. Hollenhorst. 2017. "Phosphorylation of the Oncogenic Transcription Factor ERG in Prostate Cells Dissociates Polycomb Repressive Complex 2, Allowing Target Gene Activation." *Journal of Biological Chemistry* 292 (42): 17225-35. <https://doi.org/10.1074/jbc.M117.796458>.
- Kikkawa, Y., N. Sanzen, H. Fujiwara, A. Sonnenberg, and K. Sekiguchi. 2000. "Integrin Binding Specificity of Laminin-10/11: Laminin-10/11 Are Recognized by Alpha 3 Beta 1, Alpha 6 Beta 1 and Alpha 6 Beta 4 Integrins." *Journal of Cell Science* 113 (5): 869.
- Kim, Janice P., Ken Zhang, Randall H. Kramer, Thomas J. Schall, and David T. Woodley. 1992. "Integrin Receptors and RGD Sequences in Human Keratinocyte Migration: Unique Anti-Migratory: Unique Anti-Migratory Function of A3β1 Epiligrin Receptor." *Journal of Investigative Dermatology* 98 (5): 764–70. <https://doi.org/10.1111/1523-1747.ep12499947>.

- King, Jennifer C, Jin Xu, John Wongvipat, Haley Hieronymus, Brett S Carver, David H Leung, Barry S Taylor, *et al.* 2009. "Cooperativity of TMPRSS2-ERG with PI3-Kinase Pathway Activation in Prostate Oncogenesis." *Nature Genetics* 41 (5): 524–26. <https://doi.org/10.1038/ng.371>.
- Krohn, Antje, Tobias Diedler, Lia Burkhardt, Pascale-Sophie Mayer, Colin De Silva, Marie Meyer-Kornblum, Darja Kötschau, *et al.* 2012. "Genomic Deletion of PTEN Is Associated with Tumor Progression and Early PSA Recurrence in ERG Fusion-Positive and Fusion-Negative Prostate Cancer." *The American Journal of Pathology* 181 (2): 401-12. <https://doi.org/10.1016/j.ajpath.2012.04.026>.
- Kurpakus, Michelle A, Vito Quaranta, and Jonathan C R Jones. 1991. "Surface Relocation OfA1pha6Beta4 Integrins and Assembly of Hemidesmosomes in an In Vitro Model of Wound Healing." *The Journal of Cell Biology* 115: 14.
- Landowski, T. H., J. Gard, E. Pond, G. D. Pond, R. B. Nagle, C. P. Geffre, and A. E. Cress. 2014. "Targeting Integrin  $\alpha 6$  Stimulates Curative-Type Bone Metastasis Lesions in a Xenograft Model." *Molecular Cancer Therapeutics* 13 (6): 1558–66. <https://doi.org/10.1158/1535-7163.MCT-13-0962>.
- LeBeau, Aaron M., Natalia Sevillano, Kate Markham, Michael B. Winter, Stephanie T. Murphy, Daniel R. Hostetter, James West, Henry Lowman, Charles S. Craik, and Henry F. VanBrocklin. 2015. "Imaging Active Urokinase Plasminogen Activator in Prostate Cancer." *Cancer Research* 75 (7): 1225–35. <https://doi.org/10.1158/0008-5472.CAN-14-2185>.
- Lee, Jie-Oh, Haijuan Yang, Maria-Magdalena Georgescu, Antonio Di Cristofano, Tomohiko Maehama, Yigong Shi, Jack E Dixon, Pier Pandolfi, and Nikola P Pavletich. 1999. "Crystal Structure of the PTEN Tumor Suppressor: Implications for Its Phosphoinositide Phosphatase Activity and Membrane Association." *Cell* 99 (3): 323-34. [https://doi.org/10.1016/S0092-8674\(00\)81663-3](https://doi.org/10.1016/S0092-8674(00)81663-3).
- Leinonen, K. A., O. R. Saramaki, B. Furusato, T. Kimura, H. Takahashi, S. Egawa, H. Suzuki, *et al.* 2013. "Loss of PTEN Is Associated with Aggressive Behavior in ERG-Positive Prostate Cancer." *Cancer Epidemiology Biomarkers & Prevention* 22 (12): 2333–44. <https://doi.org/10.1158/1055-9965.EPI-13-0333-T>.
- Li, Y., and P.J. Cozzi. 2007. "Targeting UPA/UPAR in Prostate Cancer." *Cancer Treatment Reviews* 33 (6): 521–27. <https://doi.org/10.1016/j.ctrv.2007.06.003>.
- Lindsay, A. J. 2004. "The C2 Domains of the Class I Rab11 Family of Interacting Proteins Target Recycling Vesicles to the Plasma Membrane." *Journal of Cell Science* 117 (19): 4365–75. <https://doi.org/10.1242/jcs.01280>.
- Lindsay, Andrew J., and Mary W. McCaffrey. 2017. "Rab Coupling Protein Mediated Endosomal Recycling of N-Cadherin Influences Cell Motility." *Oncotarget* 8 (62). <https://doi.org/10.18632/oncotarget.10513>.

- Lippert, Solvej, Kasper D Berg, Gunilla Høyer-Hansen, Ida K Lund, Peter Iversen, Ib J Christensen, Klaus Brasso, and Martin A Røder. 2016. "Copenhagen UPAR Prostate Cancer (CuPCa) Database: Protocol and Early Results." *Biomarkers in Medicine* 10 (2): 209-16. <https://doi.org/10.2217/bmm.15.114>.
- Liu, Z., J. L. Tan, D. M. Cohen, M. T. Yang, N. J. Sniadecki, S. A. Ruiz, C. M. Nelson, and C. S. Chen. 2010. "Mechanical Tugging Force Regulates the Size of Cell-Cell Junctions." *Proceedings of the National Academy of Sciences* 107 (22): 9944–49. <https://doi.org/10.1073/pnas.0914547107>.
- Llense, Flora, and Enrique Martín-Blanco. 2008. "JNK Signaling Controls Border Cell Cluster Integrity and Collective Cell Migration." *Current Biology* 18 (7): 538–44. <https://doi.org/10.1016/j.cub.2008.03.029>.
- Ilić, Duško, Yasuhide Furuta, Satoshi Kanazawa, Naoki Takeda, Kenji Sobue, Norio Nakatsuji, Shintaro Nomura, *et al.* 1995. "Reduced Cell Motility and Enhanced Focal Adhesion Contact Formation in Cells from FAK-Deficient Mice." *Nature* 377 (6549): 539–44. <https://doi.org/10.1038/377539a0>.
- Lokman, Utku, Andrew M. Erickson, Hanna Vasarainen, Antti S. Rannikko, and Tuomas Mirtti. 2018. "PTEN Loss but Not ERG Expression in Diagnostic Biopsies Is Associated with Increased Risk of Progression and Adverse Surgical Findings in Men with Prostate Cancer on Active Surveillance." *European Urology Focus* 4 (6): 867-73. <https://doi.org/10.1016/j.euf.2017.03.004>.
- Lotan, Tamara L, Wei Wei, Olga Ludkovski, Carlos L Morais, Liana B Guedes, Tamara Jamaspishvili, Karen Lopez, *et al.* 2016. "Analytic Validation of a Clinical-Grade PTEN Immunohistochemistry Assay in Prostate Cancer by Comparison with PTEN FISH." *Modern Pathology* 29 (8): 904-14. <https://doi.org/10.1038/modpathol.2016.88>.
- Ma, Zhong, Donna J. Webb, Minji Jo, and Steven L. Gonias. 2001. "Endogenously Produced Urokinase-Type Plasminogen Activator Is a Major Determinant of the Basal Level of Activated ERK/MAP Kinase and Prevents Apoptosis in MDA-MB-231 Breast Cancer Cells." *Journal of Cell Science* 114 (18): 3387.
- Mahmood, Niaz, Catalin Mihalcioiu, and Shafaat A. Rabbani. 2018. "Multifaceted Role of the Urokinase-Type Plasminogen Activator (UPA) and Its Receptor (UPAR): Diagnostic, Prognostic, and Therapeutic Applications." *Frontiers in Oncology* 8 (February). <https://doi.org/10.3389/fonc.2018.00024>.
- Makrilia, Nektaria, Anastasios Kollias, Leonidas Manolopoulos, and Kostas Syrigos. 2009. "Cell Adhesion Molecules: Role and Clinical Significance in Cancer." *Cancer Investigation* 27 (10): 1023-37. <https://doi.org/10.3109/07357900902769749>.

- Marchiò, Serena, Marco Soster, Sabrina Cardaci, Andrea Muratore, Alice Bartolini, Vanessa Barone, Dario Ribero, *et al.* 2012. "A Complex of  $\alpha_6$  Integrin and E-cadherin Drives Liver Metastasis of Colorectal Cancer Cells through Hepatic Angiopoietin-like 6." *EMBO Molecular Medicine* 4 (11): 1156–75. <https://doi.org/10.1002/emmm.201101164>.
- Mareel, Marc, and Ancy Leroy. 2003. "Clinical, Cellular, and Molecular Aspects of Cancer Invasion." *Physiological Reviews* 83 (2): 337-76. <https://doi.org/10.1152/physrev.00024.2002>.
- Margadant, C., K. Raymond, M. Kreft, N. Sachs, H. Janssen, and A. Sonnenberg. 2009. "Integrin  $\alpha_3\beta_1$  Inhibits Directional Migration and Wound Re-Epithelialization in the Skin." *Journal of Cell Science* 122 (2): 278–88. <https://doi.org/10.1242/jcs.029108>.
- Marques, Rute B., Natasja F. Dits, Sigrun Erkens-Schulze, Wytske M. van Weerden, and Guido Jenster. 2010. "Bypass Mechanisms of the Androgen Receptor Pathway in Therapy-Resistant Prostate Cancer Cell Models." Edited by Chad Creighton. *PLoS ONE* 5 (10): e13500. <https://doi.org/10.1371/journal.pone.0013500>.
- Martin-Belmonte, Fernando, Ama Gassama, Anirban Datta, Wei Yu, Ursula Rescher, Volker Gerke, and Keith Mostov. 2007. "PTEN-Mediated Apical Segregation of Phosphoinositides Controls Epithelial Morphogenesis through Cdc42." *Cell* 128 (2): 383-97. <https://doi.org/10.1016/j.cell.2006.11.051>.
- Martinez-Rico, C., F. Pincet, J.-P. Thiery, and S. Dufour. 2010. "Integrins Stimulate E-Cadherin-Mediated Intercellular Adhesion by Regulating Src-Kinase Activation and Actomyosin Contractility." *Journal of Cell Science* 123 (5): 712–22. <https://doi.org/10.1242/jcs.047878>.
- Maruthamuthu, V., B. Sabass, U. S. Schwarz, and M. L. Gardel. 2011. "Cell-ECM Traction Force Modulates Endogenous Tension at Cell-Cell Contacts." *Proceedings of the National Academy of Sciences* 108 (12): 4708–13. <https://doi.org/10.1073/pnas.1011123108>.
- Mayor, Roberto, and Sandrine Etienne-Manneville. 2016. "The Front and Rear of Collective Cell Migration." *Nature Reviews Molecular Cell Biology* 17 (2): 97–109. <https://doi.org/10.1038/nrm.2015.14>.
- McCandless, J, A Cress, I Rabinovitz, C Payne, G Bowden, J Knox, and R Nagle. 1997. "A Human Xenograft Model for Testing Early Events of Epithelial Neoplastic Invasion." *International Journal of Oncology*, February. <https://doi.org/10.3892/ijo.10.2.279>.
- Melker, Anneinieke A., and Arnoud Sonnenberg. 1996. "The Role of the Cytoplasmic Domain of Alpha6 Integrin in the Assembly and Function of Alpha6beta1 and Alpha6beta4." *European Journal of Biochemistry* 241 (1): 254–64. <https://doi.org/10.1111/j.1432-1033.1996.0254t.x>.
- Mishra, Abhinava, James Mondo, Joseph Campanale, and Denise Montell. 2019. "Coordination of Protrusion Dynamics within and between Collectively Migrating Border Cells by Myosin II." *Molecular Biology of the Cell* 30 (August): mbc.E19-02. <https://doi.org/10.1091/mbc.E19-02-0124>.

- Miyake, H, I Hara, K Yamanaka, S Arakawa, and S Kamidono. 1999. "Elevation of Urokinase-Type Plasminogen Activator and Its Receptor Densities as New Predictors of Disease Progression and Prognosis in Men with Prostate Cancer." *International Journal of Oncology*, March. <https://doi.org/10.3892/ijo.14.3.535>.
- Miyazaki, Takamichi, Sugiko Futaki, Kouichi Hasegawa, Miwa Kawasaki, Noriko Sanzen, Maria Hayashi, Eihachiro Kawase, Kiyotoshi Sekiguchi, Norio Nakatsuji, and Hirofumi Suemori. 2008. "Recombinant Human Laminin Isoforms Can Support the Undifferentiated Growth of Human Embryonic Stem Cells." *Biochemical and Biophysical Research Communications* 375 (1): 27-32. <https://doi.org/10.1016/j.bbrc.2008.07.111>.
- Mondino, Anna, and Francesco Blasi. 2004. "UPA and UPAR in Fibrinolysis, Immunity and Pathology." *Trends in Immunology* 25 (8): 450-55. <https://doi.org/10.1016/j.it.2004.06.004>.
- Montironi, Rodolfo, Roberta Mazzucchelli, and Marina Scarpelli. 2006. "Precancerous Lesions and Conditions of the Prostate: From Morphological and Biological Characterization to Chemoprevention." *Annals of the New York Academy of Sciences* 963 (1): 169–84. <https://doi.org/10.1111/j.1749-6632.2002.tb04108.x>.
- Mui, Keeley L., Christopher S. Chen, and Richard K. Assoian. 2016. "The Mechanical Regulation of Integrin–Cadherin Crosstalk Organizes Cells, Signaling and Forces." *Journal of Cell Science* 129 (6): 1093–1100. <https://doi.org/10.1242/jcs.183699>.
- Mukhopadhyay, Sanjay, Michael D. Feldman, Esther Abels, Raheela Ashfaq, Senda Beltaifa, Nicolas G. Cacciabeve, Helen P. Cathro, *et al.* 2017. "Whole Slide Imaging Versus Microscopy for Primary Diagnosis in Surgical Pathology: A Multicenter Blinded Randomized Noninferiority Study of 1992 Cases (Pivotal Study)." *The American Journal of Surgical Pathology*, September 1. <https://doi.org/10.1097/PAS.0000000000000948>.
- Nagle, Ray B, Junshan Hao, J David Knox, Bruce L Dalkin, and Anne E Cress. 1995. "Expression of Hemidesmosomal and Extracellular Matrix Proteins by Normal and Malignant Human Prostate Tissue" 146 (6): 10.
- Nagle, Raymond B., and Anne E. Cress. 2011. "Metastasis Update: Human Prostate Carcinoma Invasion via Tubulogenesis." *Prostate Cancer* 2011: 1–10. <https://doi.org/10.1155/2011/249290>.
- Nagle, Raymond B., Amit M. Algotar, Connie C. Cortez, Katherine Smith, Carol Jones, Ubaradka G. Sathyanarayana, Steven Yun, *et al.* 2013. "ERG Overexpression and PTEN Status Predict Capsular Penetration in Prostate Carcinoma: ERG & PTEN Predict Capsular Penetration." *The Prostate* 73 (11): 1233-40. <https://doi.org/10.1002/pros.22675>.

- Nguyen, Beth P., Xiang-Dong Ren, Martin A. Schwartz, and William G. Carter. 2001. "Ligation of Integrin  $\alpha_3\beta_1$  by Laminin 5 at the Wound Edge Activates Rho-Dependent Adhesion of Leading Keratinocytes on Collagen." *Journal of Biological Chemistry* 276 (47): 43860-70. <https://doi.org/10.1074/jbc.M103404200>.
- Nishiuchi, Ryoko, Junichi Takagi, Maria Hayashi, Hiroyuki Ido, Yoshiko Yagi, Noriko Sanzen, Tsutomu Tsuji, Masashi Yamada, and Kiyotoshi Sekiguchi. 2006. "Ligand-Binding Specificities of Laminin-Binding Integrins: A Comprehensive Survey of Laminin-Integrin Interactions Using Recombinant A3 $\beta$ 1, A6 $\beta$ 1, A7 $\beta$ 1 and A6 $\beta$ 4 Integrins." *Matrix Biology* 25 (3): 189–97. <https://doi.org/10.1016/j.matbio.2005.12.001>.
- Nusrat, A R, and H A Chapman. 1991. "An Autocrine Role for Urokinase in Phorbol Ester-Mediated Differentiation of Myeloid Cell Lines." *Journal of Clinical Investigation* 87 (3): 1091–97. <https://doi.org/10.1172/JCI115070>.
- Owens, David M., and Fiona M. Watt. 2001. "Influence of B1 Integrins on Epidermal Squamous Cell Carcinoma Formation in a Transgenic Mouse Model." *Cancer Research* 61 (13): 5248.
- Parsons, J. Thomas, Alan Rick Horwitz, and Martin A. Schwartz. 2010. "Cell Adhesion: Integrating Cytoskeletal Dynamics and Cellular Tension." *Nature Reviews Molecular Cell Biology* 11 (9): 633-43. <https://doi.org/10.1038/nrm2957>.
- Pawar, Sangita C., Manolis C. Demetriou, Raymond B. Nagle, G. Tim Bowden, and Anne E. Cress. 2007. "Integrin A6 Cleavage: A Novel Modification to Modulate Cell Migration." *Experimental Cell Research* 313 (6): 1080-89. <https://doi.org/10.1016/j.yexcr.2007.01.006>.
- Pećina-Šlaus, Nives. 2003. "Tumor Suppressor Gene E-Cadherin and Its Role in Normal and Malignant Cells." *Cancer Cell International* 3 (1): 17. <https://doi.org/10.1186/1475-2867-3-17>.
- Petrovics, Gyorgy, Aijun Liu, Syed Shaheduzzaman, Bungo Furasato, Chen Sun, Yongmei Chen, Martin Nau, *et al.* 2005. "Frequent Overexpression of ETS-Related Gene-1 (ERG1) in Prostate Cancer Transcriptome." *Oncogene* 24 (23): 3847–52. <https://doi.org/10.1038/sj.onc.1208518>.
- Piccolo, Stefano, Sirio Dupont, and Michelangelo Cordenonsi. 2014. "The Biology of YAP/TAZ: Hippo Signaling and Beyond." *Physiological Reviews* 94 (4): 1287–1312. <https://doi.org/10.1152/physrev.00005.2014>.
- Ports, M. O., R. B. Nagle, G. D. Pond, and A. E. Cress. 2009. "Extracellular Engagement of  $\alpha_6$  Integrin Inhibited Urokinase-Type Plasminogen Activator-Mediated Cleavage and Delayed Human Prostate Bone Metastasis." *Cancer Research* 69 (12): 5007–14. <https://doi.org/10.1158/0008-5472.CAN-09-0354>.
- Rabinovitz, Isaac, and Arthur M. Mercurio. 1996. "The Integrin A6 $\beta$ 4 and the Biology of Carcinoma." *Biochemistry and Cell Biology* 74 (6): 811-21. <https://doi.org/10.1139/o96-087>.

- Ramel, Damien, Xiaobo Wang, Carl Laflamme, Denise J. Montell, and Gregory Emery. 2013. "Rab11 Regulates Cell–Cell Communication during Collective Cell Movements." *Nature Cell Biology* 15 (3): 317-24. <https://doi.org/10.1038/ncb2681>.
- Ramovs, Veronika, Pablo Secades, Ji-Ying Song, Bram Thijssen, Maaïke Kreft, and Arnoud Sonnenberg. 2019. "Absence of Integrin A3 $\beta$ 1 Promotes the Progression of HER2-Driven Breast Cancer in Vivo." *Breast Cancer Research* 21 (1): 63. <https://doi.org/10.1186/s13058-019-1146-8>.
- Raymond, K. 2005. "Keratinocytes Display Normal Proliferation, Survival and Differentiation in Conditional 4-Integrin Knockout Mice." *Journal of Cell Science* 118 (5): 1045–60. <https://doi.org/10.1242/jcs.01689>.
- Ridley, A. J. 2003. "Cell Migration: Integrating Signals from Front to Back." *Science* 302 (5651): 1704–9. <https://doi.org/10.1126/science.1092053>.
- Rooij, Johan de, Andre Kerstens, Gaudenz Danuser, Martin A. Schwartz, and Clare M. Waterman-Storer. 2005. "Integrin-Dependent Actomyosin Contraction Regulates Epithelial Cell Scattering." *The Journal of Cell Biology* 171 (1): 153–64. <https://doi.org/10.1083/jcb.200506152>.
- Rozario, Tania, and Douglas W. DeSimone. 2010. "The Extracellular Matrix in Development and Morphogenesis: A Dynamic View." *Developmental Biology* 341 (1): 126–40. <https://doi.org/10.1016/j.ydbio.2009.10.026>.
- Rubenstein, Cynthia S., Jaime M.C. Gard, Mengdie Wang, Julie E. McGrath, Nadia Ingabire, James P. Hinton, Kendra D. Marr, *et al.* 2019. "Gene Editing of A6 Integrin Inhibits Muscle Invasive Networks and Increases Cell–Cell Biophysical Properties in Prostate Cancer." *Cancer Research* 79 (18): 4703–14. <https://doi.org/10.1158/0008-5472.CAN-19-0868>.
- Rusthoven, Chad G., Bernard L. Jones, Thomas W. Flaig, E. David Crawford, Matthew Koshy, David J. Sher, Usama Mahmood, *et al.* 2016. "Improved Survival With Prostate Radiation in Addition to Androgen Deprivation Therapy for Men With Newly Diagnosed Metastatic Prostate Cancer." *Journal of Clinical Oncology* 34 (24): 2835-42. <https://doi.org/10.1200/JCO.2016.67.4788>.
- Saramaki, O. R., A. E. Harjula, P. M. Martikainen, R. L. Vessella, T. L.J. Tammela, and T. Visakorpi. 2008. "TMPRSS2:ERG Fusion Identifies a Subgroup of Prostate Cancers with a Favorable Prognosis." *Clinical Cancer Research* 14 (11): 3395–3400. <https://doi.org/10.1158/1078-0432.CCR-07-2051>.
- Schafer, G., M. Narasimha, E. Vogelsang, and M. Leptin. 2014. "Cadherin Switching during the Formation and Differentiation of the Drosophila Mesoderm - Implications for Epithelial-to-Mesenchymal Transitions." *Journal of Cell Science* 127 (7): 1511-22. <https://doi.org/10.1242/jcs.139485>.
- Schmelz, Monika, Anne E. Cress, Katherine M. Scott, Friederike Burger, Haiyan Cui, Karim Sallam, Kathy M. McDaniel, Bruce L. Dalkin, and Raymond B. Nagle. 2002. "Different Phenotypes in Human Prostate Cancer: A6 or A3 Integrin in Cell-Extracellular Adhesion Sites." *Neoplasia* 4 (3): 243-54. <https://doi.org/10.1038/sj.neo.7900223>.



- Schreider, Cyrille, Peignon, Gregory, Tenet, Sophie, and Chamaz, Jean. 2002. "Integrin-Induced E-Cadherin-Actin Complexes." *Journal of Cell Science* 115 (3): 543–52.
- Selvaraj, Nagarathinam, Vivekananda Kedage, and Peter C Hollenhorst. 2015. "Comparison of MAPK Specificity across the ETS Transcription Factor Family Identifies a High-Affinity ERK Interaction Required for ERG Function in Prostate Cells." *Cell Communication and Signaling* 13 (1): 12. <https://doi.org/10.1186/s12964-015-0089-7>.
- Shariat, Shahrokh F., Claus G. Roehrborn, John D. McConnell, Sangtae Park, Nina Alam, Thomas M. Wheeler, and Kevin M. Slawin. 2007. "Association of the Circulating Levels of the Urokinase System of Plasminogen Activation With the Presence of Prostate Cancer and Invasion, Progression, and Metastasis." *Journal of Clinical Oncology* 25 (4): 349-55. <https://doi.org/10.1200/JCO.2006.05.6853>.
- Siegel, Rebecca L., Kimberly D. Miller, and Ahmedin Jemal. 2019. "Cancer Statistics, 2019." *CA: A Cancer Journal for Clinicians* 69 (1): 7-34 <https://doi.org/10.3322/caac.21551>.
- Smith, Harvey W., and Chris J. Marshall. 2010. "Regulation of Cell Signalling by UPAR." *Nature Reviews Molecular Cell Biology* 11 (1): 23-36. <https://doi.org/10.1038/nrm2821>.
- Song, Min Sup, Leonardo Salmena, and Pier Paolo Pandolfi. 2012. "The Functions and Regulation of the PTEN Tumour Suppressor." *Nature Reviews Molecular Cell Biology* 13 (5): 283–96. <https://doi.org/10.1038/nrm3330>.
- Spadafora, C. 2008. "Sperm-Mediated 'reverse' Gene Transfer: A Role of Reverse Transcriptase in the Generation of New Genetic Information." *Human Reproduction* 23 (4): 735–40. <https://doi.org/10.1093/humrep/dem425>.
- Sroka, I. C., C. P. Sandoval, H. Chopra, J. M. C. Gard, S. C. Pawar, and A. E. Cress. 2011. "Macrophage-Dependent Cleavage of the Laminin Receptor 6 1 in Prostate Cancer." *Molecular Cancer Research* 9 (10): 1319-28. <https://doi.org/10.1158/1541-7786.MCR-11-0080>.
- Sroka, Isis C., Todd A. Anderson, Kathy M. McDaniel, Raymond B. Nagle, Matthew B. Gretzer, and Anne E. Cress. 2010. "The Laminin Binding Integrin A6 $\beta$ 1 in Prostate Cancer Perineural Invasion." *Journal of Cellular Physiology* 224 (2): 283–88. <https://doi.org/10.1002/jcp.22149>.
- Sroka, Isis C, Harsharon Chopra, Lipsa Das, Jaime M C Gard, Raymond B Nagle, and Anne E Cress. 2016. "Schwann Cells Increase Prostate and Pancreatic Tumor Cell Invasion Using Laminin Binding A6 Integrin." *Journal of Cellular Biochemistry* 117 (2): 491–99. <https://doi.org/10.1002/jcb.25300>.
- Stewart, Rachel L., Dava West, Chi Wang, Heidi L. Weiss, Tamas Gal, Eric B. Durbin, William O'Connor, Min Chen, and Kathleen L. O'Connor. 2016. "Elevated Integrin A6 $\beta$ 4 Expression Is Associated with Venous Invasion and Decreased Overall Survival in Non-Small Cell Lung Cancer." *Human Pathology* 54 (August): 174-83. <https://doi.org/10.1016/j.humpath.2016.04.003>.

- Stipp, Christopher S. 2010. "Laminin-Binding Integrins and Their Tetraspanin Partners as Potential Antimetastatic Targets." *Expert Reviews in Molecular Medicine* 12 (January). <https://doi.org/10.1017/S1462399409001355>.
- Sun, H., R. Lesche, D.-M. Li, J. Liliental, H. Zhang, J. Gao, N. Gavrilova, B. Mueller, X. Liu, and H. Wu. 1999. "PTEN Modulates Cell Cycle Progression and Cell Survival by Regulating Phosphatidylinositol 3,4,5,-Trisphosphate and Akt/Protein Kinase B Signaling Pathway." *Proceedings of the National Academy of Sciences* 96 (11): 6199–6204. <https://doi.org/10.1073/pnas.96.11.6199>.
- Suvarna, Kim S., Christopher Layton, and John D. Bancroft, eds. 2013. *Theory and Practice of Histological Techniques*. 7. ed. Edinburgh: Elsevier Churchill Livingstone.
- Suzuki, Hiroyoshi, Diha Freije, Deborah R. Nusskern, Kenji Okami, Paul Cairns, David Sidransky, William B. Isaacs, and G. Steven Bova. 1998. "Interfocal Heterogeneity of *PTEN/MMAC1* Gene Alterations in Multiple Metastatic Prostate Cancer Tissues." *Cancer Research* 58 (2): 204.
- Talmadge, J. E., and I. J. Fidler. 2010. "AACR Centennial Series: The Biology of Cancer Metastasis: Historical Perspective." *Cancer Research* 70 (14): 5649–69. <https://doi.org/10.1158/0008-5472.CAN-10-1040>.
- Tamura, M., J. Gu, H. Tran, and K. M. Yamada. 1999. "PTEN Gene and Integrin Signaling in Cancer." *JNCI Journal of the National Cancer Institute* 91 (21): 1820–28. <https://doi.org/10.1093/jnci/91.21.1820>.
- Tamura, Masahito, Jianguo Gu, Takahisa Takino, and Kenneth M. Yamada. 1999. "Tumor Suppressor PTEN Inhibition of Cell Invasion, Migration, and Growth: Differential Involvement of Focal Adhesion Kinase and P130<sup>Cas</sup>." *Cancer Research* 59 (2): 442.
- Tamura, R. N. 1990. "Epithelial Integrin Alpha 6 Beta 4: Complete Primary Structure of Alpha 6 and Variant Forms of Beta 4." *The Journal of Cell Biology* 111 (4): 1593–1604. <https://doi.org/10.1083/jcb.111.4.1593>.
- Taylor, Barry S., Nikolaus Schultz, Haley Hieronymus, Anuradha Gopalan, Yonghong Xiao, Brett S. Carver, Vivek K. Arora, *et al.* 2010. "Integrative Genomic Profiling of Human Prostate Cancer." *Cancer Cell* 18 (1): 11–22. <https://doi.org/10.1016/j.ccr.2010.05.026>.
- Titford, M. 2005. "The Long History of Hematoxylin." *Biotechnic & Histochemistry* 80 (2): 73–78. <https://doi.org/10.1080/10520290500138372>.
- Tomlins, Scott A., Rohit Mehra, Daniel R. Rhodes, Lisa R. Smith, Diane Roulston, Beth E. Helgeson, Xuhong Cao, *et al.* 2006. "TMPRSS2:ETV4 Gene Fusions Define a Third Molecular Subtype of Prostate Cancer." *Cancer Research* 66 (7): 3396–3400. <https://doi.org/10.1158/0008-5472.CAN-06-0168>.
- Tomlins, Scott A., Bharathi Laxman, Sooryanarayana Varambally, Xuhong Cao, Jindan Yu, Beth E. Helgeson, Qi Cao, *et al.* 2008. "Role of the TMPRSS2-ERG Gene Fusion in Prostate Cancer." *Neoplasia* 10 (2): 177-188. <https://doi.org/10.1593/neo.07822>.

- Usher, Pernille Autzen, Ole Frøkjær Thomsen, Peter Iversen, Morten Johnsen, Nils Brønner, Gunilla Høyer-Hansen, Peter Andreasen, Keld Danø, and Boye Schnack Nielsen. 2005. "Expression of Urokinase Plasminogen Activator, Its Receptor and Type-1 Inhibitor in Malignant and Benign Prostate Tissue: Proteolysis in Prostate Cancer." *International Journal of Cancer* 113 (6): 870-80. <https://doi.org/10.1002/ijc.20665>.
- VanderVorst, Kacey, Courtney A. Dreyer, Sara E. Konopelski, Hyun Lee, Hsin-Yi Henry Ho, and Kermit L. Carraway. 2019. "Wnt/PCP Signaling Contribution to Carcinoma Collective Cell Migration and Metastasis." *Cancer Research* 79 (8): 1719–29. <https://doi.org/10.1158/0008-5472.CAN-18-2757>.
- Varzavand, Afshin, Justin M. Drake, Robert U. Svensson, Mary E. Herndon, Bo Zhou, Michael D. Henry, and Christopher S. Stipp. 2013. "Integrin A3β1 Regulates Tumor Cell Responses to Stromal Cells and Can Function to Suppress Prostate Cancer Metastatic Colonization." *Clinical & Experimental Metastasis* 30 (4): 541–52. <https://doi.org/10.1007/s10585-012-9558-1>.
- Varzavand, Afshin, Will Hacker, Deqin Ma, Katherine Gibson-Corley, Maria Hawayek, Omar J. Tayh, James A. Brown, Michael D. Henry, and Christopher S. Stipp. 2016. "A3β1 Integrin Suppresses Prostate Cancer Metastasis via Regulation of the Hippo Pathway." *Cancer Research* 76 (22): 6577–87. <https://doi.org/10.1158/0008-5472.CAN-16-1483>.
- Vaughan, R. B., and J. P. Trinkaus. 1966. "Movements of Epithelial Cell Sheets *In Vitro*." *Journal of Cell Science* 1 (4): 407.
- Wang, J., Y. Cai, W. Yu, C. Ren, D. M. Spencer, and M. Ittmann. 2008. "Pleiotropic Biological Activities of Alternatively Spliced TMPRSS2/ERG Fusion Gene Transcripts." *Cancer Research* 68 (20): 8516–24. <https://doi.org/10.1158/0008-5472.CAN-08-1147>.
- Wang, Mengdie, Raymond B. Nagle, Beatrice S. Knudsen, Gregory C. Rogers, and Anne E. Cress. 2017. "A Basal Cell Defect Promotes Budding of Prostatic Intraepithelial Neoplasia." *Journal of Cell Science* 130 (1): 104-10. <https://doi.org/10.1242/jcs.188177>.
- Watanabe, T., K. Sato, and K. Kaibuchi. 2009. "Cadherin-Mediated Intercellular Adhesion and Signaling Cascades Involving Small GTPases." *Cold Spring Harbor Perspectives in Biology* 1 (3): a003020–a003020. <https://doi.org/10.1101/cshperspect.a003020>.
- Weber, G. F., M. A. Bjerke, and D. W. DeSimone. 2011. "Integrins and Cadherins Join Forces to Form Adhesive Networks." *Journal of Cell Science* 124 (8): 1183–93. <https://doi.org/10.1242/jcs.064618>.
- Wei, Jueyang, Leslie Shaw, and Arthur Mercurio. 1997. "Integrin Signaling in Leukocytes: Lessons from the A6β1 Integrin." *Journal of Leukocyte Biology* 61 (May): 397–407. <https://doi.org/10.1002/jlb.61.4.397>.
- Weinell, Rolf J, Annette Rosendahl, Elisabeth Pinschmidt, Oliver Kisker, Babette Simon, and Sentot Santoso. 1995. "The (X6-1) Integrin Receptor in Pancreatic Carcinoma" 108 (2): 10.

- Weiner, A B, R S Matulewicz, S E Eggener, and E M Schaeffer. 2016. "Increasing Incidence of Metastatic Prostate Cancer in the United States (2004–2013)." *Prostate Cancer and Prostatic Diseases* 19 (4): 395–97. <https://doi.org/10.1038/pcan.2016.30>.
- Wu, L., J. C. Zhao, J. Kim, H.-J. Jin, C.-Y. Wang, and J. Yu. 2013. "ERG Is a Critical Regulator of Wnt/LEF1 Signaling in Prostate Cancer." *Cancer Research* 73 (19): 6068–79. <https://doi.org/10.1158/0008-5472.CAN-13-0882>.
- Yamada, Kenneth M., and Masaru Araki. 2001. "Tumor Suppressor PTEN: Modulator of Cell Signaling, Growth, Migration and Apoptosis." *Journal of Cell Science* 114 (13): 2375.
- Yanez-Mo, M., R. Tejedor, P. Rousselle, and F. Sanchez-Madrid. 2001. "Tetraspanins in Intercellular Adhesion of Polarized Epithelial Cells: Spatial and Functional Relationship to Integrins and Cadherins." *Journal of Cell Science* 114 (3): 577.
- Yang, Jing, Sendurai A Mani, Joana Liu Donaher, Sridhar Ramaswamy, Raphael A Itzykson, Christophe Come, Pierre Savagner, Inna Gitelman, Andrea Richardson, and Robert A Weinberg. 2004. "Twist, a Master Regulator of Morphogenesis, Plays an Essential Role in Tumor Metastasis." *Cell* 117 (7): 927–39. <https://doi.org/10.1016/j.cell.2004.06.006>.
- Yano, Hajime, Yuichi Mazaki, Kazuo Kurokawa, Steven K. Hanks, Michiyuki Matsuda, and Hisataka Sabe. 2004. "Roles Played by a Subset of Integrin Signaling Molecules in Cadherin-Based Cell–Cell Adhesion." *The Journal of Cell Biology* 166 (2): 283–95. <https://doi.org/10.1083/jcb.200312013>.
- Yoshimoto, Maisa, Anthony M Joshua, Isabela W Cunha, Renata A Coudry, Francisco P Fonseca, Olga Ludkovski, Maria Zielenska, Fernando A Soares, and Jeremy A Squire. 2008. "Absence of TMPRSS2:ERG Fusions and PTEN Losses in Prostate Cancer Is Associated with a Favorable Outcome." *Modern Pathology* 21 (12): 1451–60. <https://doi.org/10.1038/modpathol.2008.96>.
- Yu, Fa-Xing, Bin Zhao, and Kun-Liang Guan. 2015. "Hippo Pathway in Organ Size Control, Tissue Homeostasis, and Cancer." *Cell* 163 (4): 811–28. <https://doi.org/10.1016/j.cell.2015.10.044>.
- Zhong, Cuiling, Michael S. Kinch, and Keith Burridge. 1997. "Rho-Stimulated Contractility Contributes to the Fibroblastic Phenotype of Ras-Transformed Epithelial Cells." *Molecular Biology of the Cell* 8 (11): 2329–44. <https://doi.org/10.1091/mbc.8.11.2329>.

- Zhou, Bo, Katherine N. Gibson-Corley, Mary E. Herndon, Yihan Sun, Elisabeth Gustafson-Wagner, Melissa Teoh-Fitzgerald, Frederick E. Domann, Michael D. Henry, and Christopher S. Stipp. 2014. "Integrin A3 $\beta$ 1 Can Function to Promote Spontaneous Metastasis and Lung Colonization of Invasive Breast Carcinoma." *Molecular Cancer Research* 12 (1): 143-54.  
<https://doi.org/10.1158/1541-7786.MCR-13-0184>.
- Zhou, Hua, and Randall H. Kramer. 2005. "Integrin Engagement Differentially Modulates Epithelial Cell Motility by RhoA/ROCK and PAK1." *Journal of Biological Chemistry* 280 (11): 10624-35.  
<https://doi.org/10.1074/jbc.M411900200>.
- Zhou, Ming. 2018. "High-Grade Prostatic Intraepithelial Neoplasia, PIN-like Carcinoma, Ductal Carcinoma, and Intraductal Carcinoma of the Prostate." *Modern Pathology* 31 (S1): 71-79.  
<https://doi.org/10.1038/modpathol.2017.138>.